Ship Hull Optimization
in Calm Water and Moderate Sea States

Tin Yadanar Tun

Master Thesis

presented in partial fulfillment
of the requirements for the double degree:
"Advanced Master in Naval Architecture" conferred by University of Liege
"Master of Sciences in Applied Mechanics, specialization in Hydrodynamics, Energetics and Propulsion" conferred by Ecole Centrale de Nantes

developed at University of Rostock
in the framework of the

"EMSHIP"
Erasmus Mundus Master Course
in "Integrated Advanced Ship Design"

Ref. 159652-1-2009-1-BE-ERA MUNDUS-EMMC

Supervisor:	Dr.Ing. Robert Bronsart, University of Rostock Dipl.-Ing. Eva Binkowski, University of Rostock
Internship Supervisor:	Dr.-Ing. Stefan Harries, FRIENDSHIP SYSTEMS AG
Reviewer:	Prof. Florin Pacuraru, University of Galati

Rostock, February 2016

ABSTRACT

Optimization is a human trait. Mathematically speaking, it is minimizing (or maximizing) one or several objectives within a set of constraints. Hull form optimization from a hydrodynamic performance point of view in calm water and in moderate sea states is an important aspect in preliminary ship design. The challenge of this work is getting a ship with lowest energy consumption in calm water and in different sea states by various optimization approaches. Several optimization approaches were used for a hull form improvement to maximize seakeeping performance (accelerations based criteria) and minimize the ship resistance at its given displacement and its service speeds. Different sea-states of operating routes and different speeds were taken into account for the analysis of seakeeping performance of a vessel.

An academic container vessel (Duisburg Test Case developed and tested by the University of Duisburg-Essen) was taken for the study case. The parametric model of the vessel is developed by modifying the initial geometry with the use of CAESES 4.0. After getting a parametric model, it was simulated by GL Rankine, potential flow code developed by DNV GL and validated with experimental results from HSVA. After coupling GL Rankine solver with CAESES, different optimization approaches were done by using CAESES/Dakota interface. The optimization was focused on the changes of the forward part of the vessel (Bulbous bow).

While performing optimization process, not only the main objectives to minimize the energy consumption of the vessel, also computational effort (how many number of CFD runs needed) and influence of slightly changes on the operational conditions were taken into account as major criteria.

As the first approach, the optimal hull form was obtained in calm water condition by different optimization algorithms and was checked wave added resistance and seakeeping behavior in moderate sea states. In second approach, optimization process was done by considering calm water condition and also seakeeping performance in different operation profiles. Finally, the results of the optimal hull form were compared with original design.

ACKNOWLEDGEMENTS

I would like to say my deepest thanks to those who willingly helped me for this master thesis and for finishing this master course

Dipl.-Ing. Eva Binkowski and Prof. Dr.-Ing. Robert Bronsart, for making this work possible and guiding me to the success of the master thesis

Dr.-Ing. Stefan Harries, for his ideas, supervision and orientation in every detail of this research work

Prof. Philippe Rigo, as coordinator of the EMSHIP for his great effort in organizing and managing this program and for his constant help and encouragement to finish this great pleasure and challenging study period in Europe

The FRIENDSHIP SYSTEMS team that made my work possible and pleasant, receiving me with open arms and answering all my questions

DNV-GL team, especially Mr. Vladimir Shigunov, Mr. Andreas Brehm and Mr. Alexander Von-Graefe and Jonas Conradin Wagner for their valuable support and advices for technical problems.

Furthermore, I would like to say thanks to Noufal Paravilayil Najeeb, my colleague for supporting me and helping me out for everything. Finally, I would like to express my gratitude towards my family, especially my parents and my friends for supporting me and all of my teachers who taught me to be in this position.

This thesis was developed in the frame of the European Master Course in “Integrated Advanced Ship Design” named “EMSHIP” for “European Education in Advanced Ship Design”, Ref.: 159652-1-2009-1-BE-ERA MUNDUS-EMMC.

Tin Yadanar Tun – Rostock, January, 2015

TABLE OF CONTENTS

LIST OF FIGURES

LIST OF TABLES

DECLARATION OF AUTHORSHIP

I declare that this thesis and the work presented in it are my own and have been generated by me as the result of my own original research.

Where I have consulted the published work of others, this is always clearly attributed.

Where I have quoted from the work of others, the source is always given. With the exception of such quotations, this thesis is entirely my own work.

I have acknowledged all main sources of help.

Where the thesis is based on work done by myself jointly with others, I have made clear exactly what was done by others and what I have contributed myself.

This thesis contains no material that has been submitted previously, in whole or in part, for the award of any other academic degree or diploma.

I cede copyright of the thesis in favor of the University of Rostock.

Date: Signature:

1. INTRODUCTION

1.1. General

The hydrodynamic performance of a hull form in calm water and in moderate sea state is a major aspect for a naval architect in preliminary design stage. In the past, ships were designed based on the performance in calm water condition without considering the sea state of actual operation profiles and there are many attempts to optimize the calm water resistance of the vessel by varying form parameters. On the other hand, both of the global and local form parameters of a vessel influence its calm water behavior as well as its seakeeping performance depends primarily on global hull form parameters. Therefore, in recent years, the optimization of vessel both in calm water and in its seaways becomes more important for the reliable prediction of the power requirement. In the optimization process, the different algorithm is linked to the computational method to obtain an optimum hull form by several geometrical constraints such as internal fitting, displacement and stability.

There are different kinds of approaches to study hydrodynamic performance which are (a) the empirical approach that is in the form of constants, formulae and curves developed from the parent ship or similar shapes, (b) the experimental approach that is the testing of a scaled model of original hull form and analyzing the performances, expanding to full scale results and (c) the numerical approach that has become increasingly important for ship resistance and powering. Therefore, ship optimization based on CFD simulation becomes the major factor of developing new optimal ship hull forms by minimizing ship resistance. Reducing the resistance leads to less consumable power, less emissions and noises.

The optimization process is fully automated requiring no user interaction. In this thesis, the steady wave system of a ship moving through calm water is approximated by means of CFD (Computational Fluid Dynamics) simulation applying nonlinear free surface Rankine panel method of GL Rankine solver, which is in-house potential flow solver developed by DNV GL. The modelling of the geometry of the initial design, the coupling of the CFD solver and performing the optimization process to minimize the wave-making resistance were done by the use of CAESES developed by FRIENDSHIP SYSTEMS.

1.2. Benefits

Ship hull form optimization offers several benefits in the way of:

- Better understanding of the design task (and the design space),
- Creating design with superior performance (and better trade-offs),
- Allowing shorter time-to-market (and faster response to market changes),
- Reducing risk (and building confidence),
- Saving costs (and avoiding expensive late changes).

Hull form optimization is conducted both for investigating new ideas and possibilities at the initial design stage and for fine-tuning of a given design at a later stage when only small changes are still acceptable, sees Figure - 1.

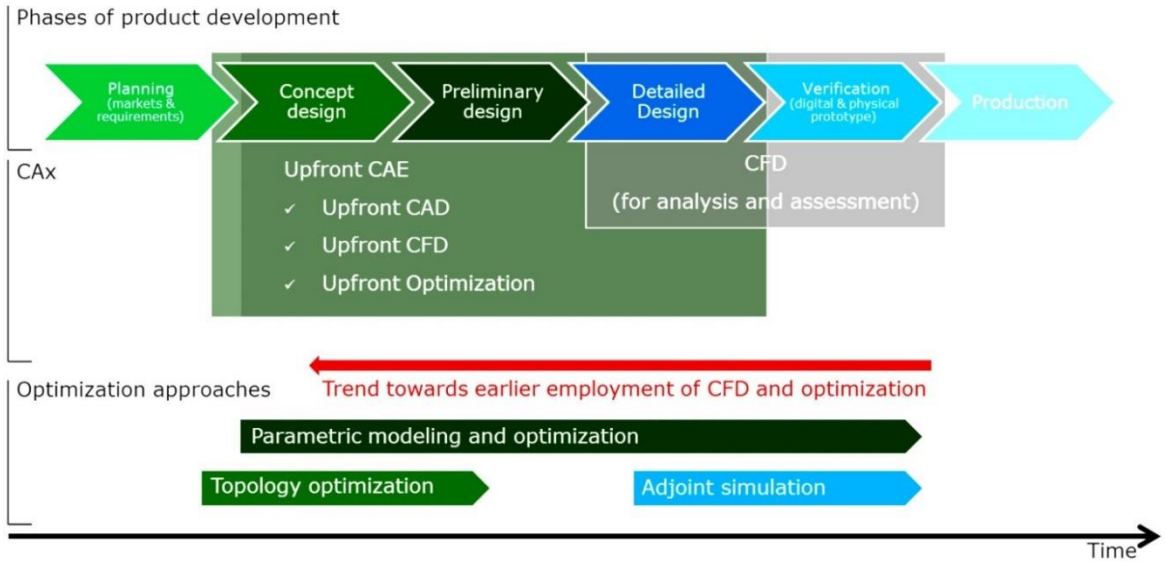

Figure - 1: Phases of Product Development [1]

1.3. Objectives

The main objective of this thesis is to study about the various approaches for the optimization of fore body (Bulbous Bow) of hull form for a container vessel based on the given technical specifications. The optimization process will be focused on minimizing the wave-making resistance of the vessel in calm water condition and added resistance in its seaway conditions. Furthermore, the coupling of newly developed in-house GL Rankine solver with CAESES, to check the resistances in both steady flow and seaway, as well as the seakeeping performances considering different scenarios of operating routes and different speeds, has to be done.

1.4. Scope of Study

In this thesis, the hull form for the specific vessel will be optimized with fully-automated process, but it is allowed to operate manually as well. The fore body of hull form is modelled as partial parametric model in CAESES and it is simulated with GL Rankine potential flow solver for obtaining the resultant resistances in calm water and in seaways, followed by validating the results from experiments which are performed in model basin at HSVA.

The optimization process will be done with CAESES/ Dakota Interface to get the optimized hull form that can be checked later for seakeeping behaviors with moderate sea states. The set-up optimization process permits to get the best hull form which is not only the resistance in calm water but also for added resistance in seaways as well.

1.5. Methods and Procedures

The original hull form trimesh of a DTC (Duisburg Test Case) container vessel, given by Duisburg University in STL format is modified in CAESES using the design parameters which control the shape of bulbous bow of the vessel. After getting a partially parametric model, the setup of GL Rankine solver is developed in order to get the simulation results such as calm water resistance, added wave resistance and 6 DOF motions. The results obtained from CFD solver are verified with the experimental results performed by HSVA towing tanks. After that, the CFD solver is coupled with CAESES to perform different optimization processes for different scenarios considering actual seaways, which cover approximately 37% of operation profiles of similar container vessels calculated by University of Rostock.

In addition to finding the optimal hull form with the minimum calm water resistance and checking seakeeping behaviors, the direct optimization of calm water resistance together with added resistance in waves will also be done. Optimization will be done especially on the fore body of the hull, (e.g. bulbous bow) because GL Rankine solver utilizes the potential flow code which is mainly effective for fore body flow of the ship and less effective for viscous flow occurred at the aft body.

The flow chart showing the step by step procedure of the entire work scope can be seen in Figure - 2.

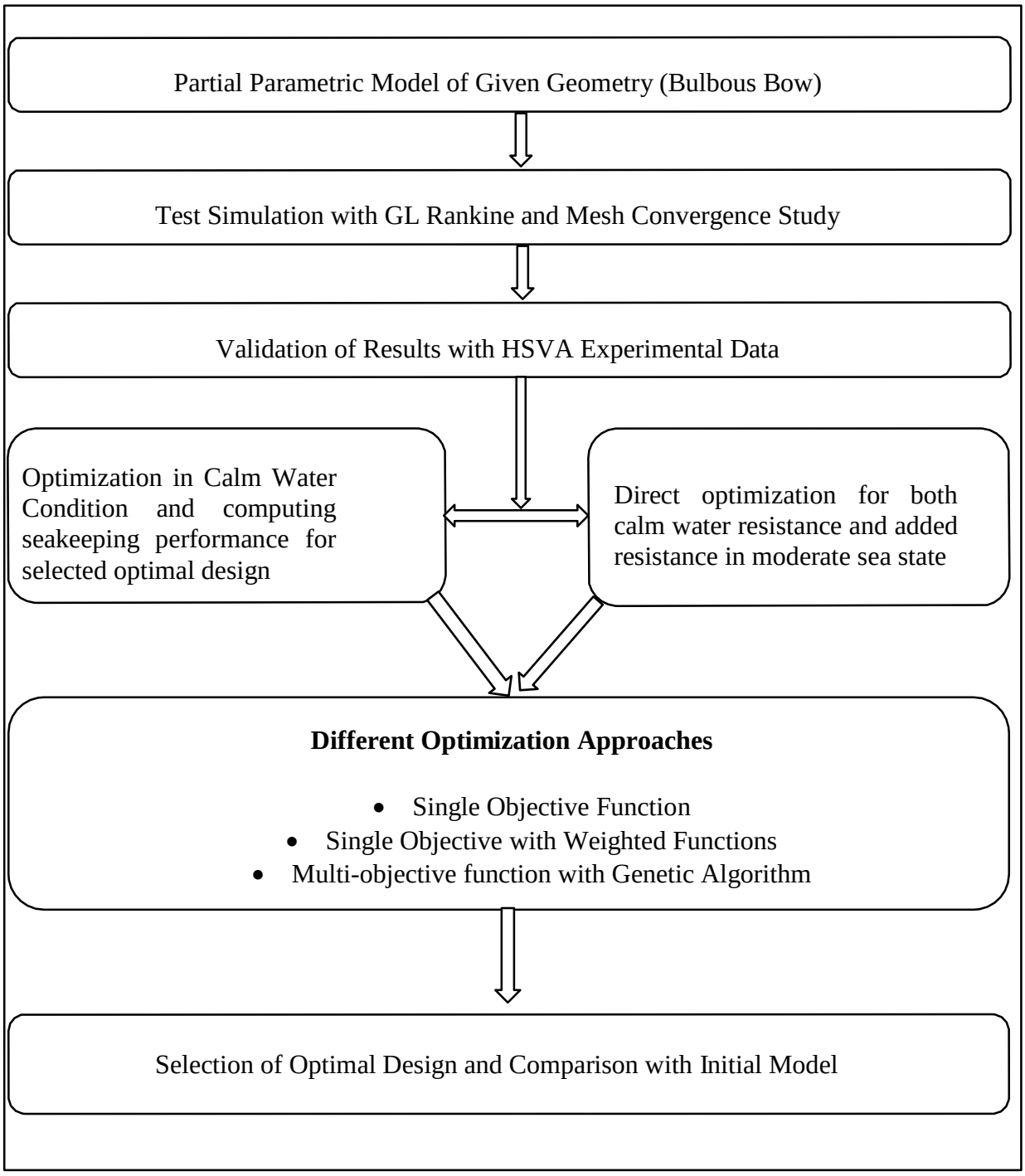

Figure- 2: Flow Chart showing Methods and Procedures

2. LITERATURE REVIEW

This thesis includes different optimization processes for the improvement of ship hydrodynamic performance such as calm water resistance, added resistance in waves for different operation profiles at different speeds and its seakeeping performances. Before starting optimization process of ship hull form, the author has done numerous engineering studies related to parametric modelling of ship hull form, coupling of GL Rankine potential flow solver with CAESES, designing the sea states of vessel's operation routes for its seakeeping performances, various optimization algorithms and so on. In this literature review, some aspects of optimization process of different hull shapes for resistance and seakeeping performance in calm water and in moderate sea states are presented for the better understanding of the problem. Prediction of Ship performances in calm and rough water is one of the most important concerns for naval architects, already at the earliest design stage. From this point of view, seakeeping performance is one of the most important performances in the ship hull form optimization (Bagheri, Ghassemi and Dehghanian, 2014 [2]).

Zhang et al (2008) [3] wrote a paper about "Parametric Approach to Design of Hull Forms" in Eslevier Journal. This paper covers the parametric modelling of the hull form with the use of form parameters and the longitudinal function curves and combining the parametric approach to CFD method for optimization. After several principle dimensions have been fixed as a result of economic and/or hydrodynamic optimizations, a subsequent improvement of the hydrodynamic performance is usually carried out to refine the design. Parameters typically used for the manipulation of wave resistance are related to the shape of the bulbous bow. (Abt et al, 2001[4]).

After designing parametric model of a vessel, numerical analysis of hydrodynamic performance has to be done by the use of CFD (computational fluid dynamics) solvers. CFD methods provide total resistance, i.e., calm water resistance and added resistance in waves. But CFD methods require too much computer resources to study the influence of various parameters on added resistance, potential flow methods are applied predominantly. (Heinrich et al, 2012 [5]). Heimann (2005) [6] wrote a PhD thesis about "CFD based Optimization of the wave-making characteristics of ship hulls" that covers a hull form optimization approach with CFD based evaluation of the nonlinear ship wave pattern, on realization of the cause and effect relation of hull variations and their impact on wave formation, which is accessed by a perturbation approach, and on wave cut analysis (WCA).

A paper about “Hull-form optimization in calm and rough water” presents a formal methodology for the hull form optimization in calm and rough water using wash waves and selected dynamic responses, respectively. A major concern of any optimization procedure is to associate the set of hull form parameters identifying the variants to a faired hull form. Parametric models offer the only way to establish this relation and to ensure that at each stage of the optimization a feasible model is produced. Then, state-of-the-art algorithms can evaluate its hydrodynamic performance both in calm and rough water by the use of Rankine-source panel method and strip theories (Grigoropoulos and Chalkias, 2009 [7]).

Genetic algorithm is inspired by the evolution theory (Darwin’s theory of biological evolution) by means of a process that is known as the natural selection and the "survival of the fittest" principle. The common idea behind this technique is similar to other evolutionary algorithms: consider a population of individuals; the environmental pressure causes natural selection which leads to an increase in the fitness of the population. It is easy to see such a process as optimization.

Consider an evaluation function to be minimized (the lower, the better). A set of candidate solutions can be randomly generated and the objective function can be used as a measure of how individuals have performed in the problem domain (an abstract fitness measure). According to this fitness, some of the better solutions are selected to seed the next generation by applying recombination and/or mutation operators to them. The recombination (also called crossover) operator is used to generate new candidate solutions (offspring) from existing ones by taking two or more selected candidates (parents) from the population pool and by exchanging some of their parts to form one or more offspring. The mutation operator is used to generate one offspring from one parent by changing some parts of the candidate solution. The application of the recombination and mutation operators causes a set of new candidates (the offspring) to compete based on their fitness with the old candidates (the parents) for a place in the next generation.

This procedure can be iterated until a solution with sufficient quality (fitness) is found or a previously set computational time limit is reached. In other words, the end conditions must be satisfied. The composed application of selection and variation operators (recombination and mutation) improves fitness values in the consecutive population. A general flowchart of genetic algorithm is shown in Figure - 3 (Bagheri et al, 2014[8]).

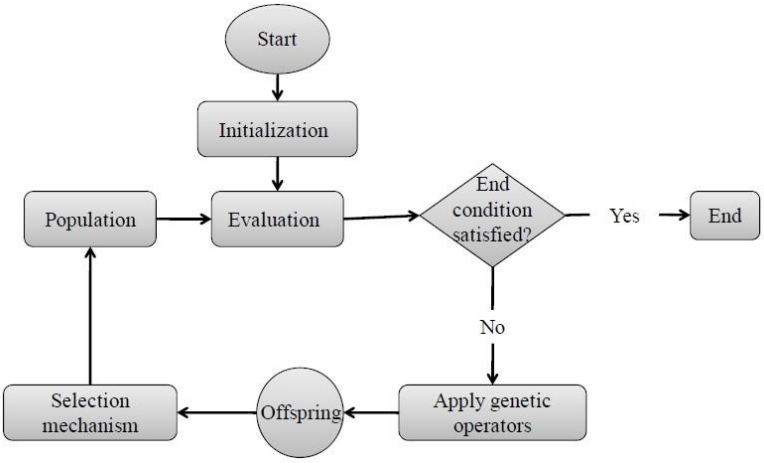

Figure - 3: General Flowchart of Genetic Algorithm [8]

In the paper "Computational Fluid Dynamics Based Bulbous Bow Optimization Using a Genetic Algorithm" (Mahmood et al, 2012 [9]), the hull form of a ship was optimized for total resistance using CFD as a calculation tool and a genetic algorithm as an optimization tool. CFD based optimization consists of major steps involving automatic generation of geometry based on design parameters, automatic generation of mesh, and automatic analysis of fluid flow to calculate the required objective/cost function.

In this thesis work, the optimization toolkit Dakota coupled with CAESES will be used for different optimization approaches. The following section will be discussed the theoretical explanation of optimization method used in CAESES/ Dakota Interface.

2.1. Advanced Design Optimization Methods in Dakota

A variety of "meta-algorithm" capabilities have been developed in order to provide a mechanism for employing individual iterators and models as reusable components within higher-level solution approaches. This capability allows the use of existing iterative algorithm and computational model software components as building blocks to accomplish more sophisticated studies such as [10]:

Hybrid minimization: In this method, a sequence of minimization methods is applied to find an optimal design point. The goal of this method is to exploit the strengths of different minimization algorithms through different stages of the minimization process.

Multi-start Local Minimization: A simple global minimization technique is to use many local minimization runs, each of which is started from a different initial point in the parameter space. This is known as multi-start local minimization. This is an attractive

method in situations where multiple local optima are known or expected to exist in the parameter space. Since solutions for different starting points are independent, parallel computing may be used to concurrently run the local minimizations.

Pareto Optimization: In Pareto optimization method, multiple sets of multi-objective weightings are evaluated. Dakota performs one multi-objective optimization problem for each set of multi-objective weights. The collection of computed optimal solutions forms a Pareto set, which can be useful in making trade-off decisions in engineering design. Since solutions for different multi-objective weights are independent, parallel computing may be used to concurrently execute the multi-objective optimization problems.

Surrogate-Based Minimization: Surrogate models approximate an original, high fidelity "truth" model, typically at reduced computational cost. In the context of minimization (optimization or calibration), surrogate models can speed convergence by reducing function evaluation cost or smoothing noisy response functions.

2.2. Brief Overview of Optimization Methods used in CAESES

The following two methods are the surrogate based optimization methods coupled with CAESES as preconfigured input templates.

(a) Local Optimization Efficient- Internally, this method creates a surrogate model (response surface) and conducts a local optimization on this model. For the initial surrogate model, existing point data can be used e.g. from a previous sensitivity analysis. During the run, the surrogate model is iteratively fine-tuned: the optimum design from the local search is evaluated and the information is added to the surrogate model – which step by step increases the quality of the model.

(b) MOGA Global Optimization Efficient- In this method, a MOGA is conducted on a surrogate model that is iteratively built-up. For the initial model, data from a previous run (e.g. sensitivity analysis) can be recycled as well. With this approach, the method might be suitable even for rather expensive evaluations [11].

The author studied a lot of reference works for optimization of hull forms for resistance and seakeeping behaviors and different optimization algorithms. However, there are not many research works in optimization of hull form, minimizing total resistance in both calm water and in sea states with different draft and speed variations according to vessel's operation profile. Therefore, this thesis will be focused on this specific work by the use of new potential flow solver, GL Rankine coupling with CAESES.

3. CASE STUDY

Hydrodynamic optimization of ships not only targets energy efficiency but also the performance of ships in moderate and heavy sea states. The research and development project, called PerSee which stands for "Performance von Schiffen im Seegang" (performance of ships in sea-states), aims at establishing new processes for the optimization of ships in moderate seas, considering the effects of waves on both hull forms and propellers, and at identifying safety requirements for ships in heavy seas. Operational scenarios as well as minimum speed and power requirements are considered. The engineers from Friendship Systems become a part of the project called PerSee, which studies the optimization of ships in sea states. Within the project, Friendship Systems further strengthens its CAE platform CAESES. Main R&D targets are further ease in setting up complex processes that involve several simulation tools and improved usability in creating and understanding complex parametric models [12]. In this PerSee project, among different coordinated work packages, Friendship Systems has to perform parametrical optimization of the hull shape under operating conditions in seaways [13]. In this thesis work, the new DTC (Duisburg Test Case) container vessel is needed to optimize for calm water resistance and motion performances in moderate seaways by applying the in-house potential flow solver called GL Rankine in CAESES.

3.1. Main Characteristics of the Vessel

The study relies on a DTC container vessel. Duisburg Test Case (DTC) is a hull design of a modern 14000 TEU post-panamax container carrier, developed at the University of Duisburg-Essen, Duisburg, Germany. Table-1 shows main particulars in the design loading condition and Figure -4 shows the original hull form design [14].

Table - 1: Main Dimensions of DTC in Design Loading Condition

Length Between Perpendiculars	L_{pp} [m]	355.0
Waterline Breadth	B_{wl} [m]	51.0
Design Draft Amidships	T_{Dm} [m]	14.5
Moulded Depth	D [m]	32.0
Block Coefficient	C_B [-]	0.661
Volume Displacement	V [m^3]	173467.0
wetted surface under rest waterline without appendages	S_W [m^2]	22032.0

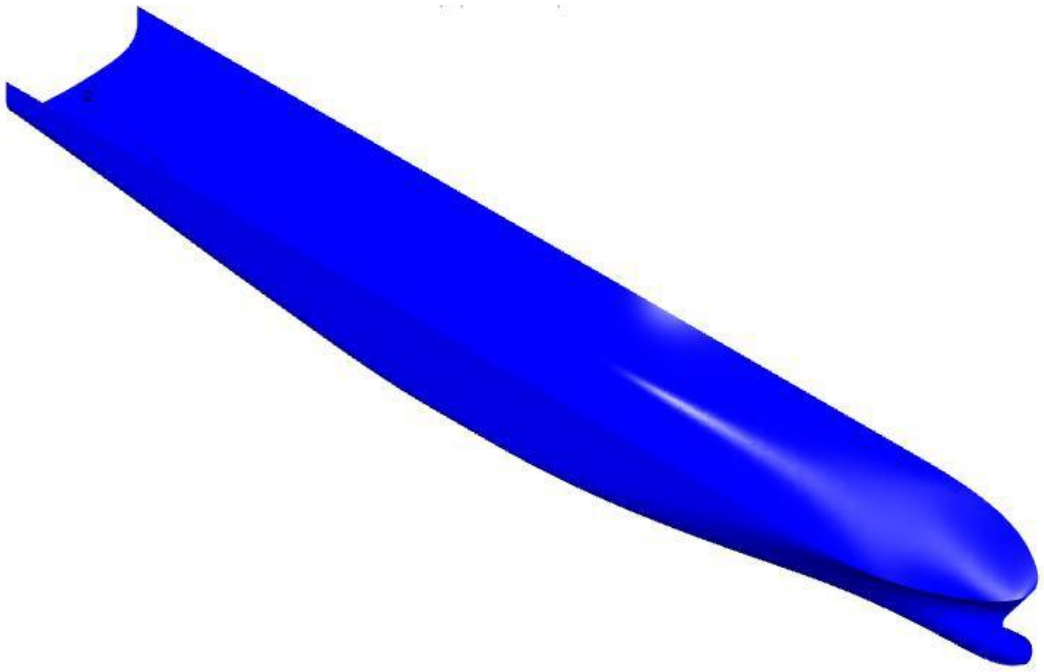

Figure- 4: Original Hull Form Design

3.2. Operational Profile

The robustness of the hull form is checked according to the operational profile, the observed variation on draft and speed of the ship. As this container vessel has not been built and it is only in preliminary design state, the operating information of this vessel is statistically derived from similar vessels in operation.

The wave scenario that the vessel has to deal with are resulted for specific wave height ($H_{1/3}$) and are chosen for three operating conditions, covering 50% of the total operating time by the vessel as mentioned in Figure-5. The weighted values w_{total} is represented in the percentage of the respective operating conditions with respect to total operating time of the vessel.

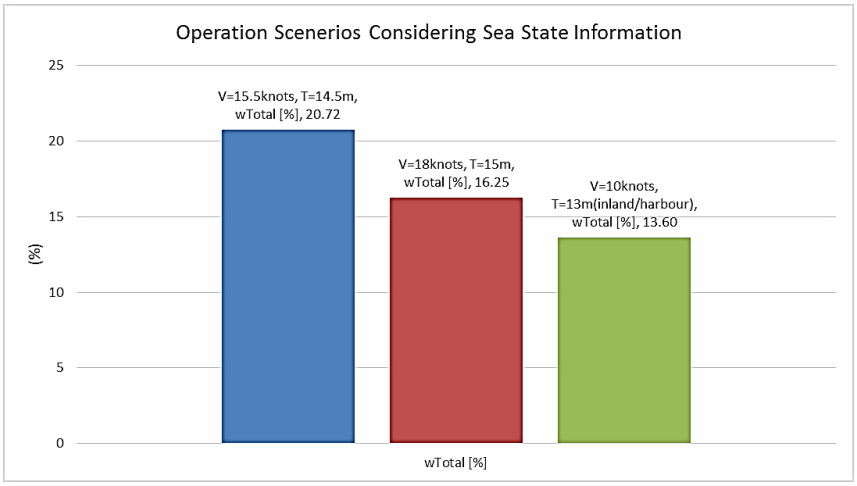

Figure- 5: Operation Scenarios Considering Actual Sea State Information

Figure-6 shows the operation scenarios without consideration of any sea state information (fast speed / draft combination) covering 46% of the total operating time.

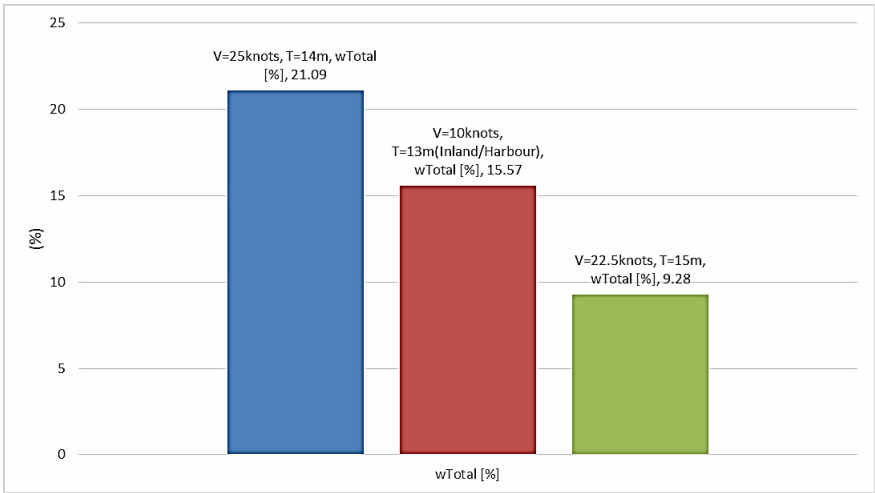

Figure- 6: Operation Scenarios without Considering Actual Sea State Information

Since the main objective of this thesis is to get optimal hull for both calm water and actual sea state condition, the operation scenario by considering sea state was chosen as following.

Operation Condition 1: V=15.5 knots and T= 14.5m
Operation Condition 2: V=18.0 knots and T= 15.0m
Operation Condition 3: V=10.0 knots and T= 13.0m

Nevertheless, V_1 = 15.5 knots and V_2=18.0 knots are to be used as the main condition for optimization process at the design draft of T=14.5m. Different optimization approaches will be done with the above two speeds and afterwards, the robustness checking according to the draft variation will be performed. For each optimal hull model, the comparison of its hydrodynamic performance will be done for different operation conditions.

4. GEOMETRICAL MODELLING

The optimization of a ship's resistance (to be minimized) is concerned with the geometric entities that describe the shape variation. Therefore, geometrical modelling plays an important role and many optimization processes follow the repetitive sequence of shape generation, analysis and performance assessment. Since CFD analysis constitutes time-consuming part of an optimization process, the outcome depends on the quality of geometric modelling. For complex shapes, a high level of sophistication is needed to reduce the number of parameters that control the geometry.

In the context of optimization of the vessel's hydrodynamic performance, a conventional non-parametric approach has numerous disadvantages because the geometry is typically generated from low level entities. The challenge lies in establishing a functional description of the modelling problem that corsets undesirable shapes without impairing the necessary freedom of variation. An excellent approach that allows this is parametric modelling [15].

Hydrodynamic optimization is an iterative and interactive design process. The process starts with a pre-processing phase in with a parametric model is established and a detailed analysis of the initial design is carried out, implying grid variation studies, convergence test and accuracy check for the CFD analysis. Then it follows the actual optimization phase by varying the design parameters along with their appropriate bounds.

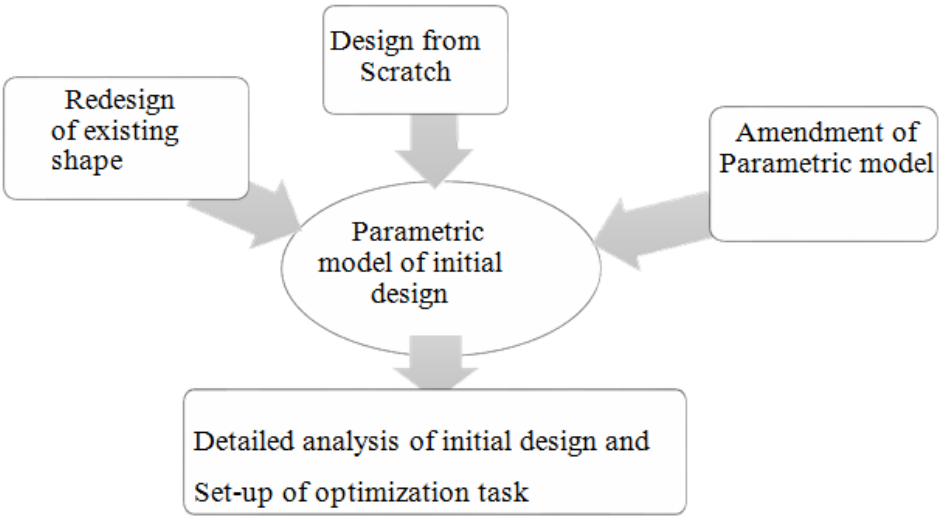

Figure- 7: Process flow of parametric model in optimization

For shape optimization using CFD, special parametric models are needed, so-called engineering models, which describe the product with as few significant parameters as possible, sometimes deliberately leaving out characteristics of lesser importance. These models address the concept and the preliminary design phases, focusing on simulation-ready CAD, and are realized within upfront CAD systems. Two major traits of upfront CAD are distinguished: Fully-parametric modelling and partially-parametric modelling [1].

In fully-parametric modelling, the entire shape is defined by means of parameters. Some parameters may be at a high level like the length, width and height of a vessel. Other parameters may determine details like an entrance angle at a particular location. Typically, many parameters are set relative to or as combinations of other parameters. Any shape is realized from scratch and variants are brought about by simply changing the values of one or several parameters. For optimization, fully-parametric modeling is very powerful since it enables both large changes in the early design phase and small adjustments when fine-tuning at a later point in time.

In partially-parametric modelling, only the changes to an existing shape are defined by parameters while the baseline (initial design model) is taken as input. Partially-parametric models are usually quick and fairly easy to set up. When compared to fully-parametric models they typically contain less knowledge (intelligence) about the product. In general, it is more difficult to excite large modifications. After all, the new shapes are derived from the baseline and, thus, cannot look totally different. Still, they are well suited for fine-tuning without much overhead. Prominent representatives of partially-parametric modelling are morphing; free-form deformation and shift transformation (e.g. shifts in coordinate direction, radial shifts).

Shift transformations typically change any point in space by adding a certain displacement depending on the point's initial position. It can be applied to both continuous data (e.g. surface patches) and discrete data (e.g. points, offsets, tri-meshes as used for data exchange via STL). Figur-8 gives an example realized in CAESES, showing a vertical shift of a container ship's bulbous bow.

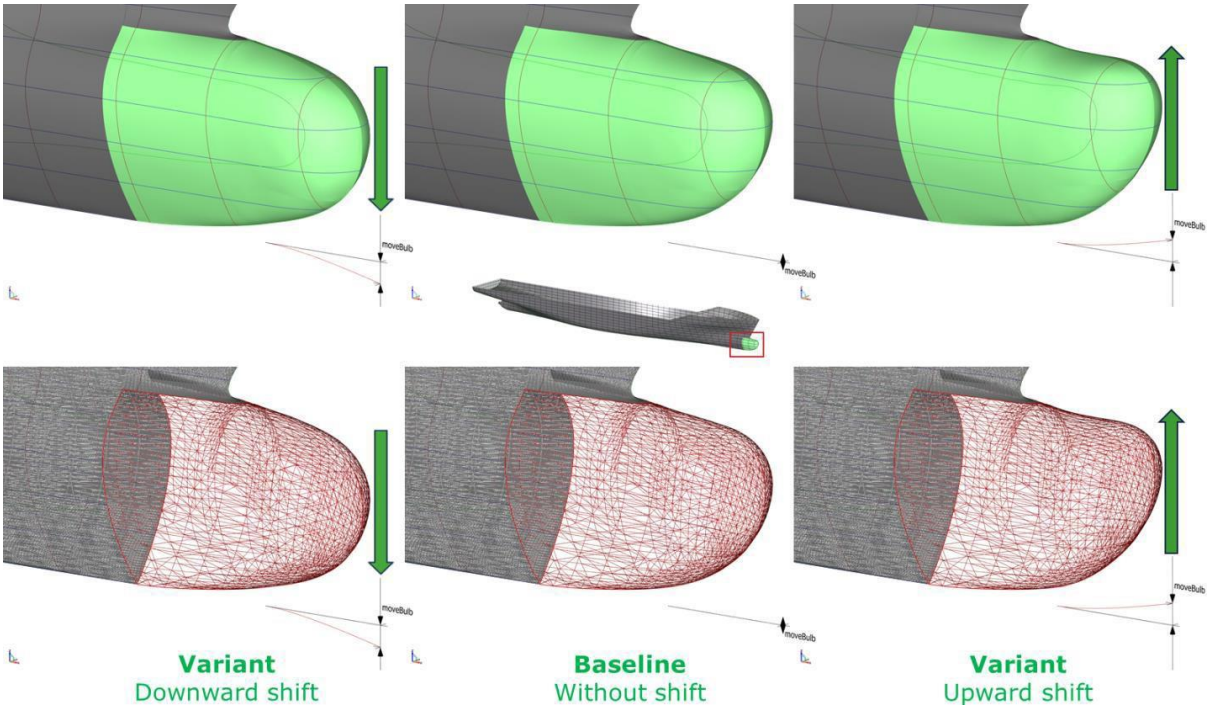

Figure- 8: Partially-parametric model for a downward vertical shift (left column), the baseline (middle) and an upward vertical shift (right column) applied to both B-spline surface patches and tri-meshes [1]

4.1. Partially-parametric Model

Since the idea of this research work is to minimize the resistance by refitting a bulbous bow, the parametric model for this task was focused on the bulbous bow region only and maintained the section shape at the forward perpendicular. Instead of implementing a completely new geometry for this study, a partial parametric model was implemented. Such model relies on a baseline geometry definition which is modified by means of various shift and scaling functions. In order to optimize the vessel, some parameters are selected to control the changes on the selected area of the geometry. The selection of parameters was based on an extended study of the influence of each variable regarding it optimization improvement i.e. the "capability" of each parameter on reducing the wave resistance and total resistance of the vessel.

First, the initial geometry of the DTC container vessel is imported to CAESES as a tri-mesh as used for data exchange via STL format [see in Figure-9]. The surface delta shift method was used to get partial parametric model in order to get different bulb shape by changing selected design parameters.

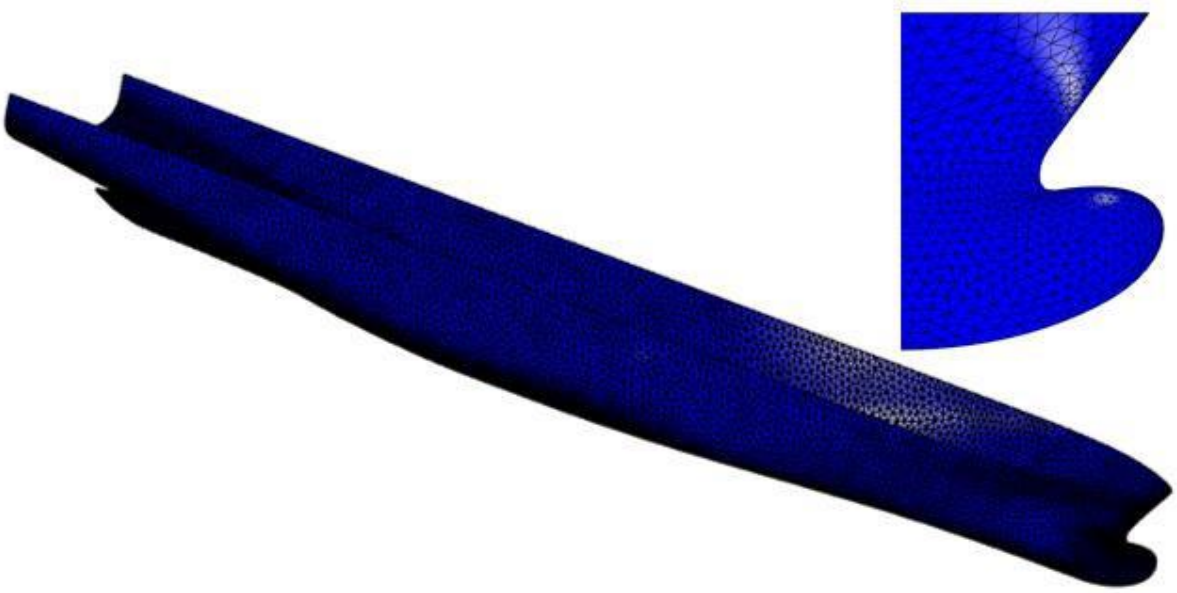

Figure- 9: Base Model Geometry in Tri-mesh STL format

First the principal parameters such as length overall, length between perpendiculars, beam, deck height and XFwdBase (the forward end position of Flat of Bottom), etc., were set-up. Then, the parametric bulb modification parameters were defined for the variation of shape.

Firstly, the feature definition curves for variation of bulb in x, y and z directions. Then, the surfaces based on those feature definition curves are generated in order to perform surface delta shift to baseline (initial design). The detail information about the usage of surface delta shift in order to get parametric model was omitted in this thesis.

The following figures 10 and 11 show the step by step procedure in order to get the partial parametric model for the bulbous bow shape variation.

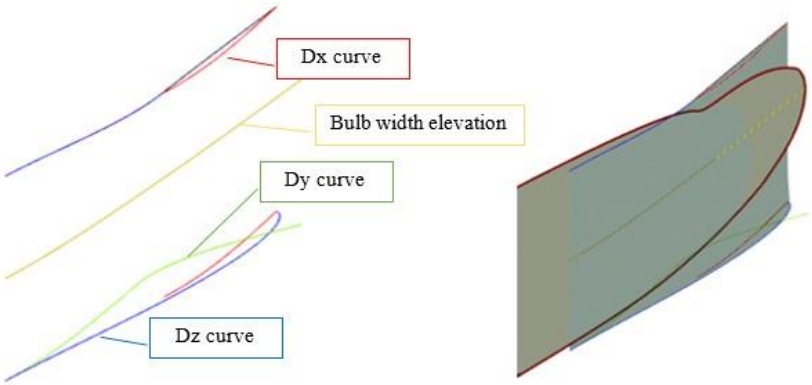

Figure- 10: Feature definition curve generation and surface generation for surface delta shift

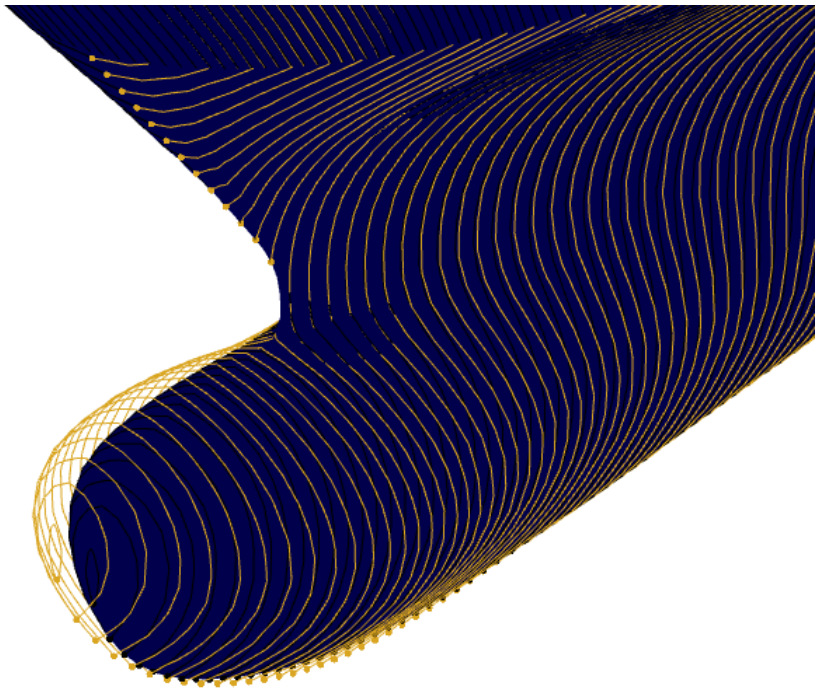

Figure- 11: Initial mesh (Blue) and new sections after surface delta shift

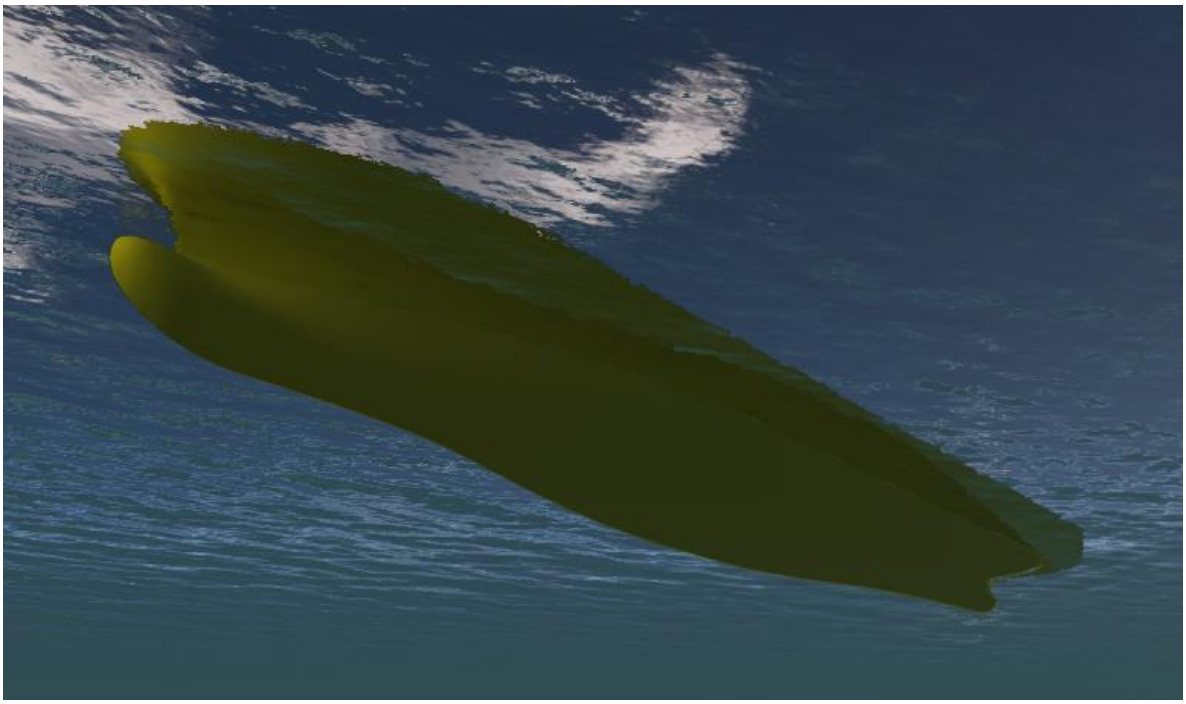

Figure- 12: Partial parametric model. Diver view created at CAESES

4.2. Selection of Design Parameters

After generating the partial parametric model, there are 14 parameters controlling the bulbous bow shape variation in total. Some parameters have large effect on the changing of the bulb geometry and some only have little influence. Furthermore, the principal parameters that define the main dimension of the hull form cannot be changed.

The number of design parameters should be as minimum as possible in order to be more efficient in the optimization process. The large number of design variables can lead to the very large amount of designs while combining all parameters. The design of experiments (DoE) study provides information to classify the design variables in order of influence to the resistance reduction. Therefore, it is necessary to define the important design variable parameters in order to save computational time and to be user-friendly for those who do not know the detail of the parametric model.

(a) **Dx Bulb** – A longitudinal shift of the bulb sections to allow elongation or shortening of the bulbous bow. The variation range for the longitudinal position of bulb tip from base design is from -2 m to +2 m.

(b) **Dy Bulb** – In order to allow for changes in width of the bulb, a scaling function has been used which gradually decreases when approaching the forward perpendicular to match the unaltered hull shape. The variation range for the half width of the bulb from base design is from -1 m to +2 m.

(c) **Dz Bulb**– a vertical shift of the bulb sections to allow the bulbous bow tip to be lowered or raised with respect to the baseline bulb. As the bulb geometry at the FP could not be changed, this shift was fading out when approaching the FP. The variation range of bulb tip elevation from the original base design is from -1.5m to 1.5m.

(d) **Bulb top tangent at FP**– It is the inclination of the after part of the bulb that connects it to the hull. It ranges from -5 degree to 11 degree.

(e) **Entrance Angle DWL** – Controls the entrance angle of the waterline at the bow regarding the X-Y plane. Changing the angle of DWL at forward perpendicular at design waterlines, ranging from -1 degree to 1 degree (zero degree for base design).

As above, there are 5 design parameters for optimization process. In Figure-13, the examples of the effect of design parameters on changing the shape of hull form are illustrated.

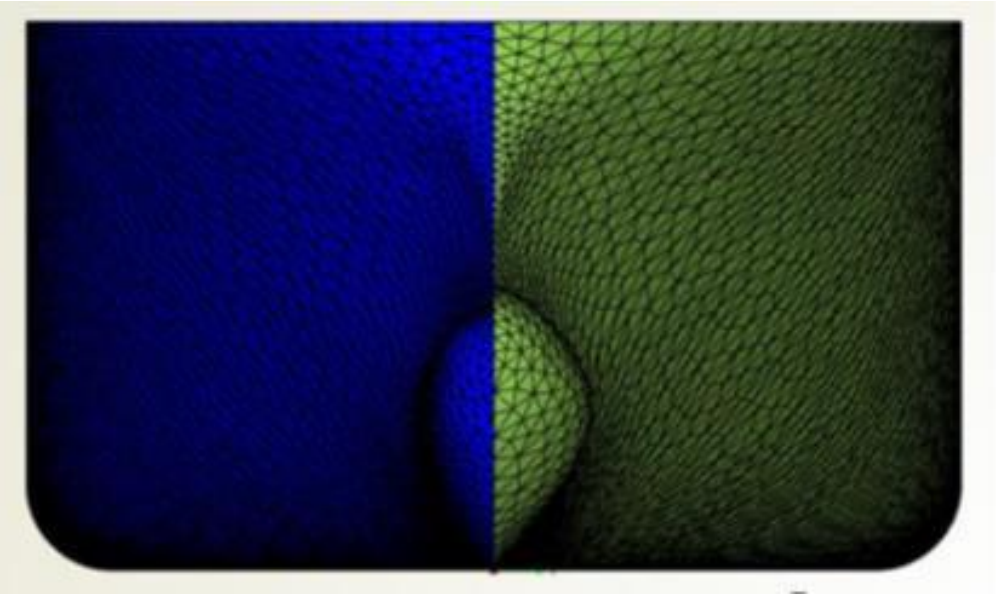

Figure- 13: Varying of bulbous bow shape by controlling design parameters in transverse direction [Initial mesh (left) and modified mesh (right)]

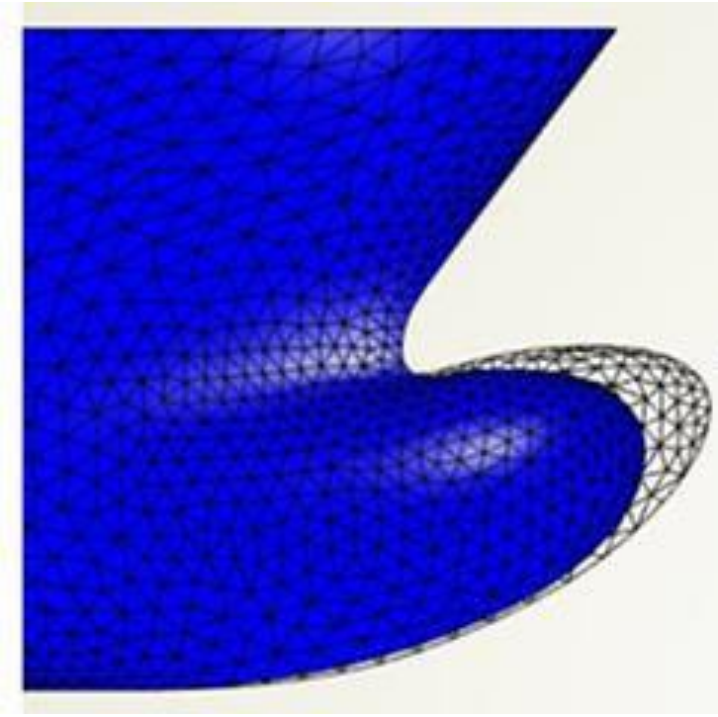

Figure- 14: Varying of bulbous bow shape by controlling design parameters in longitudinal direction [Initial meshes (blue) and modified mesh (grey)]

Appendix A1 show the study of each variable parameter affecting on the wave resistance and total resistance of the ship at the experimental speeds of 20 knots and 25 knots by using Direct Search Method. From the results shown in Appendix A1, finally, above 5 design variables were used in order to continue optimization process.

5. COMPUTATIONAL FLUID DYNAMICS (CFD) METHOD

In assessment of ship hull's hydrodynamic performance optimization, CFD solvers play an important role to compute the flow fields around the hull for different operation conditions. The accuracy, computation time and reliability are to be considered while choosing CFD solver for the optimizing process. There are a lot of effective, reliable and fast CFD tools for evaluating the numerical solution of wave flows. RANSE CFD solvers can obtain very accurate results. But, these tools require too much computational time when different operation conditions are to be considered. Furthermore, the more accurate and detailed methods, the more costly they are [see in Figure- 15]. Thus, it is very important to choose the CFD tool to be used in order to achieve well representing results for the study within the minimum cost possible.

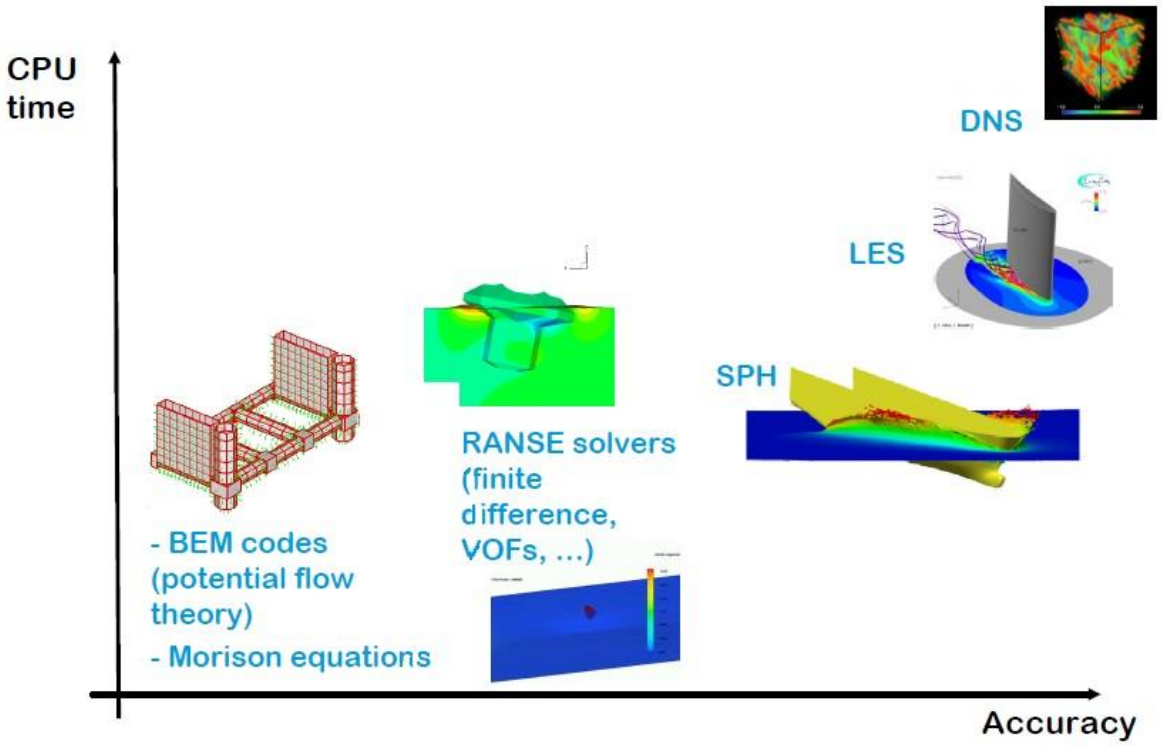

Figure- 15: CFD methods with their accuracy and CPU time (Ferrant (2013) [16])

At early design stage, potential flow code solvers are utilized practically. For the design task at hand, the most important objective was the wave making resistance of the hull at the considered speed. Rankine panel codes considering the nonlinear free-surface boundary condition are the standard tool of choice to assess wave making and support bulbous bow design. In Rankine Panel method, the source strength on each panel is adjusted to fulfil the various boundary conditions, namely zero normal velocity on the hull and kinematic and dynamic boundary

conditions on the water surface. The ship's dynamic floating position and the wave formation are computed iteratively. After each iteration step, the geometry of the free surface is updated and the sinkage, trim, heel are adjusted. The calculations are considered to be converged when all forces and moments are in balance and all boundary conditions are fulfilled. Having determined the source strengths, the pressure and velocity at each point of the flow field can be calculated. The wave resistance can be computed by integrating the pressure over wetted surface of the hull.

In potential flow theory, viscous effects such as a recirculation zone at the stern cannot be calculated correctly. However, in hull optimization studies, the focus is on the forebody, to be precise, on the bulbous bow shape where potential flow approximates the real conditions well. The total resistance is predicted on the basis of the non-viscous resistance components from the CFD simulation and an estimate of the viscous components by the ITTC method which may optionally be based on local flow properties, or by an accompanying boundary layer computation.

In this case, potential flow code GL Rankine developed by DNV-GL was used to calculate the wave resistance and total resistance in steady flow computation and added resistance in waves for seakeeping analysis.

5.1. GL Rankine Solver

The program GL Rankine can be used for the following computations [18]:

- resistance in calm water, taking into account shallow water and channel walls
- dynamic squat in calm water, taking into account shallow water and channel walls
- linear transfer functions of ship motions in regular waves
- sectional loads, relative motions and accelerations in waves
- mapping of pressure distributions onto nodes of a finite-element mesh
- hydrodynamic interaction of ships with the same forward speed and course

5.1.1. Use of GL Rankine Solver

Since GL Rankine solver does not have Graphical User Interface (GUI), it has to be run with executable xml file, which is called config.xml or other arbitrary name, in the command line. This file includes all the command for computation and input and output files such as geometry of hull form or result files.

Firstly, a body part surface is exported by CAESES as a watertight trimesh hull without deck and transom stern in STL format. The triangles should be small enough to resolve the ship geometry.

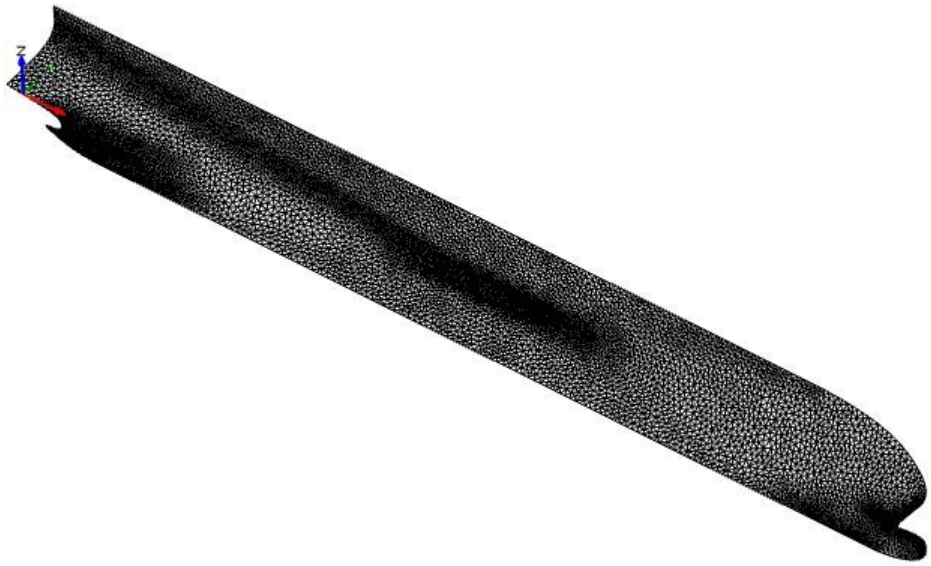

Figure- 16: Typical STL triangular grid of a ship half

After importing triangular grid surface of a ship half, the panel grid generation was done. It is needed to generated the unstructured grid on the body surface properly to resolve steady wave resistance and at slow speed, the amount of panels is typically about 4000 on one side of the submerged body. But, the structured quadrilateral grid for free surface can be generated automatically based on the ship size and speed. For Froude number smaller than 0.15, it is quite difficult to obtain the convergent solution by this method.

The body panel generation was done by using the factors; 'lMid', 'lBow', 'lAft', 'zAft' and 'zBow' [details can be seen in user manual]. The variation of the height of panel grid above the waterline at bow and aft region (zAft and zBow) should be careful since it is proportional to stagnation height, $z= u^2/2g$ for non-linear steady simulation where 'u' is the forward ship speed. The other parameters such as relaxation factor and wave damping factor that effect on convergence of the iteration will be kept as default values.

The unstructured panel grid on the ship hull consists of triangles covering the wetted surface up to the steady flow waterline. The panel grid on the ship's hull is used both for steady flow and seakeeping computations; the panel grid on the free surface is automatically adapted to the characteristic wave lengths of the problem.

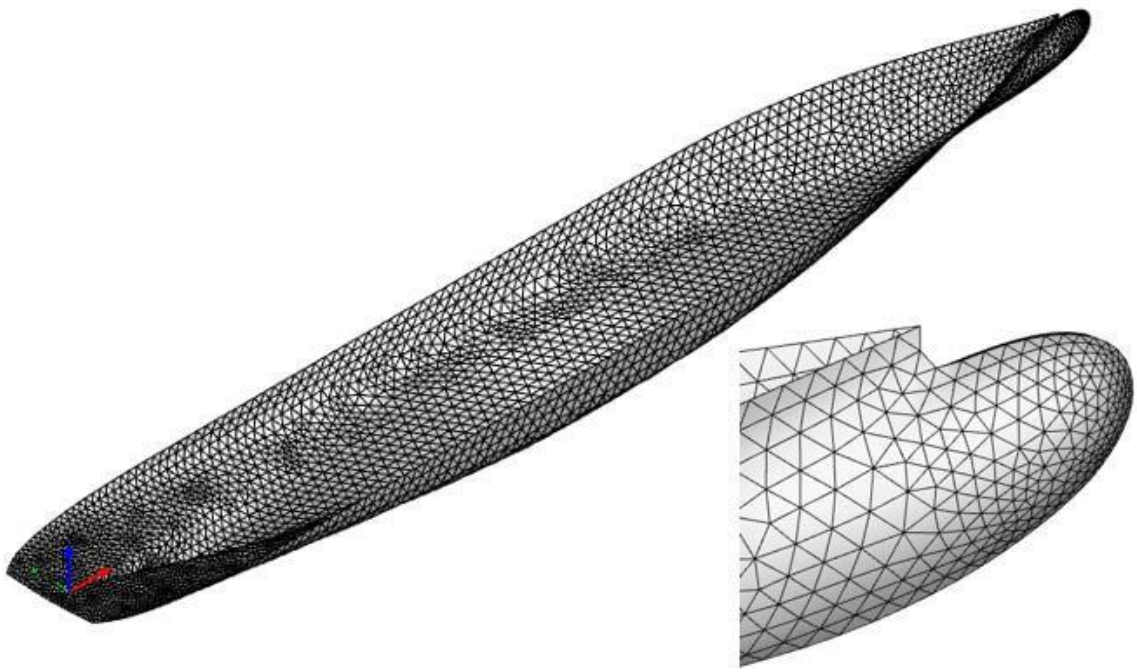

Figure- 17: Typical panels generated by GL Rankine on a STL surface

After the panel grid generation for the hull underwater surface, the rectangular panel grids generation of free surface was created automatically depending on the ship size and forward speed.

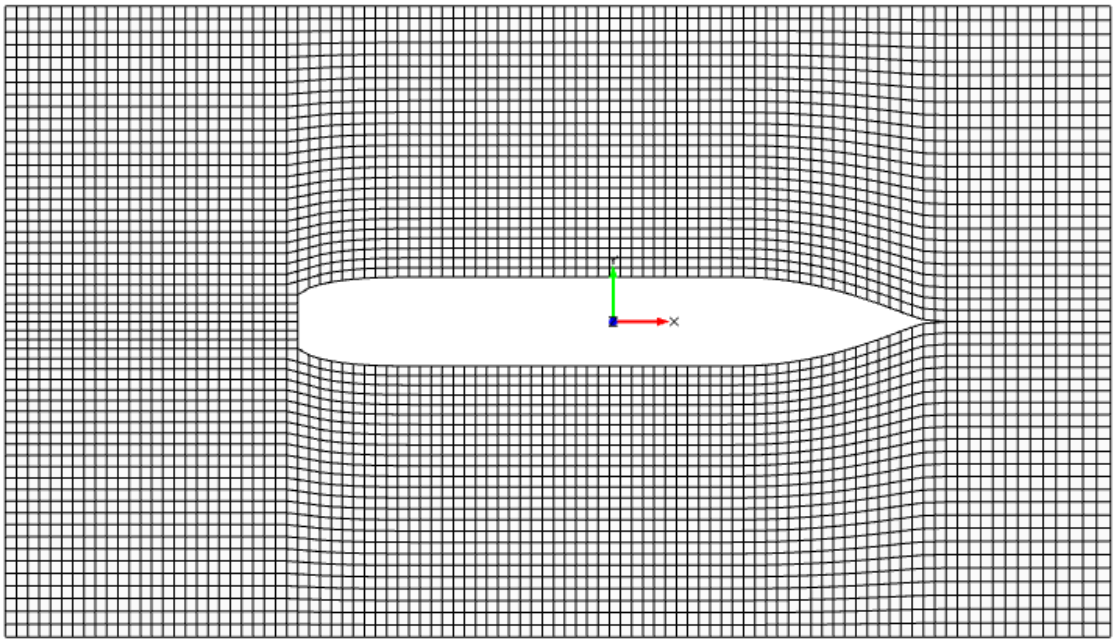

Figure- 18: Automatically created structured free surface mesh in GL Rankine depending on speed

The nonlinear part of GL Rankine predicts the steady flow around a ship using nonlinear free surface condition. The fluid is assumed to be inviscid, incompressible and irrotational. Therefore a velocity potential exists, which has to fulfil the Laplace equation (conservation of mass) as well as kinematic and a dynamic boundary conditions on the free surface ('no flow through the surface' and 'atmospheric pressure at the surface', respectively).

Because the free surface boundary condition is nonlinear an iterative solution is required. An under relaxed Newton-like iteration for the residuum is used. After determining the potential, the forces and moments acting on the ship are computed by integration and obtained the wave resistance, frictional resistance (calculated by ITTC 1978) and total resistance of the vessel in calm water condition.

For motion in waves, forces and moments acting on the ship surface depends linearly on the incoming wave amplitudes for this method in linear response computation. By superimposing the potential from the stationary problem and the potential of periodical flow which oscillates with the wave frequency, the total potential needed for seakeeping analysis is calculated.

The method GL Rankine calculates ship motions and loads in waves, taking into account interaction between the steady flow at constant forward speed and the periodic flow in waves. The method is based on the linearization of the flow and ship motions due to incoming waves with respect to the nonlinear steady flow produced by the ship motion in calm water with constant speed, taking into account ship wave and dynamic squat. Therefore, seakeeping computations are preceded by the solution of the steady flow problem.

The seakeeping contributions, considered up to first order, depend linearly on wave amplitude, while the steady flow solution is fully nonlinear with respect to free surface deformations, dynamic trim and sinkage and all boundary conditions. In addition, quadratic transfer functions (i.e., forces and moments proportional to wave amplitude squared) are computed to obtain added resistance and side drift force in waves.

The detailed explanation about how to coupled GL Rankine software connector with CAESES was omitted in this thesis. The set up input XML file for steady flow computation and seakeeping computation are shown in Appendix A2.

After the set-up for GL Rankine coupled with CAESES is done, detailed analysis of initial base design has to be performed such as implying grid variation studies, convergence test and accuracy check for the CFD analysis with experimental data in both calm water and in waves.

The results for each analysis can be seen in the sections 5.2 and 5.3.

5.2. Mesh Dependency on Numerical Results

In this part, the variation of C_W coefficients in base model for Froude numbers of 0.174, 0.200 and 0.218, which correspond with ship speed of 20 knots, 23 knots and 25knots respectively, will be checked for different hull grids. While changing the hull grid parameters, only the grid length at the bow, mid and aft region will be changed. The variation of the height of panel grid above the waterline at bow and aft region should be careful since it is proportional to stagnation height, $z= V^2/2g$ for non-linear steady simulation. The other parameters such as relaxation factor and wave damping factor that effect on convergence of the iteration will be kept as default values.

Table - 2: Variation of grid parameters

Parameters	**mesh 1**	**mesh 2**	**mesh 3**	**mesh 4**	**mesh 5**
lMid	5	4	4	3.5	3
lBow	3	3	2.5	2.5	2
lAft	3	3	2.5	2.5	2

According to GL Rankine user manual, zAft = min (0.3 z, lAft) and zBow = min (0.5z to 1.0z, lBow), where LAft = approximate grid length at aft region, lBow= approximate grid length at bow region and $z = u^2/2g$. According to the variation of zAft and zBow for different Froude numbers, the number of panel generated of the hull is also different as shown in Table 3.

Table - 3: Number of Panels for Different Froude Numbers

	Number of panels				
Fn	**Mesh 1**	**Mesh 2**	**Mesh 3**	**Mesh 4**	**Mesh 5**
0.174	2204	2965	3383	3888	5374
0.200	2312	3008	3424	3943	5527
0.218	2299	3048	3409	4004	5527

The free surface mesh is generated by default parameter according to different forward speed. The free surface mesh around the hull for resistance calculation is generated as the structured rectangular mesh.

Table - 4: Wave resistance coefficients for different mesh

Cw x e4(-)	mesh1	mesh2	mesh3	mesh4	mesh5
Fn=0.174	1.3668	1.4863	1.4530	1.2277	1.2864
Fn=0.200	1.3753	1.3065	1.4516	1.2307	1.1362
Fn=0.218	1.8082	1.8784	2.1613	1.9535	1.4200

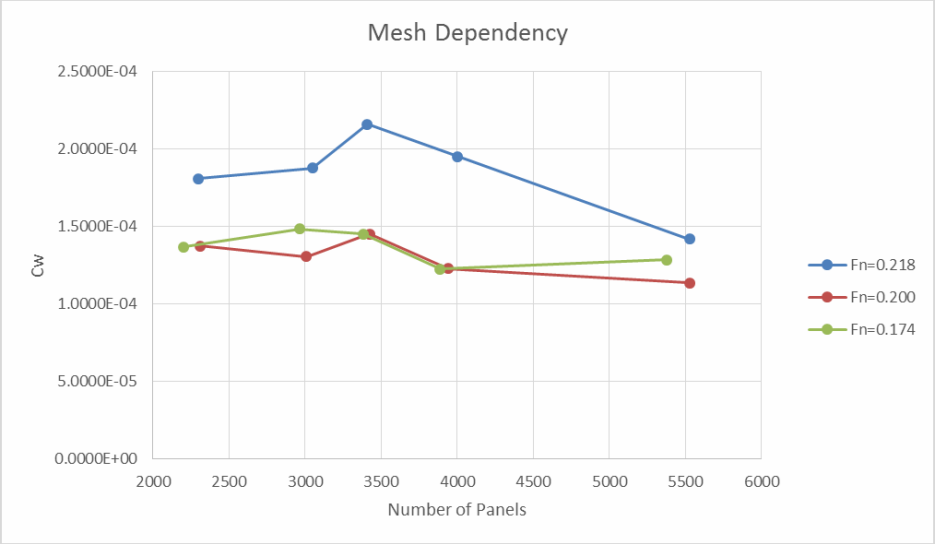

Figure- 19: Mesh Dependency for different Froude Numbers

While changing the mesh parameters, it should be noted that the maximum number of panels generated below waterline is 10000 as default. Table 4 and Fig.19 show the wave resistance coefficient for different mesh at Fr =0.174, 0.200, 0.218. It can be seen that the mesh dependency is quite sensitive to the numerical results of wave resistance coefficient obtained from GL Rankine solver.

For panel grid generation of the model, it should be nice to follow the standard recommendation such as 1% of LPP of ship for panel size in middle section and 0.7% for that in forward or aft section.

As summary, the final mesh of hull panel generation is chosen for **mesh 3** with **LAft, LBow = 0.7% of LPP = 2.5 m** and **LMid = 1% of LPP = 4m** [approximately 3500 panels on hull, approximate computation time= 15 minutes for each simulation in Intel® Core™ i5-3230M CPU @ 2.60GHz, RAM 4GB].

All the remaining works such as verification with experimental data and optimization processes will be done with the same mesh parameters [as shown above- mesh3].

5.3. Validation of Numerical Results with Experimental Data

After the mesh parameters analysis was done, the coupling of GL Rankine config file with CAESES was fixed and validated with the experimental results that are done in in the model test basins SVA Potsdam (resistance and propulsion tests), Nietzschmann (2010), and HSVA (roll decay tests), Schumacher (2011) in order to explore the accuracy of the results that come out from GL Rankine solver.

5.3.1. Description of Experiment

Duisburg Test Case (DTC) is a hull design of a modern 14000 TEU post-panamax container carrier, developed at the Institute of Ship Technology, Ocean Engineering and Transport Systems (ISMT). Although the hull form exists only as a virtual CAD model and as two models in different scales, the lines of the hull represent a typical hull form for modern post-panamax container vessels.

Table - 5: Particulars of model scale and full scale of DTC container vessel

	Symbol	Full Scale	Model Scale
Scale	λ [-]	59.407	
Length Between Perpendiculars	L_{pp} [m]	355.0	5.976
Waterline Breadth	B_{wl} [m]	51.0	0.859
Design Draft Amidships	T_{Dm} [m]	14.5	0.244
Moulded Depth	D [m]	32.0	0.538
Block Coefficient	C_B [-]	0.661	0.661
Volume Displacement	V [m^3]	173467.0	0.827
wetted surface under rest waterline without appendages	S_W [m^2]	22032.0	6.243
Transverse metacentric height	GM_T[m]	1.37	0.023
Vertical center of gravity	KG [m]	23.68	0.399
Height of metacenter above BL	KM_T [m]	25.05	0.422
Radius of gyration k_{xx}	k_{xx} [m]	20.25	0.341
Radius of gyration k_{yy}	k_{yy}[m]	88.19	1.485
Radius of gyration k_{zz}	k_{zz}[m]	88.49	1.490

5.3.2. Comparisons of Result Values for Calm Water Resistance

Resistance was measured at six forward speeds, corresponding to Froude numbers from 0.17 to 0.218 and full-scale advance speeds Vs from about 20.0 to 25.0 knots. The hull was ballasted at the design draft 14.5 m with zero trim, and was free in trim and sinkage. Tests were carried out at water kinematic viscosity = 1.09E-06 m^2 /s and density 998.8 kg/m^3.

Table 5 shows the experimental results referring to the model scale, including model speed V_m [m/s], Froude number, Reynolds number, total resistance R_T [N] and its non-dimensional coefficient C_T, frictional resistance R_F [N] and its non-dimensional coefficient C_F, and non-dimensional wave resistance coefficient C_W.

$$C_{Tm} = \frac{R_{Tm}}{0.5 \times \rho_m \times S_m \times V_m^2} \quad (1)$$

$$C_{Fm} = \frac{0.075}{(\log(Re_m) - 2)^2} \quad (2)$$

$$C_{wm} = C_{Tm} - (1 + k) \times C_{Fm} \quad (3)$$

The form factor k was found from a RANSE-CFD simulation for a double-body flow at the model scale as k = 0.094. By Froude number similitude, the coefficients of the residual resistances of the model scale and full scale are the same and therefore, C_w for full scale is obtained. By following the same procedure as the model scale, the total resistance coefficient of the full scale ship (C_{TS}) is achieved.

Table - 6: Results of resistance model tests

Vs (kn)	Vm(m/s)	Fn_m	$Re_m \times 10^{-6}$	$C_{Tm} \times 10^3$	$CF_m \times 10^3$	$C_w \times 10^4$	R_{Tm}(N)	R_{Wm}(N)
20	1.335	0.174	7.3198	3.6606	3.1695	1.9316	20.34	1.0733
21	1.401	0.183	7.6816	3.6049	3.1423	1.6714	22.06	1.0228
22	1.469	0.192	8.0545	3.5880	3.1160	1.7907	24.14	1.2048
23	1.535	0.200	8.4164	3.6019	3.0919	2.1935	26.46	1.6113
24	1.602	0.209	8.7837	3.6231	3.0687	2.6590	28.99	2.1276
25	1.668	0.218	9.1456	3.6695	3.0471	3.3594	31.83	2.9141

For the range of Froude numbers used in experimental data, the CFD simulations in GL Rankine for the final mesh panel hull and free surface are performed to compute non-dimensional resistance coefficients (C_T, C_F and C_W). The results are as follow in Table 7.

Table - 7: Results of GL Rankine Simulations

Parameters	Base Model simulation with final mesh					
Vs [knots]	20	21	22	23	24	25
lMid[m]	4	4	4	4	4	4
lBow [m]	2.5	2.5	2.5	2.5	2.5	2.5
lAft [m]	2.5	2.5	2.5	2.5	2.5	2.5
zBow [m]	2.5	2.5	2.5	2.5	2.5	2.5
zAft [m]	1.62	1.78	1.96	2.14	2.33	2.5
no. of panels	3383	3339	3346	3424	3323	3409
FS no. of panels	2503	2142	1809	1504	1296	1058
Trim(degree)	0.056	0.065	0.074	0.083	0.09	0.1
Sinkage(m)	-0.235	-0.262	-0.292	-0.322	-0.355	-0.389
Wetted surface(m^2)	22077	22078	22084	22087	22097	22109
Cw $\times 10^4$	1.4530	1.2799	1.3522	1.4516	1.5874	2.1613

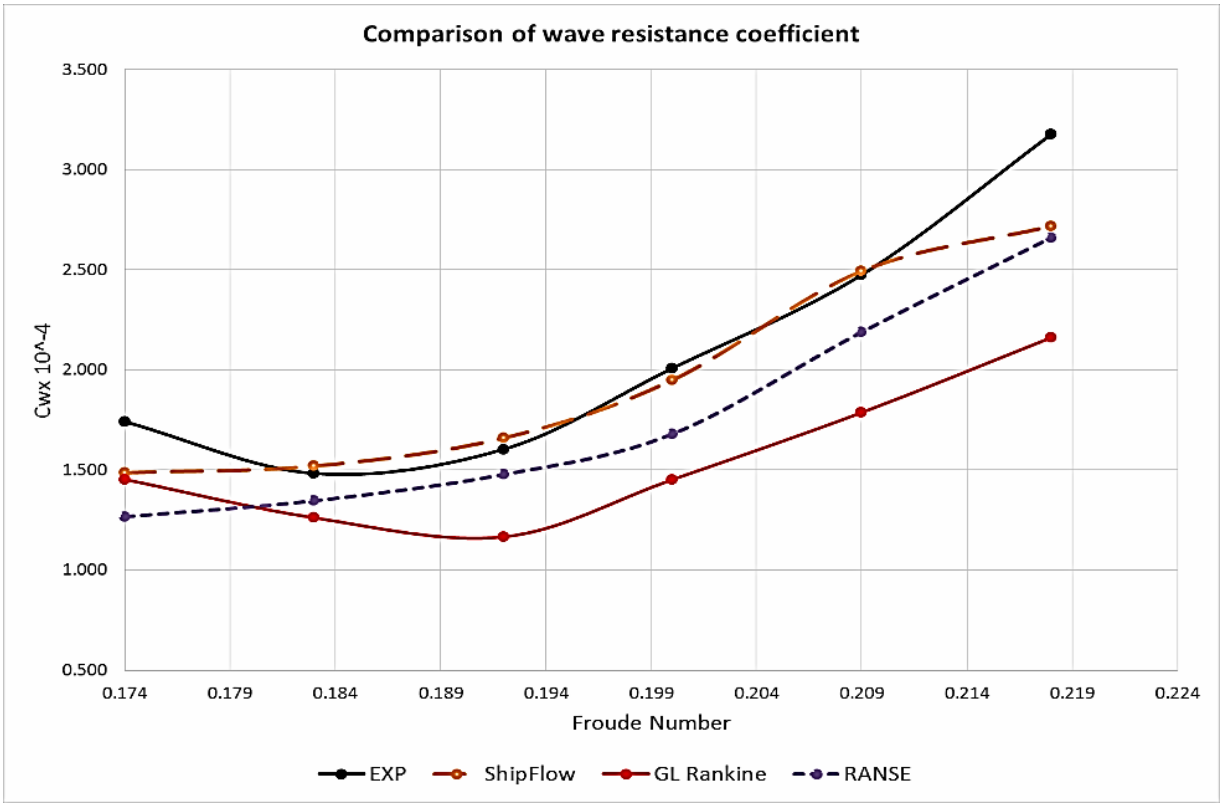

Figure- 20: Comparison of Wave Resistance Coefficients (Cw)

The comparison of the numerical results simulated by GL Rankine and the experimental results performed by HSVA are described along with the results obtained from ShipFlow and RANSE simulations in Fig.20. It can be seen that the numerical simulation was done for 6 different forward speeds and its curve shows the same curvature as experimental data.

In order to compare the total resistance of the vessel in calm water condition, the form factor of k= 0.117 (obtained from University of Duisburg, Personal Communication) was used for full scale.

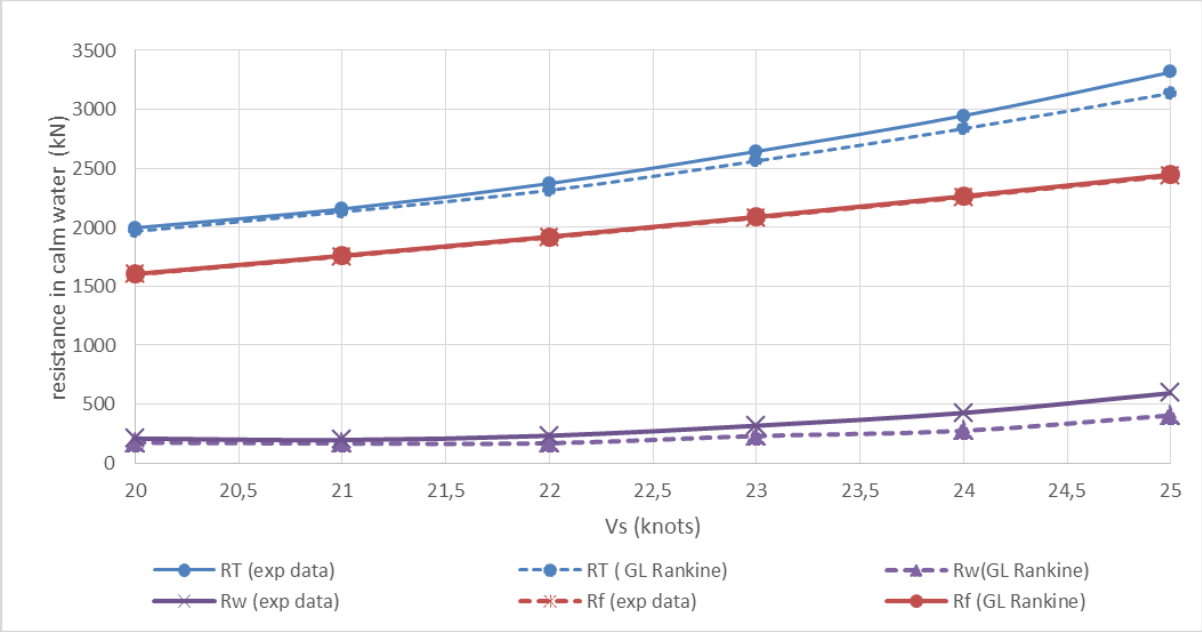

Figure- 21: Comparison of resistance in calm water condition

The frictional resistance has small variation due to the difference of the wetted surface area and also for the wave resistance. By using k=0.117, the total resistance at 20 knots has the decrement of 1.5% in numerical results compared to that in experimental results, while the total resistance at 25 knots is reduced 6% in simulation. These differences are in the range of acceptable limit and it can be said that GL Rankine has the relevant accuracy.

5.3.3. Comparisons of Result Values for Wave Added Resistance

Model tests for added resistance in waves use either self-propelled or towed models. Self- propelled models eliminate the influence of the towing equipment on model motions; however, the influence of motions and waves on the thrust deduction factor (required to estimate the added resistance) remains a factor of uncertainty. Towed models have either restrained surge motion or they are connected by soft springs to the towing carriage. Restraining the surge motion may influence added resistance, especially if it interferes with

pitch and heave motions. Thus, the arrangement with springs appears more appropriate. Another difficulty with experiments for added resistance in waves is that added resistance (average longitudinal force over time) is small compared to the amplitude of force variations. Thus, errors in measuring these forces might be comparable to or even exceed the average force itself. Further, added resistance is sensitive to the quality of wave generation and wave measurement, especially in short waves, because, unlike linear reactions, added resistance depends on wave amplitude squared [5].

The towing test in regular waves was performed at the draught of 14.5 m with a DTC model at the speed of 16 knots. The wave added resistance (R_{AW}) is achieved by extracting the calm water resistance from the total resistance of the model in waves. The transfer function and the non-dimensional coefficient of the wave added resistance are computed by using the Equations. 4 and 5. Assuming the wave added resistance coefficients of both model and full scale ship are the same, the transfer function of wave added resistance of the DTC is obtained by using the same equations as in model scale.

$$\text{Transfer function of } R_{AW} = \frac{R_{AW}}{\zeta_a^2} \tag{4}$$

$$\text{Non} - \text{dimensional added resistance coefficient} = C_{AW} = \frac{R_{AW}}{\rho.g.(\frac{B^2}{Lwl})\zeta_a^2} \tag{5}$$

The following result table shows the added resistance coefficient obtained from Experiments and RANSE CFD results using Comet for design draft 14.5m at 16 knots forward speed [Sebastian, personal communication].

Table - 8: DTC added resistance coefficient results

DTC Added Resistance Coefficient

lambda/L	Amplitude	CFD_CAW	EFD_CAW
0.220	0.025	2.062	1.889
0.280	0.049	1.755	1.523
0.360	0.068	1.910	1.671
0.440	0.095	2.099	1.953
0.600	0.059	2.639	
0.800	0.078	4.488	
0.910	0.071	5.245	4.757
1.000	0.080	4.970	4.642
1.090	0.088	4.401	4.377
1.200	0.080	3.541	
1.400	0.100	2.328	
1.800	0.100	1.048	
2.500	0.100	0.395	

For the numerical results, the simulation is done by GL Rankine solver with the same wave amplitudes as the experiment in head waves (180˚). The comparison is shown in Fig. 22 for the speed of 16 knots at T=14.5m, describing the wave added resistance (C_{AW}) versus the ratio between wavelengths of incoming waves to ship length waterline.

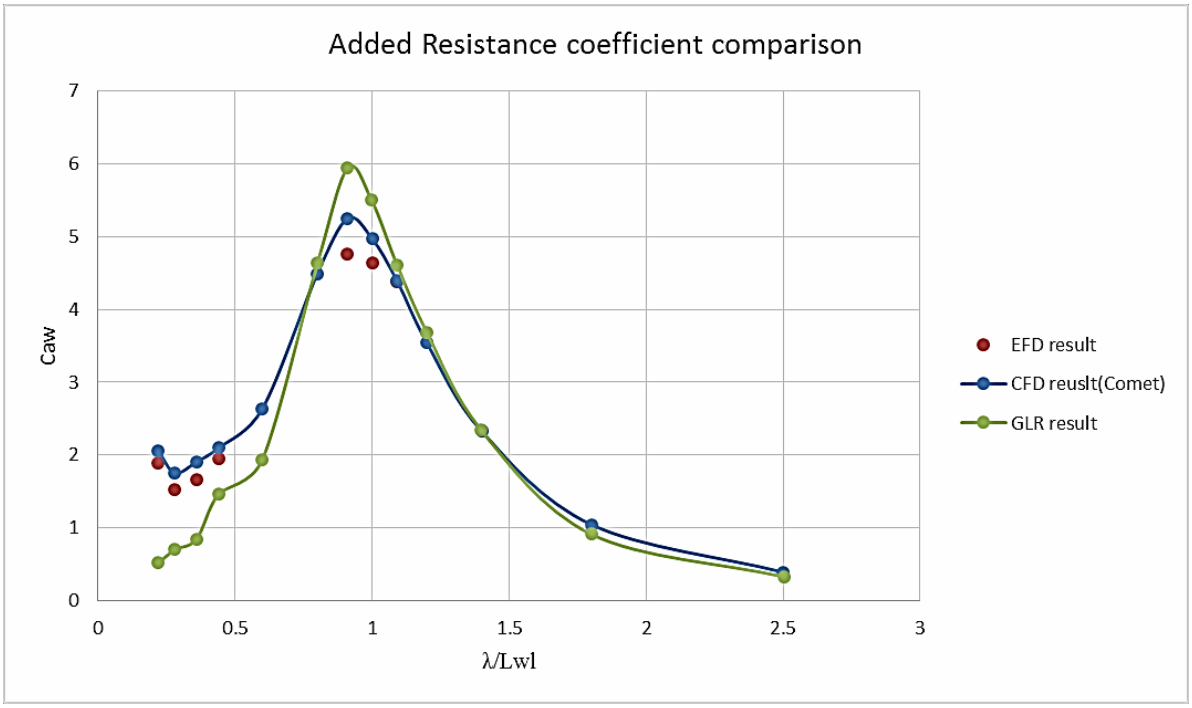

Figure- 22: Comparison of added wave resistance coefficient (T=14.5m, Vs = 16 knots)

It is observed that the large difference between results of the test evaluations, especially in short waves. The RANSE computations are quite similar to experimental results and to the results of the potential code in medium and long waves. But they show relative errors in the short waves region. This demonstrates the inherent difficulty to obtain reliable estimates of added resistance in short waves.

The trends for the results have a certain amount of similarity. The potential flow solver GL Rankine can deliver inaccurate results, especially for full hull forms and short waves, for which the added resistance is increasingly affected by the viscous effects. The potential flow theory based GL Rankine method is preferred over RANS code with respect to the computational effort.

6. OPTIMIZATION PROCESSES IN CALM WATER CONDITION

Marine designs have different features with complex shapes. In order to get the best design, optimization becomes to play an important role. However, it takes a lot of computational time and costly. Therefore, performing optimization tasks should be done with effective algorithms without doing any experiments. Nowadays, with the numerous optimization methods, thousands of designs can be simulated and optimized in a short time. In this section, optimization process in calm water condition, calculating the total resistance of the ship will be done with different methods. While performing optimization, the objective functions are to minimize total resistance at the design draft of 14.5m with two operating speeds of 15.5 knots and 18 knots as already explained in Section 3.2.

6.1. Design of Experiments

In this part, the optimization processes applied to perform a study of the design space. Usually the Design of Experiments (DoE) is driven by a random or quasi-random process (SOBOL in CAESES) and it has a big importance as well to drives the optimization process towards the global optimum and not to local minimum when performing deterministic optimization process. Designers can determine simultaneously the individual and interactive effects of many factors that could affect the output results of the design with DOE as illustrated in Figure- 23.

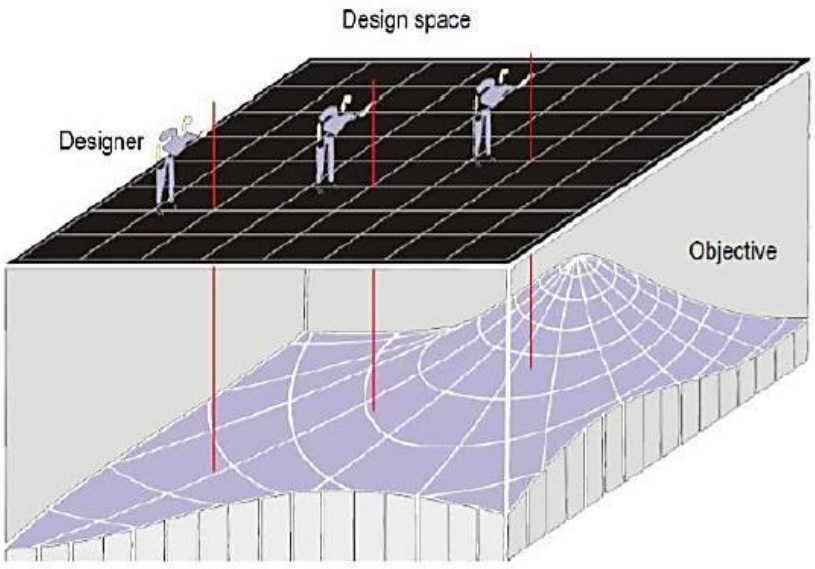

Figure- 23: Exploration of Design Space [23]

Appendix A3 shows the sampling of design space obtained from SOBOL with 150 designs in order to get the feasible design with all ranges of design variables. With these results from design of experiment, the best design can be selected and on it, the optimization method performed.

6.2. Single Objective Optimization

For single objective optimization process, Local Optimization Efficient method in CAESES/ Dakota interface was used starting from the initial design selection from Design of Experiments (SOBOL). This method is surrogate-based local optimization. For the initial surrogate model, data is taken from Design of Experiments. During the run, the surrogate model is iteratively fine-tuned: the optimum design from the local search is evaluated and the information is added to the surrogate model – which step by step increases the quality of the model.

1st Case - minimize total resistance at V=15.5knots at design draft of 14.5m

The Figure 24 presents the results for the optimization process together with the designs obtained on the DoE study, displayed by their indexes (order of creation) and in the ordinate is the difference in total resistance (%) relative to the base model.

$$Difference\ in\ R_T(\%) = \frac{Design\ R_T - Base\ R_T}{Base\ R_T} \times 100\% \quad (6)$$

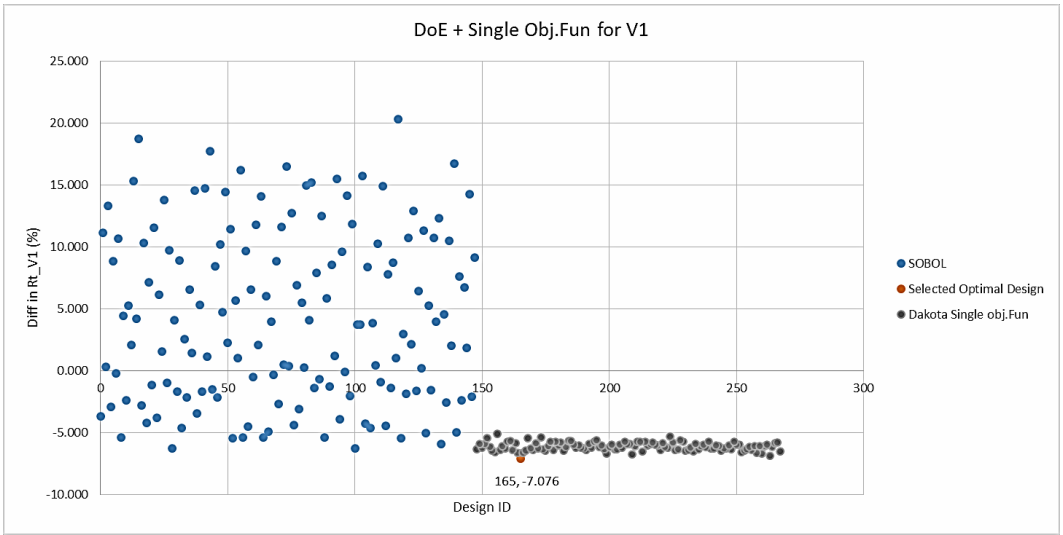

Figure- 24: Single objective optimization at 15.5 knots

The optimized model for V_1=15.5 knots was chosen from Dakota single objective optimization process and it was named SO_V15.5 which stands for single objective optimization for 15.5 knots. It has the reduction in total resistance, where the viscous effects are estimated from GL Rankine, of 7.08% related to the base model. The optimized geometry has a longer and narrower bulb as can be observed in Figure-27. Furthermore, the bulb tip elevation becomes higher and the entrance angle becomes a bit wider than the base model.

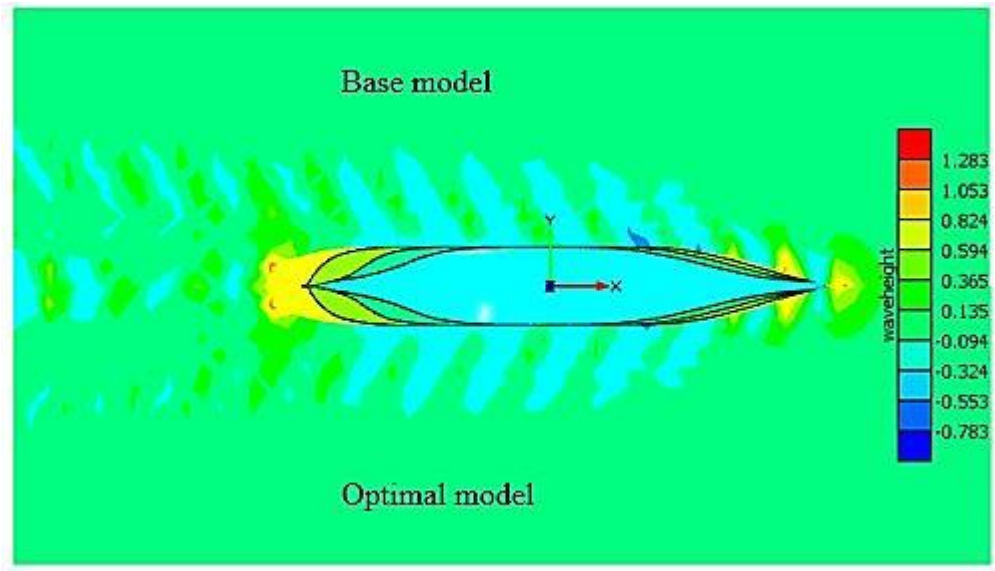

Figure- 25: Wave height comparison between Base model and optimal model

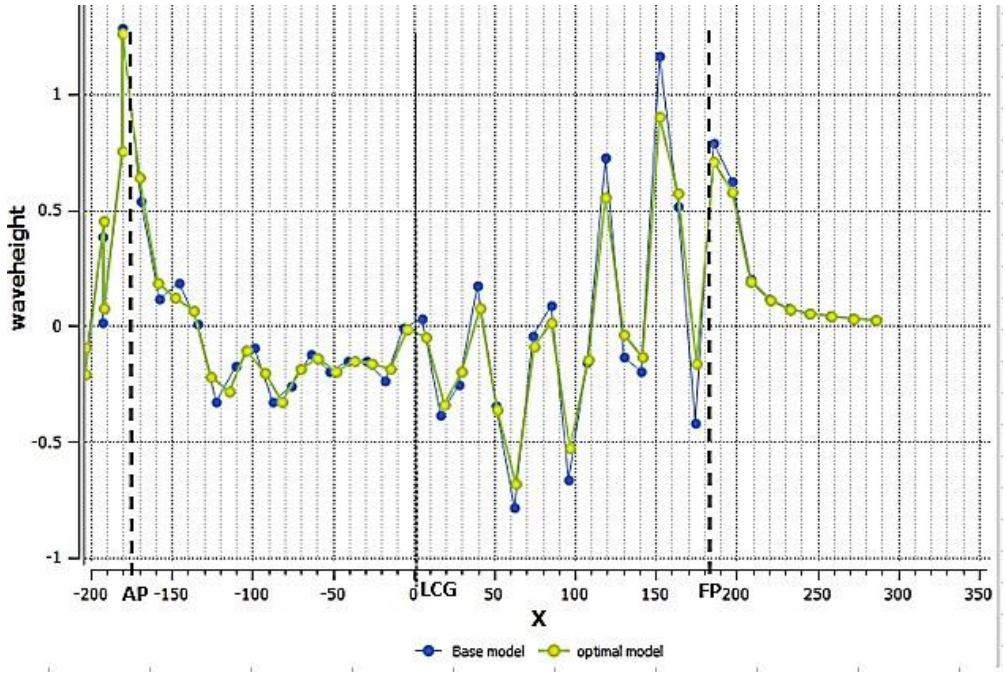

Figure- 26: Wave profile comparison between base and optimal model (V=15.5 knots)

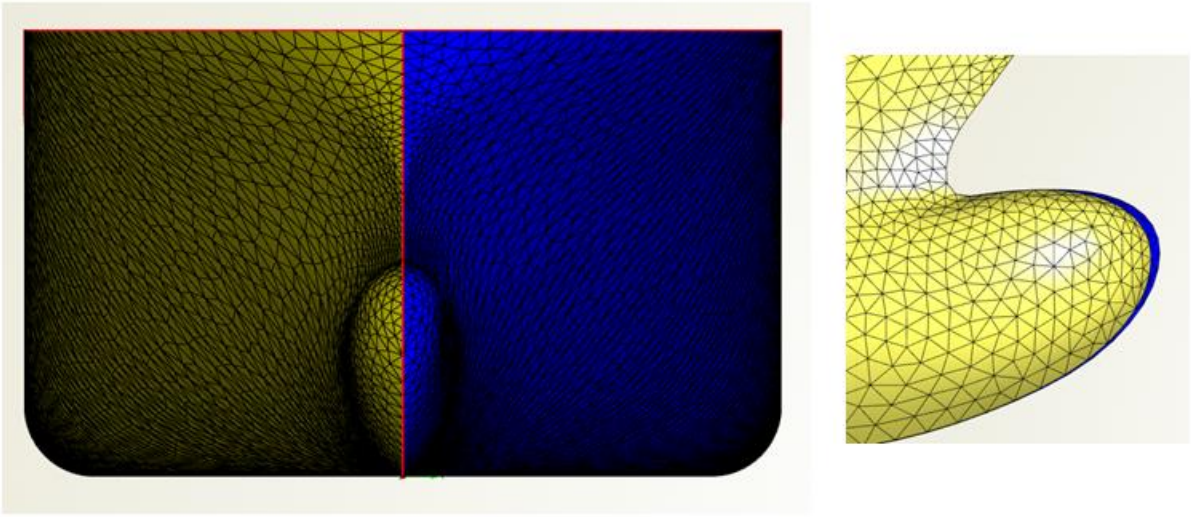

Figure- 27: Base model and optimal model comparison (V =15.5 knots)

(initial mesh – yellow and optimal model mesh- blue)

2nd Case - minimize total resistance at V=18 knots at design draft of 14.5m

The same procedure is applied to optimize the model at 18 knots with Dakota/ Local optimization efficient strategy. Figure-28 presents the results for the optimization process together with the designs obtained on the DoE study, displayed by their indexes (order of creation) and in the ordinate is the difference in total resistance (%) relative to the base model for 18 knots.

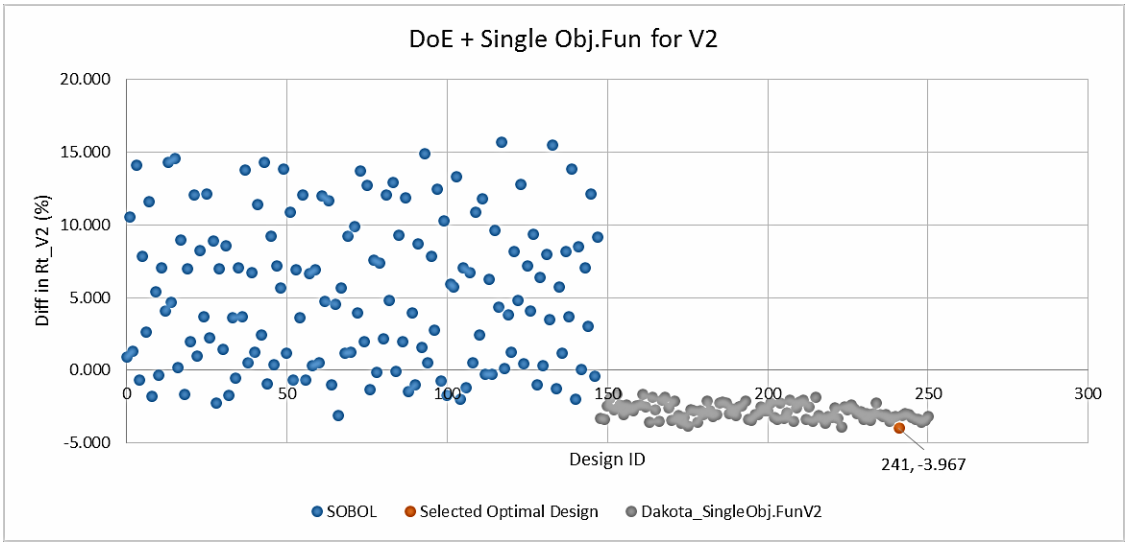

Figure- 28: Single objective optimization at 18 knots

In comparison with based model, the optimal model for V=18 knots has a reduction of 3.97% in total resistance of the ship. The optimized geometry has a bit shorter and narrower bulb as can be observed in Figure-30. Furthermore, the bulb tip elevation becomes higher and the entrance angle becomes wider than the base model.

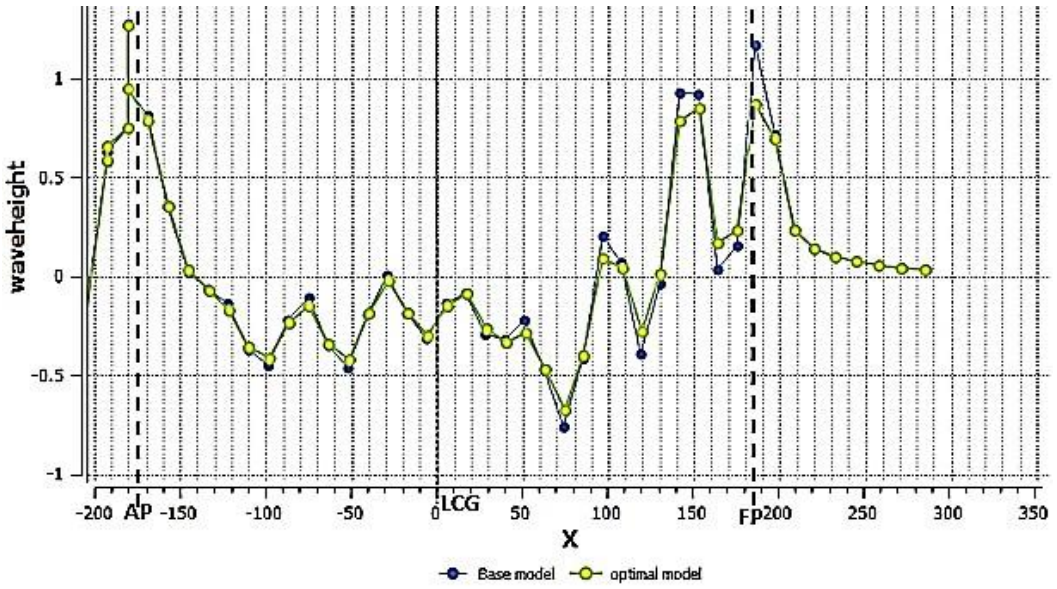

Figure- 29: Wave cut comparison between base and optimal model (V=18 knots)

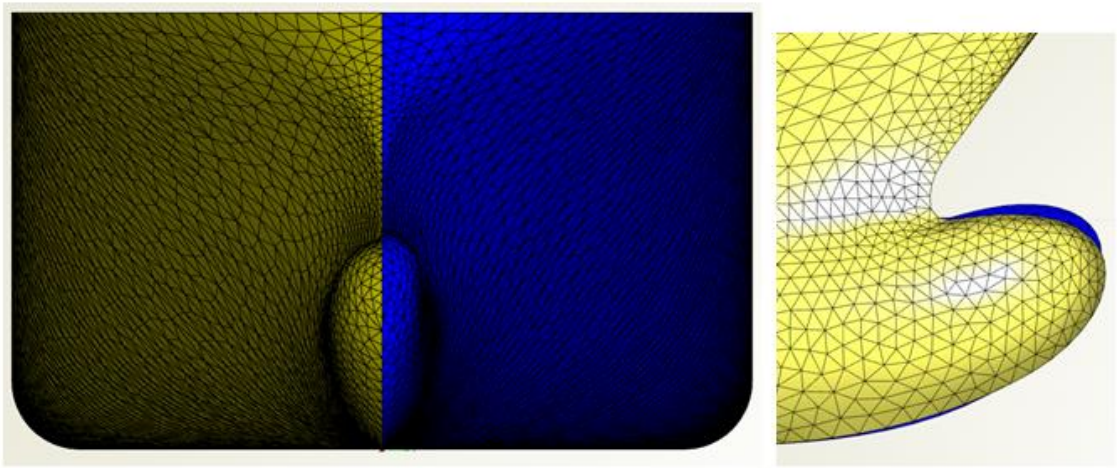

Figure- 30: Base model and optimal model comparison (V =18 knots)

(initial mesh – yellow and optimal model mesh- blue)

When comparing both models, optimized for V_1 and V_2 in both operating conditions, the results can be observed as following in Figure- 31.

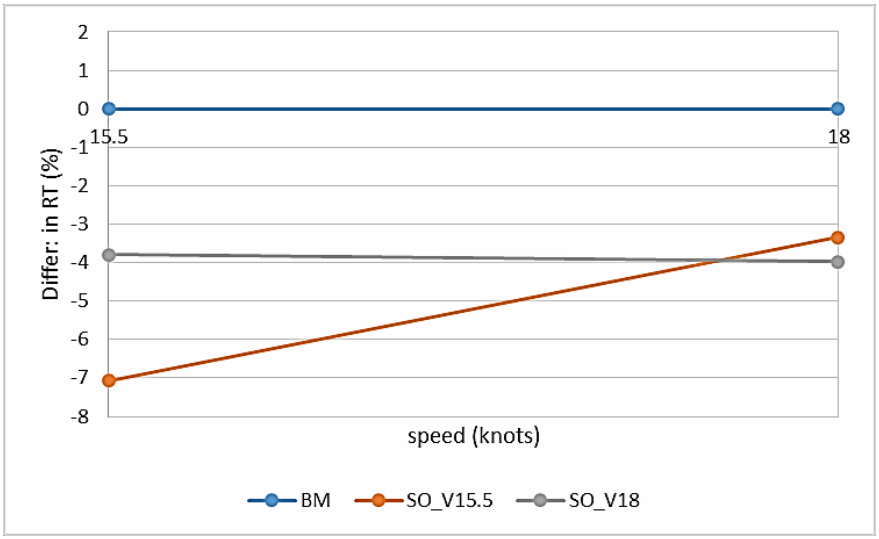

Figure- 31: Comparison of Single objective optimization for 15.5 knots and 18 knots

6.3. Single Objective Optimization with Weighted Functions

Multi-objective optimization can be performed by using the weighted function in the single objective optimization functions. For the consideration of two different operational conditions as objective function on the optimization process, several techniques were used where the conditions are defined by the variation of the velocity (V_1= 15.5 knots and V_2= 18 knots). A single objective optimization was performed in each case by surrogate-based local optimization method and the multi-objective function (MoF) is defined as following:

$$MoF = \alpha \times R_{TV1} + (1-\alpha) \times R_{TV2} \quad (6)$$

Where, R_{TV1} and R_{TV2} are total resistance at the speeds of V_1= 15.5 knots and V_2= 18 knots respectively and α is the weight function coefficient ($0<\alpha < 1$).

If α = 0 or α = 1, it is a single objective problem where only one condition is considered and the results would be similar to those observed previously in Section 6.2. Three different values for the weight coefficients were considered:

i. α = 0.25
ii. α = 0.50
iii. α = 0.75

6.3.1. α = 0.25

The weight of 0.25 means that 25% for the objective function is due to the resistance of the vessel at velocity V_1 and 75% related to the resistance of the vessel at velocity V_2. It can also be observed that the total resistance is reduced by 5.71% at 15.5 knots and 3.75 % at 18 knots compared to the base model.

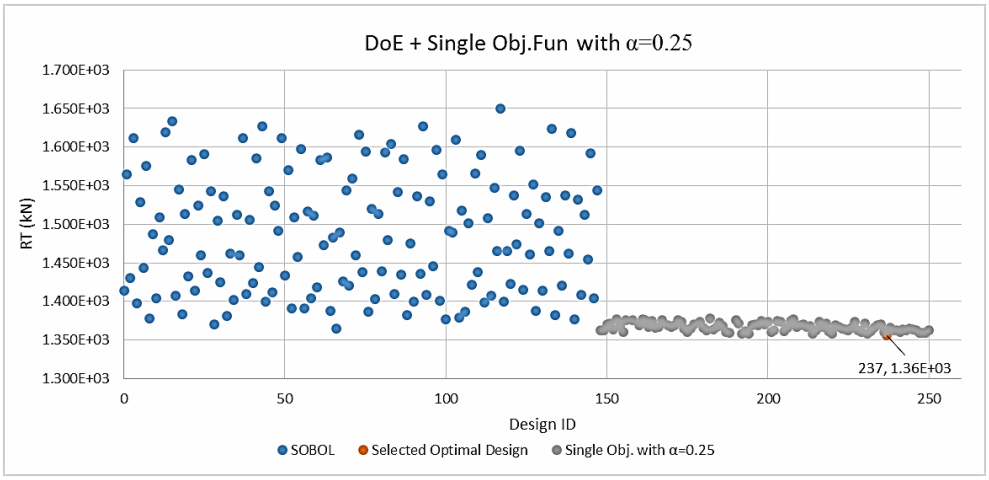

Figure- 32: Single objective optimization with α= 0.25

6.3.2. α = 0.50

The weight of 0.50 means that 50% for the objective function is due to the resistance of the vessel at velocity V_1 and 50% related to the resistance of the vessel at velocity V_2. The total resistance of the selected optimal model is reduced by 6.97% at 15.5 knots and 3.923 % at 18 knots compared to the base model.

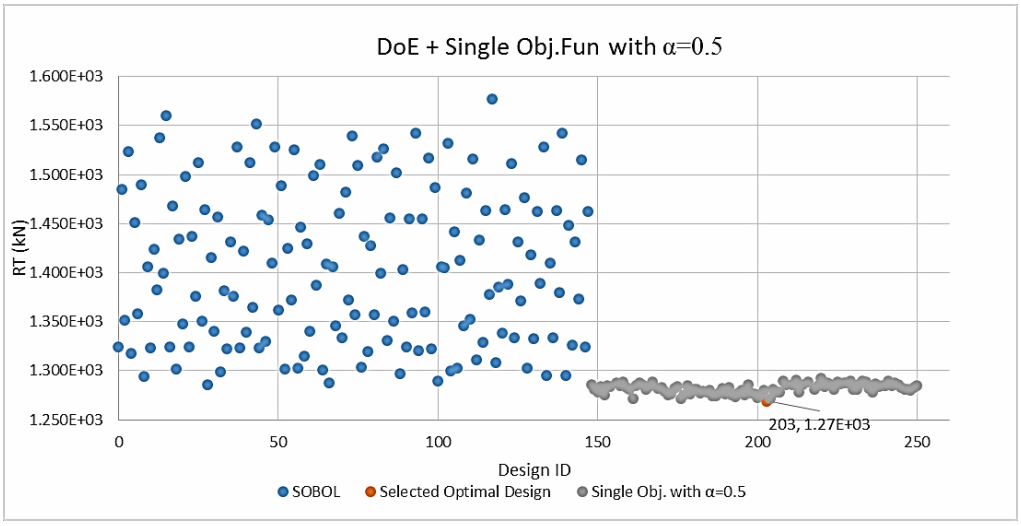

Figure- 33: Single objective optimization with α= 0.50

6.3.3. $\alpha = 0.75$

The weight of 0.75 means that 75% for the objective function is due to the resistance of the vessel at velocity V_1 and 25% related to the resistance of the vessel at velocity V_2. The total resistance of the selected optimal model is reduced by 7.00% at 15.5 knots and 3.91 % at 18 knots compared to the base model. It means that as the weight function coefficient used for V_1 is increased, the reduction % of total resistance in V_1 related to base model is also increased.

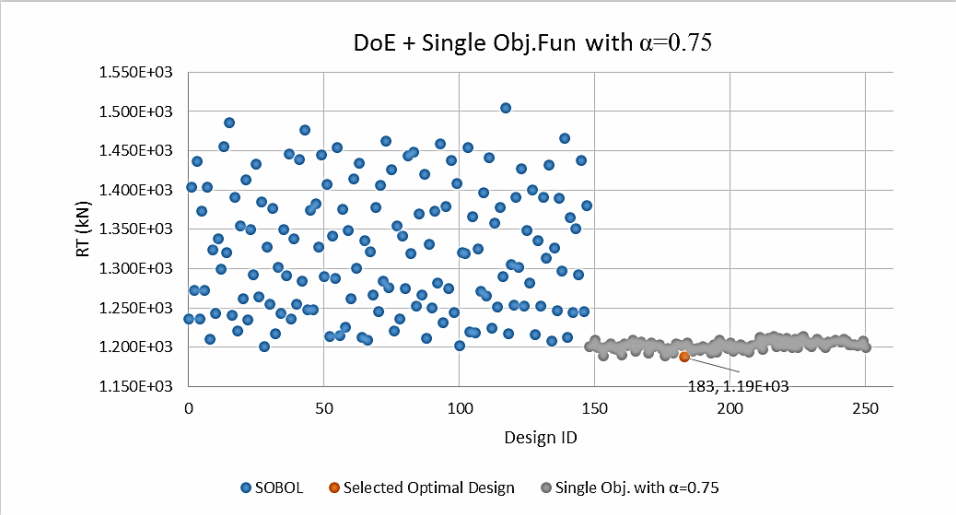

Figure- 34: Single objective optimization with α= 0.75

Table - 9: Result summary for single objective optimization processes

		V(knots)	15.5		18	
			R_{TV1} (kN)	Diff (%)	R_{TV2}(kN)	Diff(%)
		Base model	1190.31	-	1489.08	-
SO_V18	α=0	Obj.fun: $(0\times R_{TV1}) + (1\times R_{TV2})$	1145.08	-3.80	1430.01	-3.97
SO_α_0.25	α=0.25	Obj.fun: $(0.25\times R_{TV1}) + (0.75\times R_{TV2})$	1122.40	-5.71	1430.28	-3.75
SO_α_0.50	α=0.50	Obj.fun: $(0.5\times R_{TV1}) + (0.5\times R_{TV2})$	1107.34	-6.97	1430.67	-3.92
SO_α_0.75	α=0.75	Obj.fun: $(0.75\times R_{TV1}) + (0.25\times R_{TV2})$	1106.89	-7.01	1430.89	-3.91
SO_V15.5	α=1.00	Obj.fun: $(1\times R_{TV1}) + (0\times R_{TV2})$	1106.08	-7.08	1439.44	-3.33

It can be observed in Table 9 that when varying the weight for R_{TV1}, the higher is the weight, the better is the improvement regarding to reduce total resistance at V1=15.5 knots. In addition, the weighted method possible the optimization of the vessel for multiple objectives (Minimization of R_{TV1} and R_{TV2}), while using the surrogate-based local optimization method.

6.4. Multi-objective Optimization

In general, there is no design in which all the functions are minimal as there is no unique optimum design to a multi-objective optimization problem. However, there is a set of points that represents the best compromise between the various objectives called Pareto Frontier. Genetic algorithms are used to perform multi-objective optimization.

In this work, the surrogate-based global optimization strategy was used for multi-objective optimization process in CAESES with Dakota. The advantage of this method is the speed of the convergence of the design objective functions.

The multi-optimization process was performed for 350 designs in which 30 designs were chosen as the samples for initial surrogate model. The process took 5 days approximately running in a computer with the processor of Core ™ i7-2760QM CPU @ 2.40 GHz, RAM 8GB.

The template of Dakota surrogate based global optimization in accordance to the recommendation of the specialist and developers of the CAESES for this study can be seen in Appendix A4.

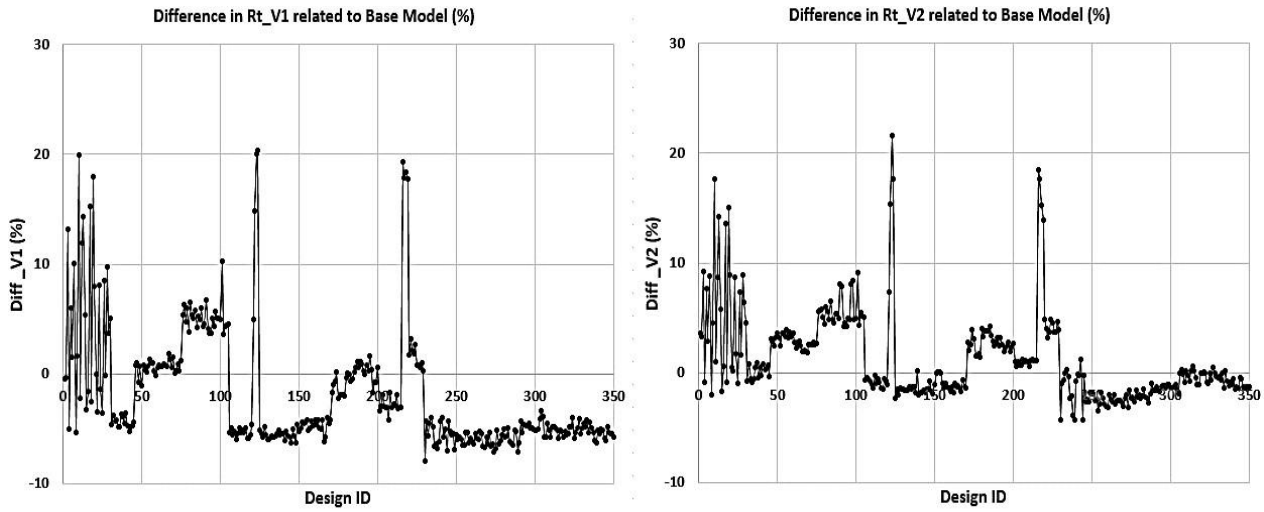

Figure- 35: Convergence study of surrogate based global optimization

Finally, the results for the multi-objective optimization by means of genetic algorithms with surrogate modal can be seen in Fig. 36. In Fig.37, the same results are presented with a zoom in the area of interest, designs that have reduced resistance when compared to the base model (negative values in the graphic). The total resistance related to base model is approximately 6.5% reduction at 15.5 knots and 3% reduction at 18 knots for the selected design 1 (MO_des270). And 6.2% and 4.31% reduction at 15.5 knots and 18 knots respectively for selected deign 2 (MO_des 239).

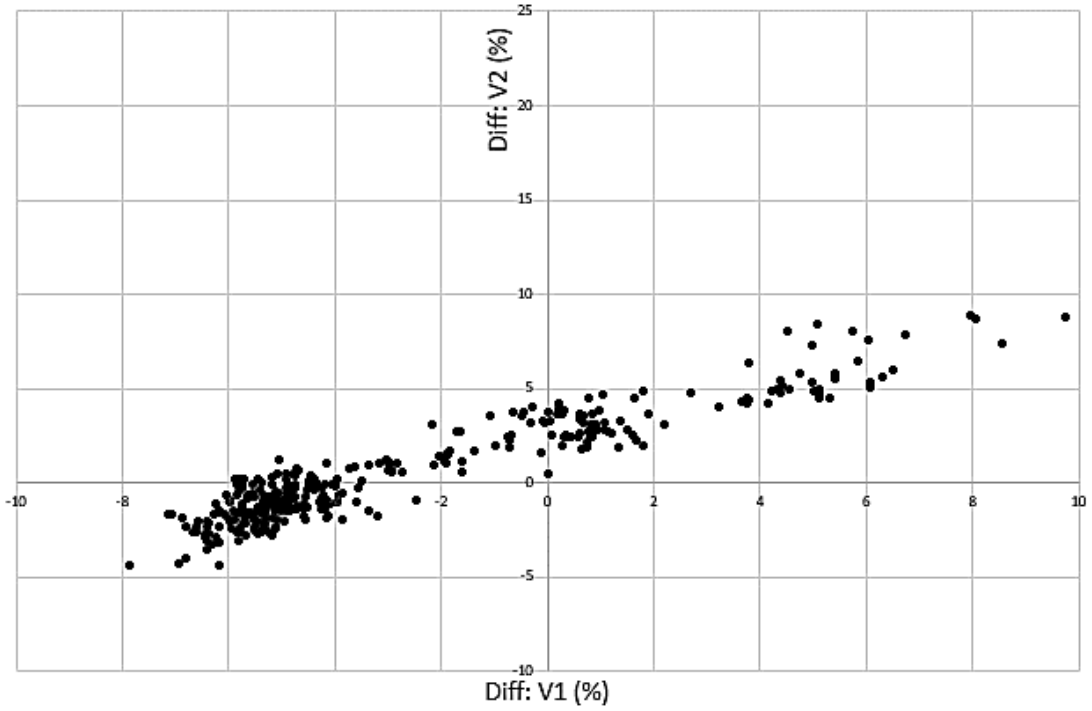

Figure- 36: Multi-Objective Optimization (Dakota- SBGO)

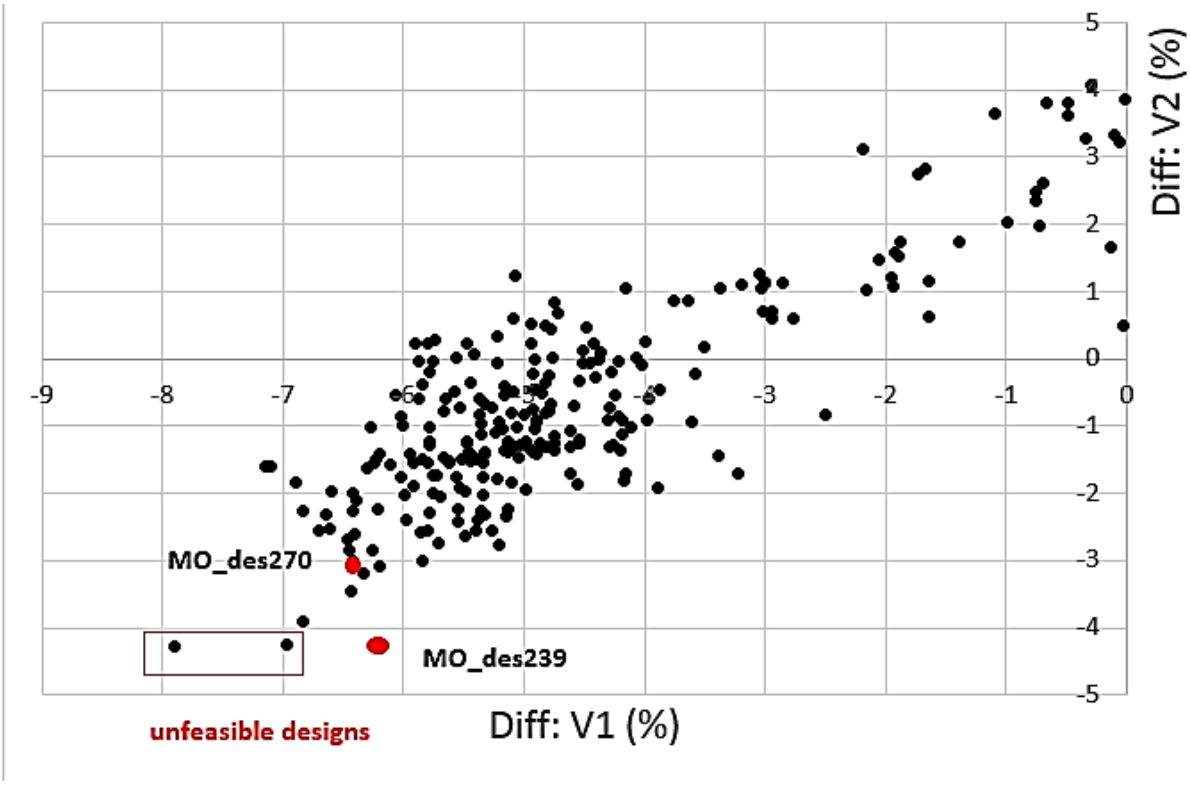

Figure- 37: Multi-Objective Optimization (Dakota- SBGO) zoomed in design of interest

6.5. Sensitivity Analysis

Optimum designs via different methods were performed for two different speeds at the design draft of 14.5 m. The robustness of the design is evaluated regarding the sensitivity to uncertainties variations on the draft of the vessel. For the sensitivity analysis, the best achieved designs of some of the optimization processes were selected and the R_{TV1} and R_{TV2} for several draft values were studied. The selected designs for the sensitivity analysis are as follows:

(1) SO_$V_{15.5}$ - the optimal design obtained for single objective optimization for R_{TV1}

(2) SO_V_{18} - the optimal design obtained for single objective optimization for R_{TV2}

(3) SO_α_0.25 - the optimal design obtained for single objective optimization with weighted coefficient of 0.25

(4) SO_α_0.50 - the optimal design obtained for single objective optimization with weighted coefficient of 0. 50

(5) SO_α_0.75 - the optimal design obtained for single objective optimization with weighted coefficient of 0.75

(6) MO _des270 - the optimal design obtained from multi-objective optimization

(7) MO _des238 - the optimal design obtained from multi-objective optimization

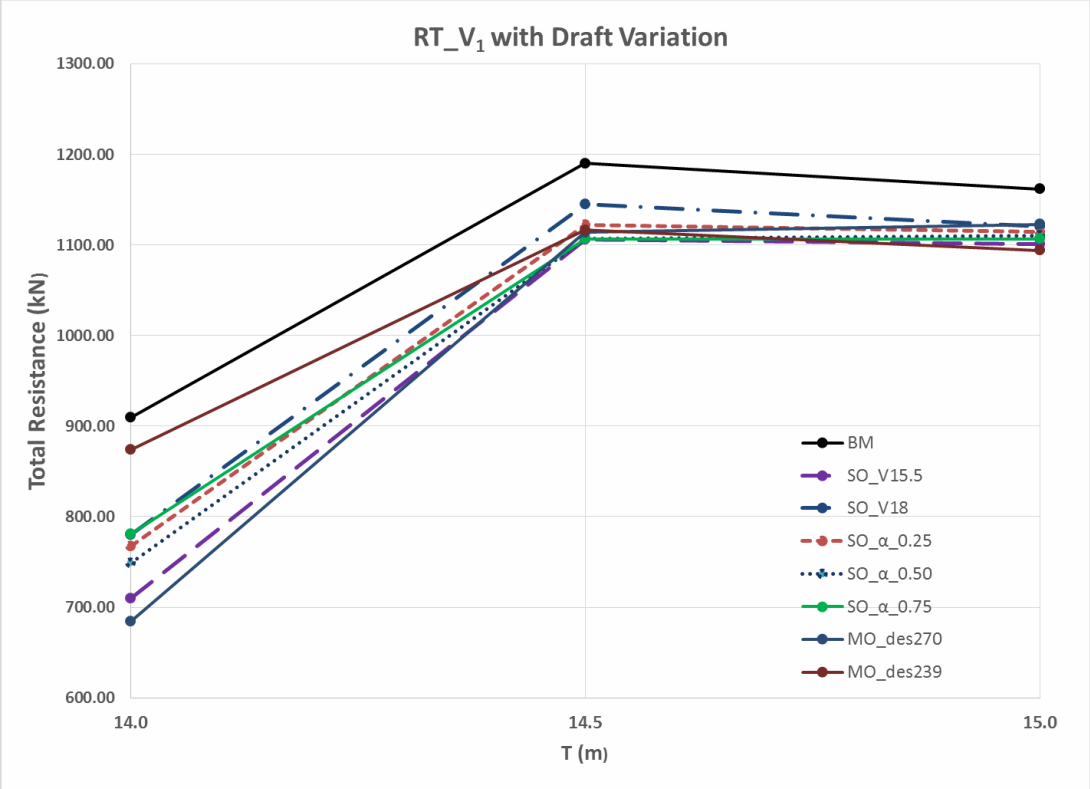

Figure- 38: Sensitivity analysis of draft variation for selected designs at V1 = 15.5 knots

(Optimization was performed at T=14.5m)

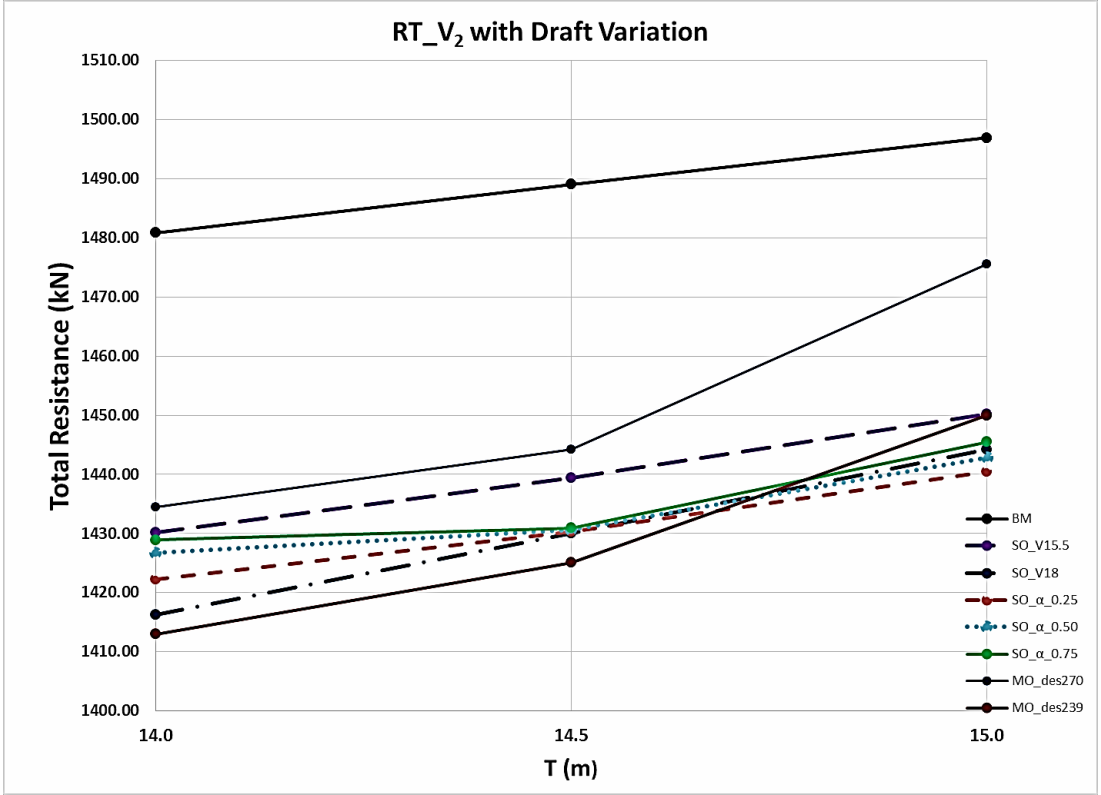

Figure- 39: Sensitivity analysis of draft variation for selected designs at V2 = 18 knots

(Optimization was performed at T=14.5m)

Figures 38 and 39 show the variation of the resistance due to changes in the draft for the condition of V_1 = 15.5 knots and V_2 = 18 knots respectively, for the selected designs with the draft variation from 14.0 m to 15.0 m. The results of base model obtained for 15.5 knots at different drafts show that the performance of the initial model is sensitive to change the draft. But, it can be observed that the selected optimal models for the condition of T=14.5 m have an improvement not only for this draft, but also for the others tested (T=14.0m and 15.0m) with same behavior as base model.

6.6. Analysis of Optimal Models at Different Operation Conditions

Since the optimization process was performed for V_1 = 15.5 knots and V_2 = 18 knots at the design draft of T =14.5m, the performance of the selected optimal models from each optimization process were analyzed for different operation conditions as shown below.

Slow Speed Scenario: OC1: V= 15.5 knots, T=14.5 m (w_{Total} = 20.72%)

OC2: V= 18.0 knots, T=15.0 m (w_{Total} = 16.25%)

High Speed Scenario: OC3: V= 22.5 knots, T=15.0 m (w_{Total} = 9.28%)

OC4: V= 25.0 knots, T=14.0 m (w_{Total} = 21.09%)

Experimental Results: OC5: V= 20.0 knots, T=14.5 m

OC6: V= 25.0 knots, T=14.5 m

Each of the optimal models obtained from different optimization processes was analyzed for six operation conditions and the results can be seen in Table 10 and Figure-40.

Table - 10: Total resistance (kN) for selected optimal models at different operation conditions

				Total Resistance in calm water							
	Vs	Vs	T	**BM**	**SO_V15.5**	**SO_V18**	**SO_α_0.25**	**SO_α_0.50**	**SO_α_0.75**	**MO_des270**	**MO_des239**
	[knots]	[m/s]	[m]	[kN]	[kN]	[kN]	[kN]	[kN]	[kN]	[kN]	[kN]
OC 1	15.5	7.9732	14.5	1190	1106	1145	1122	1107	1107	1114	1116.5
OC 2	18	9.2592	15	1496	1450.25	1444.28	1440.46	1442.88	1445.48	1475.54	1450
OC 3	22.5	11.574	15	2351	2346	2374	2347	2344	2346	2346	2355
OC 4	25	12.86	14	2886	2880	2900	2892	2894	2893	2876	2860
OC 5	20	10.288	14.5	1844	1810	1775	1752	1780	1796	1785	1889
OC 6	25	12.86	14.5	2966	2936	2967	2979	2950	2971	2990	2995

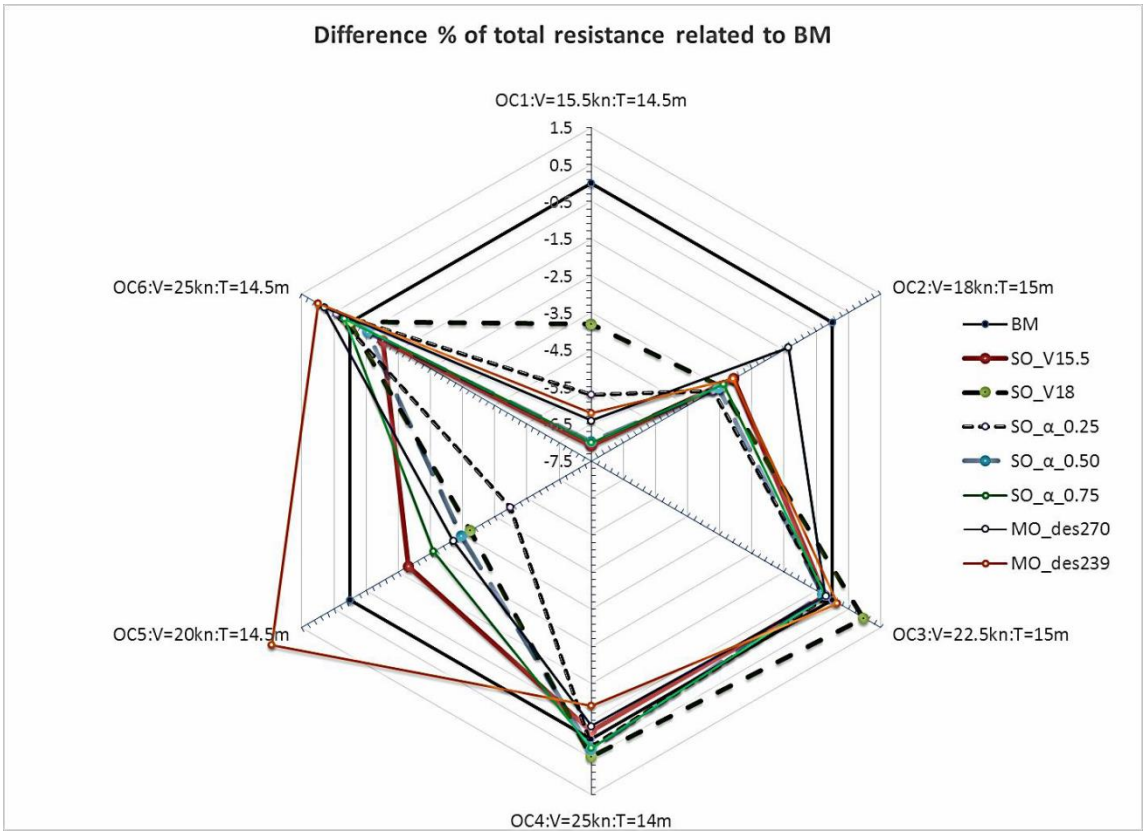

Figure- 40: Comparison of Difference in R_T (%) related to base model at different operation conditions

From Figure-40, we can see that the optimal model named SO_V15.5 (red colour line) has the improvement in all operation conditions.

7. SEAKEEPING ANALYSIS IN MODERATE SEA STATES

As one of the main objectives of this thesis, the analysis of added resistance due to waves has to be done after optimization in calm water conditions. Since the container vessel has not been built yet, the wave data and the study of sea states are done from statistical data of existing similar vessels. This process is performed by specialists from University of Rostock. The wave scenario data that the vessel has to deal with are resulted for all specific wave height ($H_{1/3}$) and wave period (T_1) are chosen for three operating conditions covering 50.60% of the total operating time by the vessel. The wave scenario data of one operation condition [T =15m, V=18knots] can be seen as the scatter diagrams in Figure- 41.

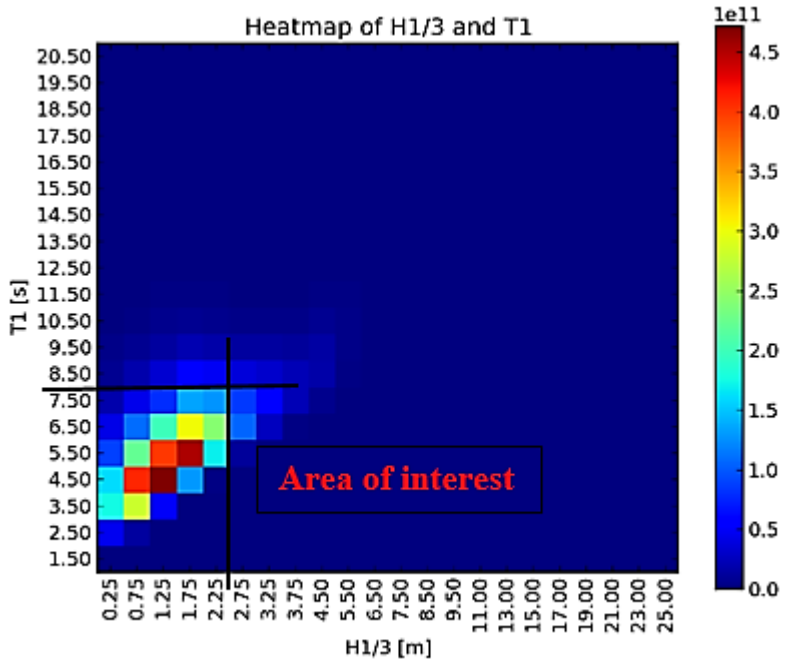

Figure- 41: Scatter Diagram of wave data at T= 15m, V=18 knots

7.1. Added Wave Resistance Due to Head Waves for Initial Model

The most reliable way to determine the increase of resistance due to the effect of waves is to carry out seakeeping tests in regular waves of constant wave height, and different wave lengths and directions at various speeds according to ITTC 7.5-022-07-02.2 [19]. The added wave resistance due to head wave for different wave period and wave height can be calculated by the use of equation 7.

$$R_{AW} = 2 \times \int_0^{\infty} \frac{R_{wave}(\omega, Vs)}{\zeta_A^2} \; S_f(\omega)\, d\omega \qquad (7)$$

Where,

R_{AW} = mean added resistance increase in long-crested irregular head waves

R_{AW} / ζ_A^2 = quadratic transfer function of the mean longitudinal drift force obtained from GL Rankine

$S_f(\omega)$ = frequency spectrum, for ocean waves modified Pierson-Moskowitz type

$$S_f(\omega) = \frac{A_f}{\omega^5} . \exp(-\frac{B_f}{\omega^4}) \quad (8)$$

$$A_f = 173.\frac{H_{1/3}^2}{T_1^4} \quad (9)$$

$$B_f = 691.\frac{1}{T_1^4} \quad (10)$$

The result of added wave resistance due to head waves for the initial model can be seen in Figures 42 and 43 for different wave periods and significant wave heights.

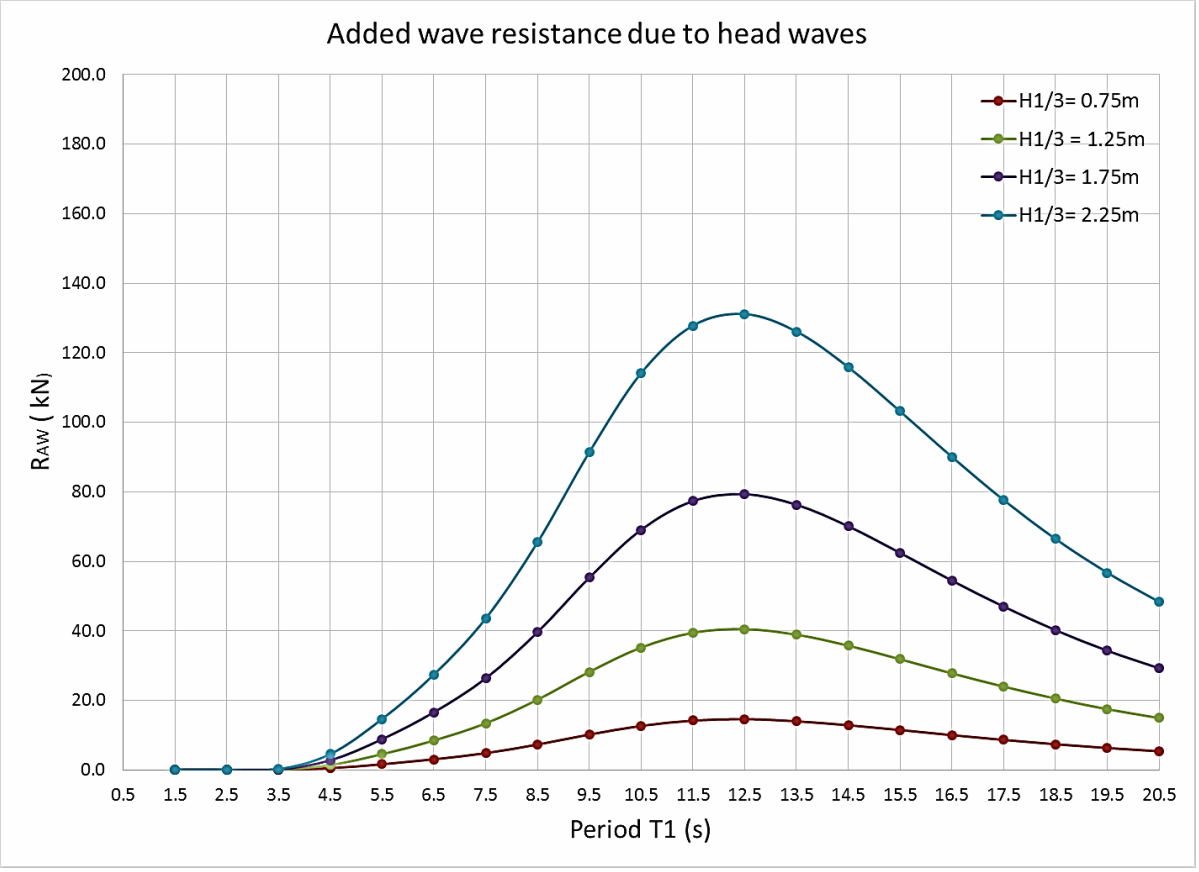

Figure- 42: Added wave resistance due to head waves for the initial base model

(V = 15.5 knots, T=14.5m)

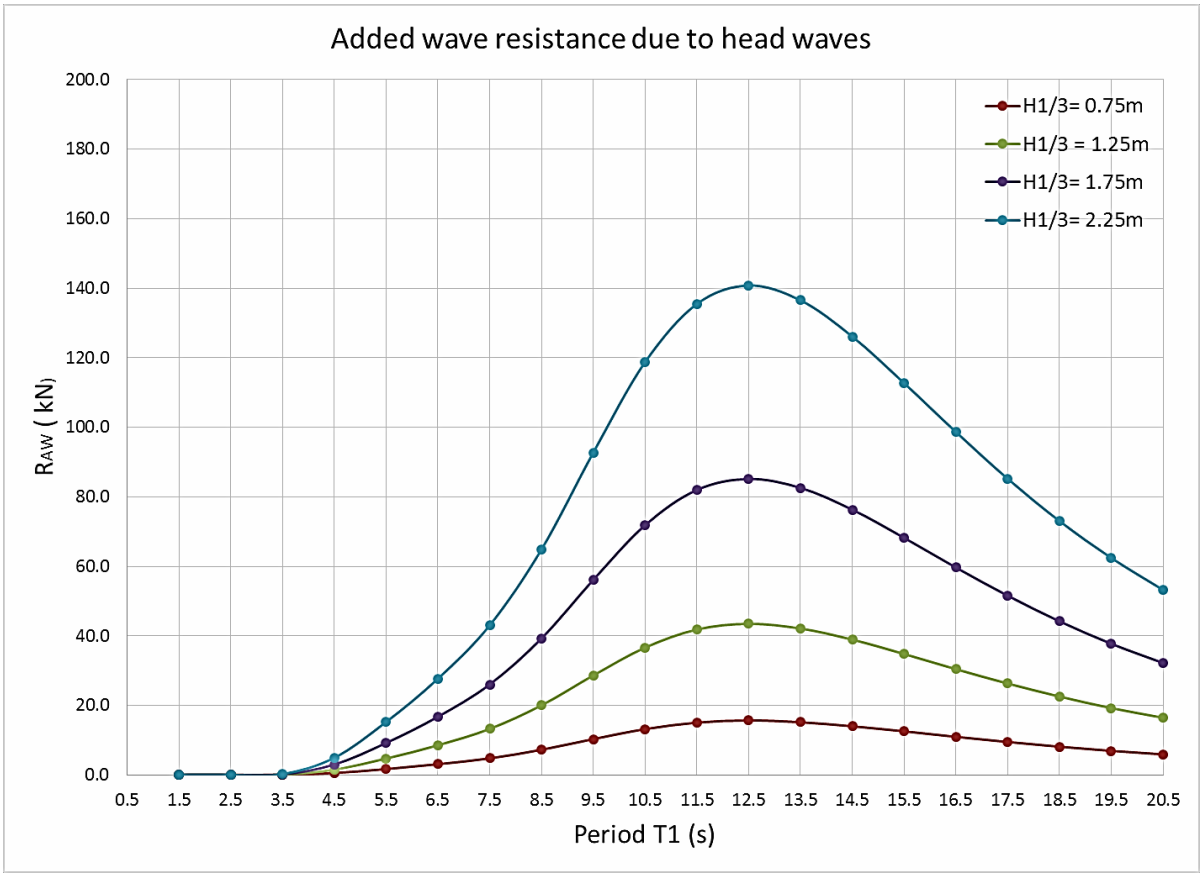

Figure- 43: Added wave resistance due to head waves for the initial base model

(V = 18.0 knots, T=14.5m)

The added wave resistance related to total resistance in calm water (%) for the area of interest was calculated and shown in Figures. 44 and 45.

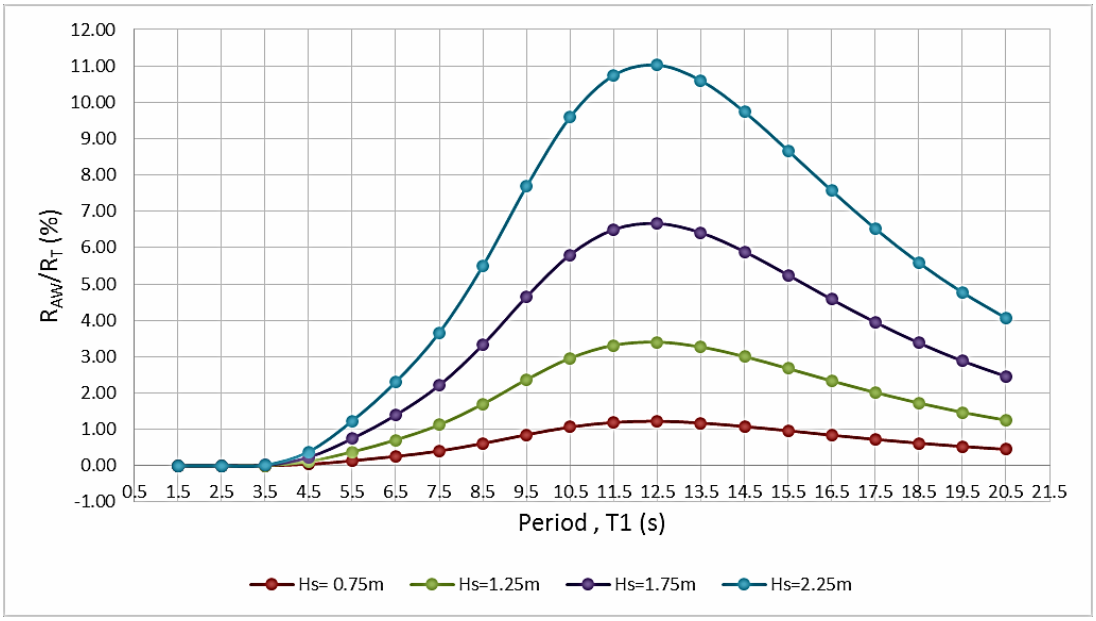

Figure- 44: Added wave resistance due to head waves for initial base model for area of interest only

(V = 15.5 knots, T=14.5m)

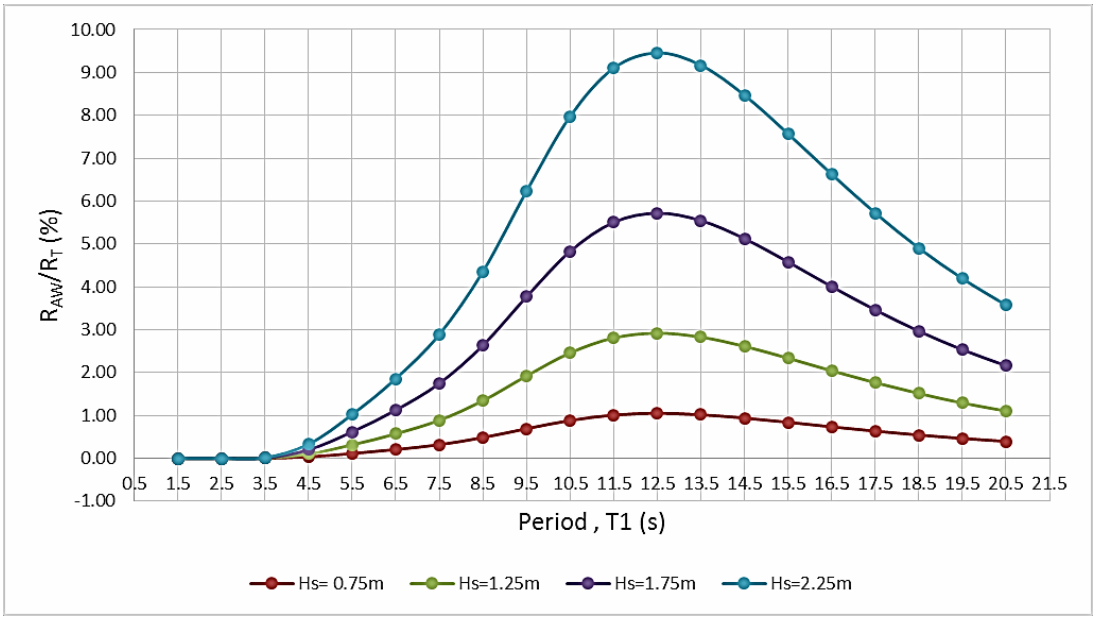

Figure- 45: Added wave resistance due to head waves for initial base model for area of interest only (V = 18 knots, T=14.5m)

7.2. Added Wave Resistance Comparison of Optimal Models

Although the hull form has been optimized for two speeds in calm water condition, seakeeping performance of each optimum design is checked by simulating the design in the selected sea state with GL Rankine solver. In order to compare the seakeeping performance, each calm water combination is added its most frequent sea state, which has the advantage of not increasing the number of combinations of optimization process. Table 11 shows the wave scenario data that the vessel has to deal with for two operating conditions.

Table - 11: Wave scenario data for two operation conditions

Operation Condition	Speed , Vs	Draft , T	Peak Period, T_P	Significant Wave Height, $H_{1/3}$
[-]	[knots]	[m]	[sec]	[m]
OC 1	15.5	14.5	12.5	1.25
OC 2	18	15	12.5	1.75

By using the most frequent wave height of each condition and the peak period observed from wave spectrum, the added wave resistance was calculated for selected optimal models from single objective optimization process in calm water conditions. The results of each model and the difference % related to the base model (BM) were shown in Table 12. It can be seen that the optimal models obtained from the optimization in calm water conditions at T=14.5m have the improvement regarding to not only calm water resistance but also for added resistance in

waves for V_1=15.5 knots while the added resistance in waves for V_2=18 knots got the higher results than the base model. But the total resistance in waves of different optimal models has the improvement in both operational conditions.

Table - 12: Comparison of total resistance due to waves of optimum models at two speeds

		Calm Water Resistance	Added Wave Resistance	Total Resistance
Designs		**[kN]**	**[kN]**	**[kN]**
BM	15.5 knots	1190	40.5	1230.5
	18 knots	1489	87	1576
SO_V15.5	15.5 knots	1106	39.4	1145.4
	Diff: from BM	-7.06%	-2.72%	-6.92%
	18 knots	1439	87.5	1526.5
	Diff: from BM	-3.36%	0.575%	-3.14%
SO_V18	15.5 knots	1145	40	1185
	Diff: from BM	-3.78%	-1.235%	-3.7%
	18 knots	1430	87.7	1517.7
	Diff: from BM	-3.96%	0.805%	-3.7%
SO_α_0.25	15.5 knots	1122	40.2	1162.2
	Diff: from BM	-5.71%	-0.74%	-5.55%
	18 knots	1430.3	87.4	1517.7
	Diff: from BM	-3.75%	0.46%	-3.71%
SO_α_0.50	15.5 knots	1107.34	39.8	1147.14
	Diff: from BM	-6.97%	-1.73%	-6.77%
	18 knots	1431	87.8	1518.8
	Diff: from BM	-3.92%	0.92%	-3.63%
SO_α_0.75	15.5 knots	1107	40	1147
	Diff: from BM	-7.01%	-1.235%	-6.786%
	18 knots	1431	87.9	1519
	Diff: from BM	-3.91%	1.034%	-3.62%
MO_des 270	15.5 knots	1114	39.2	1153.2
	Diff: from BM	-6.41%	-3.21%	-6.282%
	18 knots	1475	87.1	1562.1
	Diff: from BM	-1.37%	0.11%	-0.9%
MO_des 239	15.5 knots	1116	39.8	1155.8
	Diff: from BM	-6.22%	-1.73%	-6.07%
	18 knots	1425	87.6	1512.6
	Diff: from BM	-4.30%	0.69%	-4.023%

7.3. Direct Optimization of Total Resistance in Waves

After the optimization of hull form in calm water conditions and analysis of added resistance in waves for optimal hull forms were done, the direct optimization of total resistance in waves for moderate sea states, summing the total resistance in calm water and added resistance due to head waves, was performed. The optimization was done of the wave scenario as shown in section 7.2 with the most frequent wave height and the peak period of 12.5s in the wave direction of 180 degrees.

The set-up file for GL Rankine was coupled with CAESES for both steady flow and seakeeping computations. The two result files obtained from GL Rankine gave the total resistance in calm water condition and the added wave resistance for sea state and by summing up; the total resistance in waves was calculated. Then, the model was optimized directly for the total resistance in waves for two operation conditions, V_1 = 15.5 knots, T_1=14.5m and V_2= 18 knots, T_2 = 15m.

In this stage of finding the total resistance in waves directly, the single objective optimization with Dakota was omitted since the computation time in GL Rankine for both steady flow and seakeeping computations took approximately one hour for each design variant. Therefore, Design of Experiments was performed for 300 design variants by using only SOBOL in CAESES and the best design was selected from 300 designs which give the minimum total resistance in waves for the selected sea state.

The Figure 46 and 47 present the results of total resistance in waves for the designs obtained on the DoE study, displayed by their indexes (order of creation) and in the ordinate of the difference in total resistance (%) relative to the base model.

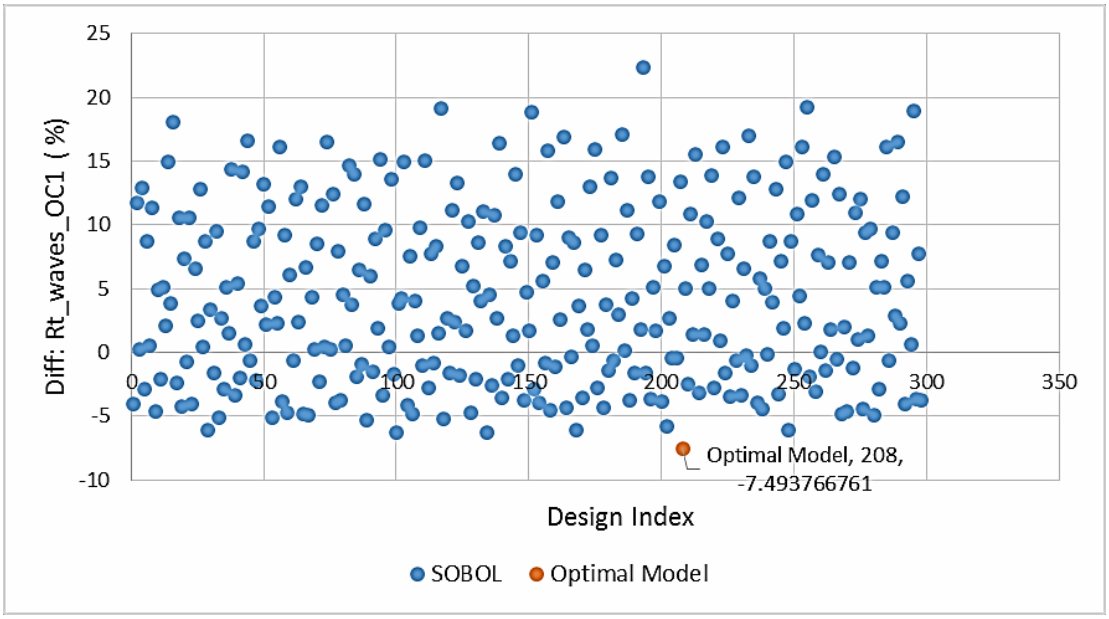

Figure- 46: DoEs by SOBOL and Optimal Model for V1 = 15.5 knots, T1=14.5m

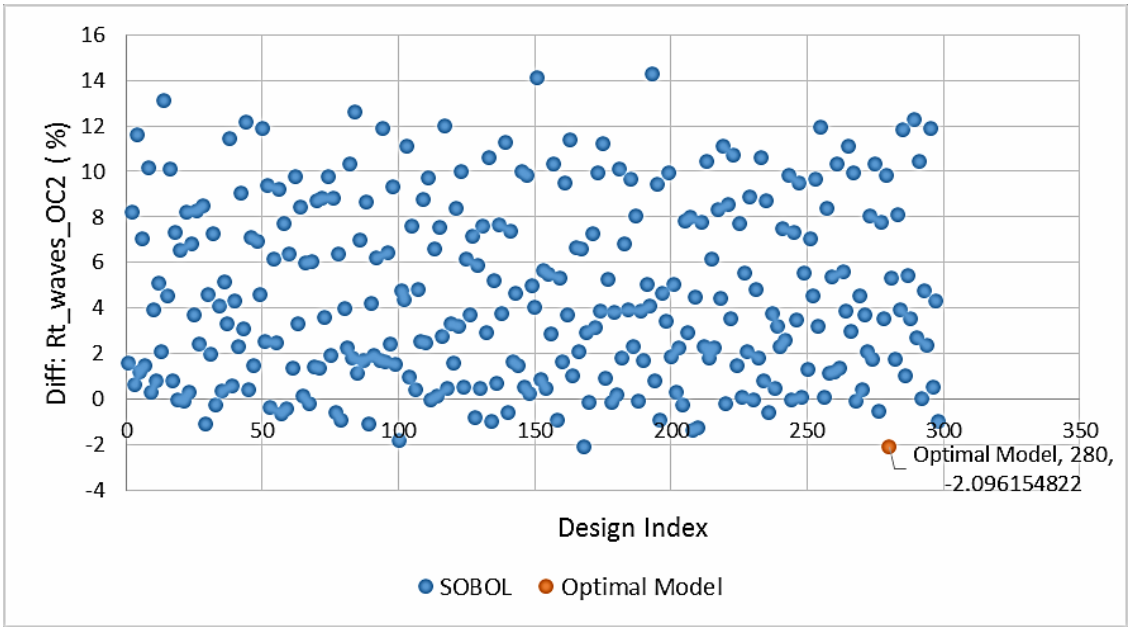

Figure- 47: DoEs by SOBOL and Optimal Model for V2 = 18 knots, T2=15m

When compared to the base model, the optimal model for operation condition 1 (Index-208) had the reduction of 7.494% in the total resistance in waves and that for operation condition 2 (Index-280) had the reduction of 2.1% in the total resistance in waves.

The comparison of the geometry of the bulbous bow for the selected optimal models for the two operation conditions and the comparison of total resistance in waves related to base model at different wave heading angles can be seen in the next section.

8. RESULTS AND ANALYSIS

8.1. State of the Art in Optimization for Calm Water Conditions

In Table 13, the number of CFD runs necessary to perform the optimization for each method is presented side by side with final performance obtained (Total resistance in waves) relative to the base model for the speed of V_1 = 15.5 knots and V_2 = 18 knots at the design draft of T=14.5m.

Table - 13: Number of CFD runs and Total resistance in waves related to base model %

			Design	CFD run (DoE+Opt)	Performance	
					V_1	V_2
Optimization in Calm Water Conditions	**Single Objective**	**DoE+ surrogate based local optimization**	SO_V15.5	267	-6.92%	-3.14%
			SO_V18	250	-3.7%	-3.7%
	Multi-Objective	**S.Obj with w=0.25**	SO_α_0.25	254	-5.55%	-3.71%
		S.Obj with w=0.5	SO_α_0.50		-6.77%	-3.63%
		S.Obj with w=0.75	SO_α_0.75		-6.786%	-3.82%
		Dakota MOGA (surrogate based global optimization)	MO_des 270	350	-6.282%	-0.9%
			MO_des 239		-6.07%	-4.023%

From the results in Table 13, it can be observed that when the objective function is to minimize the total resistance in V_1= 15.5 knots, the greater the weighted function coefficient, the better the improvement of the results of V_1. When comparing the optimum designs obtained by the several optimization processes some trends of the form characteristics are observed in Table 14.

Table - 14: Geometry trend of the optimized bulbous bow

Designs	Length	Width	Height	Bulb tangent at top (0 deg for Base model)	Entrance angle (0 deg for base model)	Difference in final volume
SO_V15.5	23%longer	99%narrower	21%higher	-1.8deg	35% wider	-0.12%
SO_α_0.75	6%longer	97.8%narrower	93%higher	7deg	85% wider	-0.12%
SO_α_0.50	11%longer	99.5%narrower	75%higher	5.3deg	99% wider	-0.11%
SO_α_0.25	17%shorter	99%narrower	59%higher	9.5deg	63% wider	-0.10%
SO_V18	12%shorter	97%narrower	70%higher	9.12deg	55% wider	-0.13%
MO_des 270	8.3%shorter	99.3%narrower	39%lower	-4.6deg	39% wider	-0.13%
MO_des 239	99 %longer	99%narrower	72%higher	8.5deg	80% wider	-0.15%

The analysis is performed by the relative value of the design variable that defines the geometry. For example, the bulbous bow for the first case presents a value 99% narrower which means that the parameter that controls the width of the bulb is in between the mean value (base model) and the lower bound, in 99% of that range.

8.2. Optimal Model Selected from the Optimization in Calm Water

Considering the performance of the designs obtained with single objective and multi-objective optimization processes, the design SO_V15.5 is selected as final optimal model. This model has the improvement in total calm water resistance of 7.06% and 3.36% for 15.5 knots and 18 knots respectively at the design draft T=14.5m . This model also has the improvements in different operation conditions [Figure- 48].

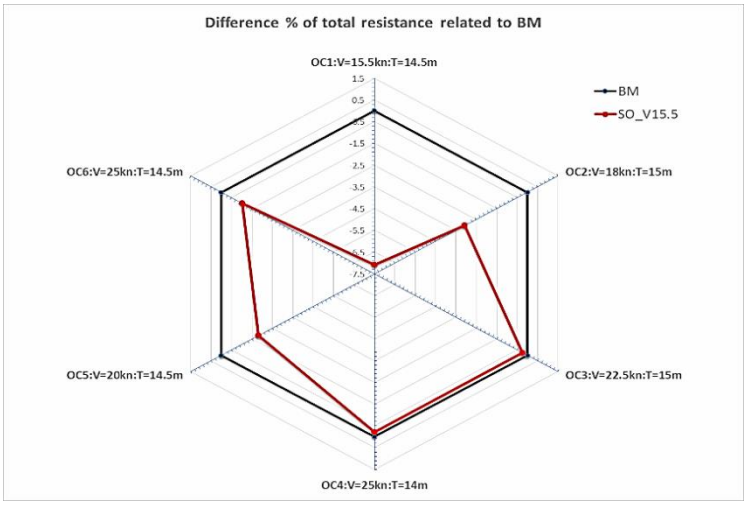

Figure- 48: Comparison of Diff: % in R_T for different operation conditions

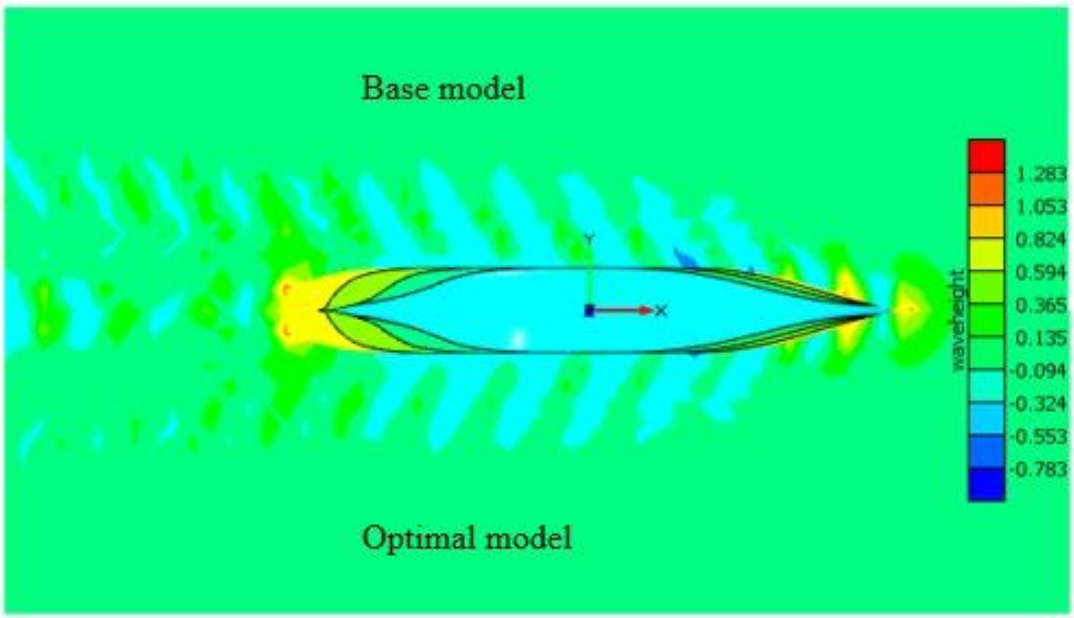

Figure- 49: Wave pattern of the optimal and base hull form (V=15.5knots, T=14.5m)

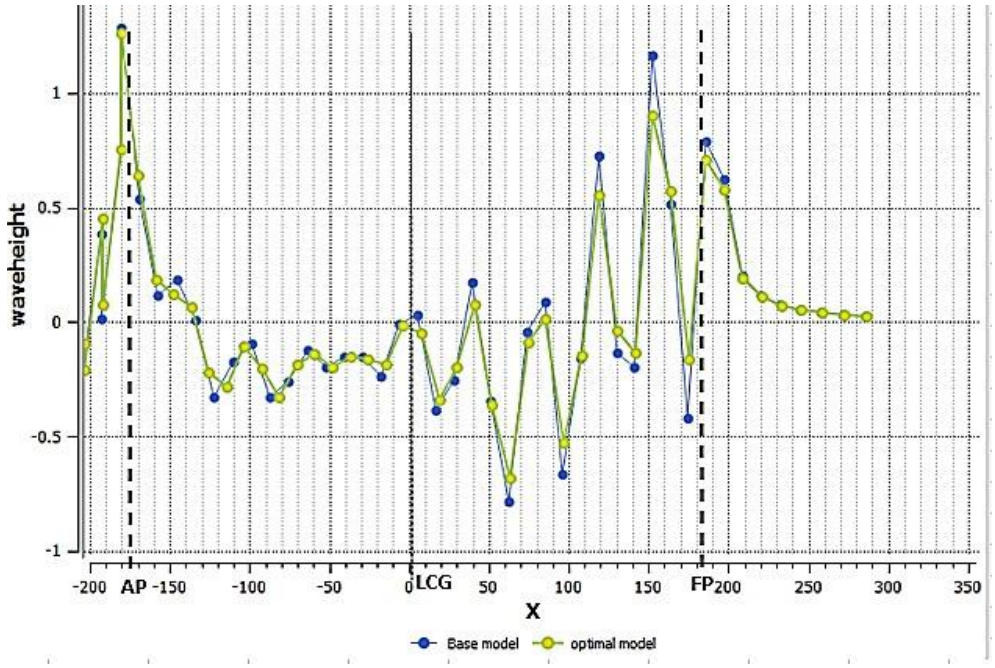

Figure- 50: Wave Profile for Base and Optimum model (V=15.5knots, T=14.5m)

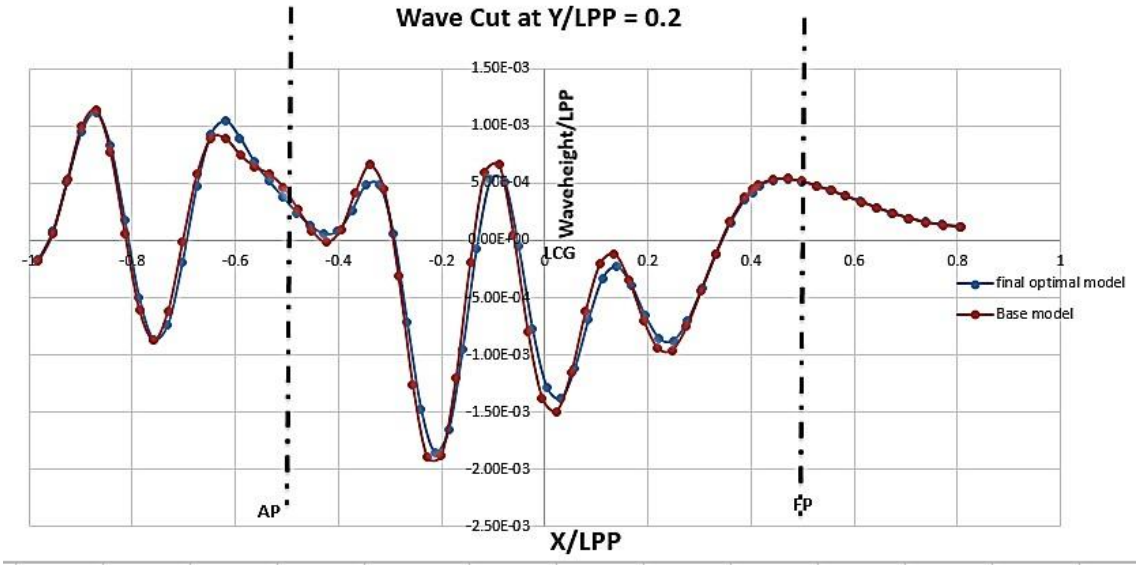

Figure- 51: Wave Cut at Y/LPP=0.2 for Base and Optimum model (V=15.5knots, T=14.5m)

The variation of the wave generated by the vessel can also be observed by the wave cut far from the body presented in the Figure-51. The differences in the wave pattern and wave cut are due to variations on the hull form as presented in Figure-52. In Figure-52, it can be observed that only the forebody of the vessels present some differences. The bulbous bow is a bit narrower and longer than the base model. The bulb tip elevation becomes a bit higher than the base model.

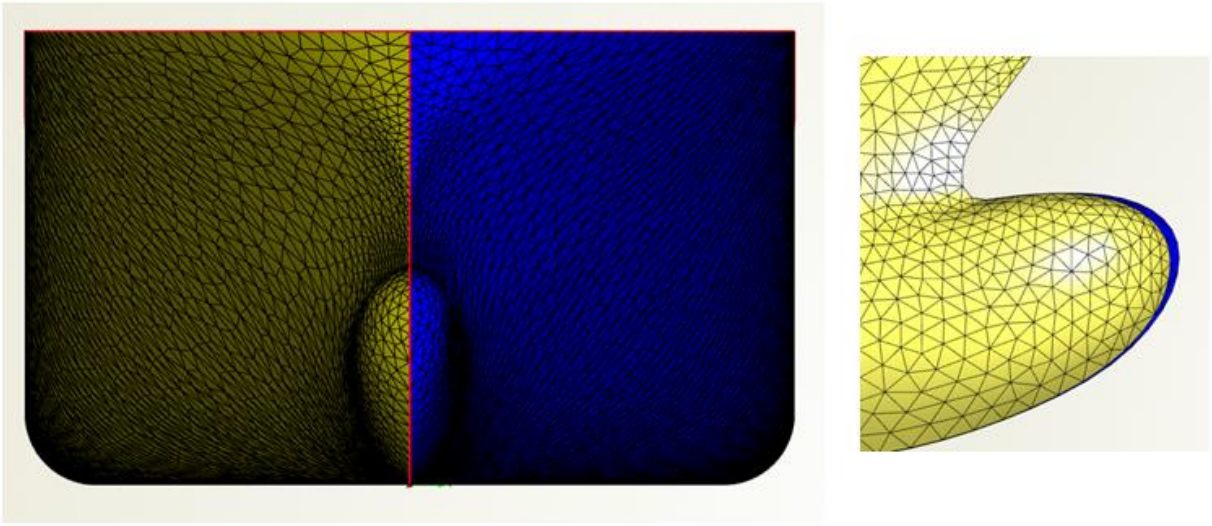

Figure- 52: Base model and final optimal model comparison (V =15.5 knots, T= 14.5m)

In Figures 53 to 55, the total resistance of the vessel in calm water condition for initial model and final optimal model are presented for three different drafts (T= 14 m, 14.5 m, 15 m) at the velocities from 15.5 knots to 25 knots.

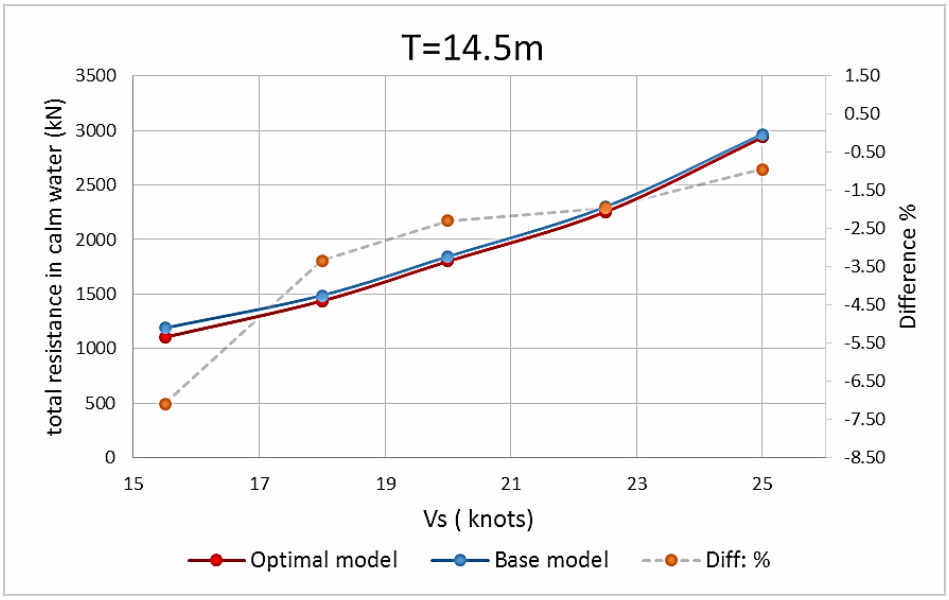

Figure- 53: Total resistance of base model and optimal model at whole range of operational speeds at T=14.5m [In the secondary axis the relative difference in percentage is presented]

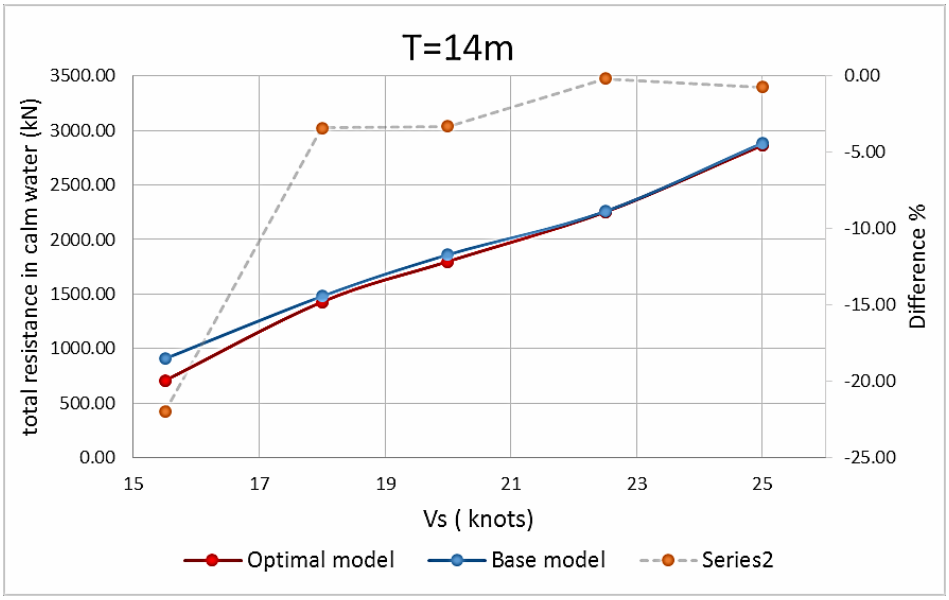

Figure- 54: Total resistance of base model and optimal model at whole range of operational speeds at T=14.0m

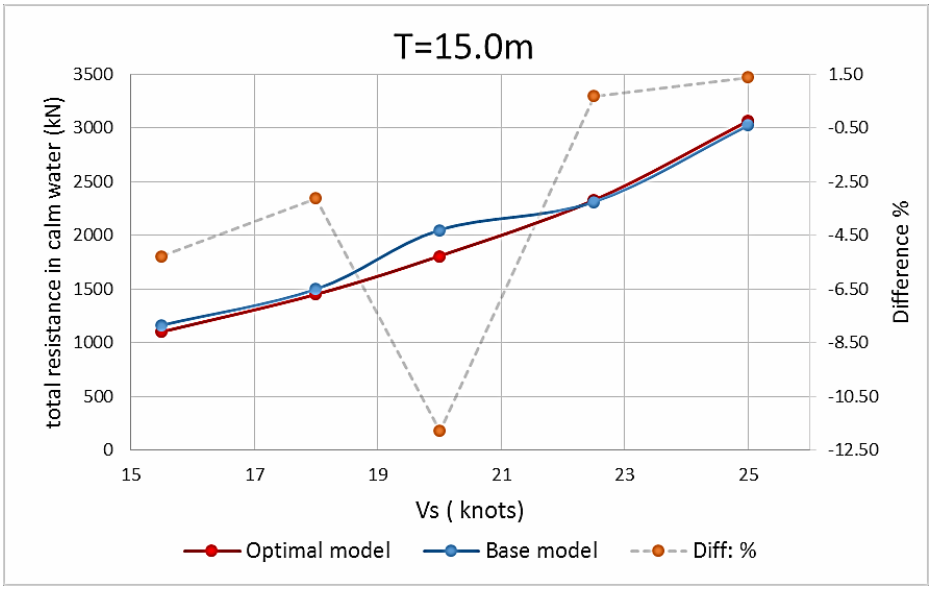

Figure- 55: Total resistance of base model and optimal model at whole range of operational speeds at T=15.0m

The optimization process was performed for a fixed draft of 14.5 m, however the optimum vessel present a good performance not only at this draft but also for different drafts conditions. Leading to the conclusion, the optimized model has a level of sensitivity, regarding uncertainties on the draft value, similar to the base model. In conclusion, the selected design from the optimization presents a good behavior at variations on the draft, and also has the improvement in the total resistance for the main operational velocities.

8.3. Optimal Model Selected from the Direct Optimization in Sea States

As in calm water condition, the final performance obtained (Total resistance in waves) relative to the base model for the speed of V_1 = 15.5 knots, T_1=14.5m and V_2 = 18 knots, T_2=15m was tabulated as following.

Table - 15: CFD runs and Total resistance in waves related to base model % in sea states

		Design	CFD run (DoE)	Performance	
				V_1=15.5kn	V_2= 18 kn
Optimization in sea states	DoE(SOBOL)	SO_Rt_OC1 (ID_208)	300	-7.5%	-1.36%
		SO_Rt_OC2 (ID_280)	300	-4.88%	-2.1%

From the results in Table 15, it can be observed that when the objective function is to minimize the total resistance in V_1= 15.5 knots at T_1=14.5m, the total resistance in waves have the reduction of -7.5 % for the objective operation condition and -1.36% for the another operation condition for the same optimal model. Similarly, when the objective function is to minimize the total resistance in V_2= 18 knots at T_2=15m, the total resistance in waves have the reduction of -4.88 % for the objective operation condition and -2.1% for another operation condition. It means that the selected optimal models for each operation condition have the improvement in the performance not only for the objective function but also for another function.

When comparing the optimum designs obtained by the two operation conditions, some trends of the form characteristics are observed in Table 16.

Table - 16: Geometry trend of the optimized bulbous bow (optimization in sea states)

	Bulbous bow characteristics				
Designs	Length	Width	Height	Bulb tangent at top (0 deg for Base model)	Entrance angle (0 deg for base model)
SO_Rt_OC1 (ID_208)	73%longer	87%narrower	27%higher	-3.56deg	61% wider
SO_Rt_OC2 (ID_280)	82%longer	72.5%narrower	87%higher	8deg	57% wider

As per table 16, the bulb is longer in length, narrower in width and higher in the bulb tip height when compared to the base model. When the objective function is to minimize the total resistance in waves for operation condition V_1 =15.5 knots and T_1=14.5m, the bulb tangent at the top becomes flatter than the base model. But for the other objective function, that becomes fuller than the base model. In order to get the faired incident waves due to the shape variation, the wave entrance angle becomes 61% and 57% wider than the base model at the respective operation condition.

8.3.1. Analysis of the Optimal Models for Different Wave Heading Angles

Since the direct optimization in sea states was performed only due to the head waves (180 deg) for both operation conditions, the selected optimal models from SOBOL was analyzed for different wave heading angles, such as 30 deg off bow and 60 deg off bow and compared the performance for those angles with the base model.

The set-up file for seakeeping computation in GL Rankine was modified to calculate the average drift force for different frequency range with the heading angle 180 deg, 150 deg and 120 deg. The result file obtained from the seakeeping computation was imported to the MATLAB code, named 'Added Resistance.m', prepared by the author in order to compute the maximum added wave resistance for the selected wave scenario. The detail of the computation steps in MATLAB code can be seen in APPENDIX- A5.

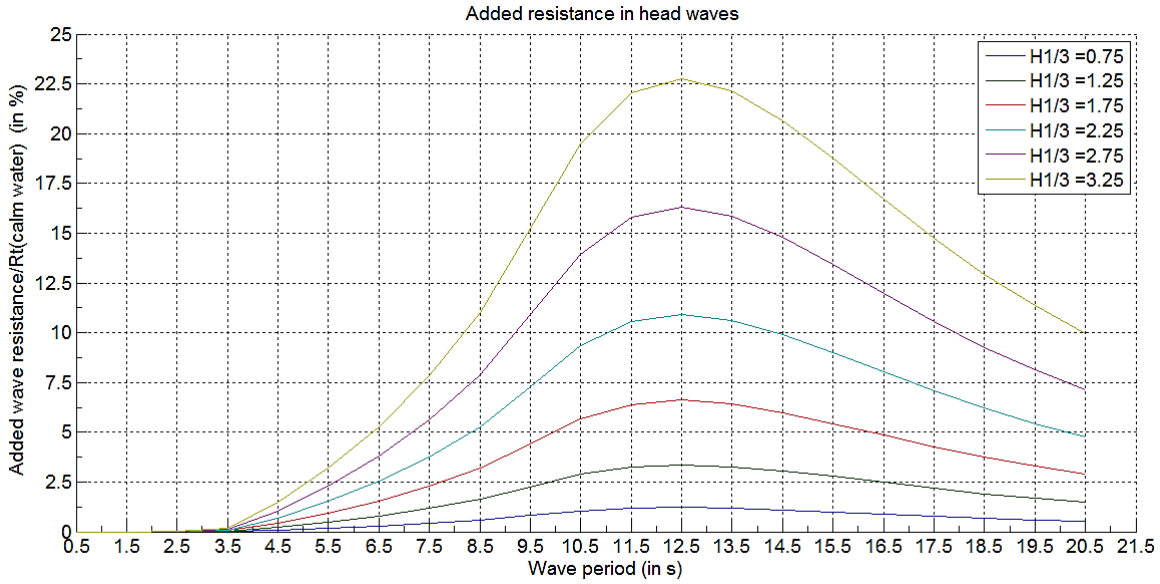

Figure- 56: Added wave resistance/ Rt (Calm water) (%) for head waves

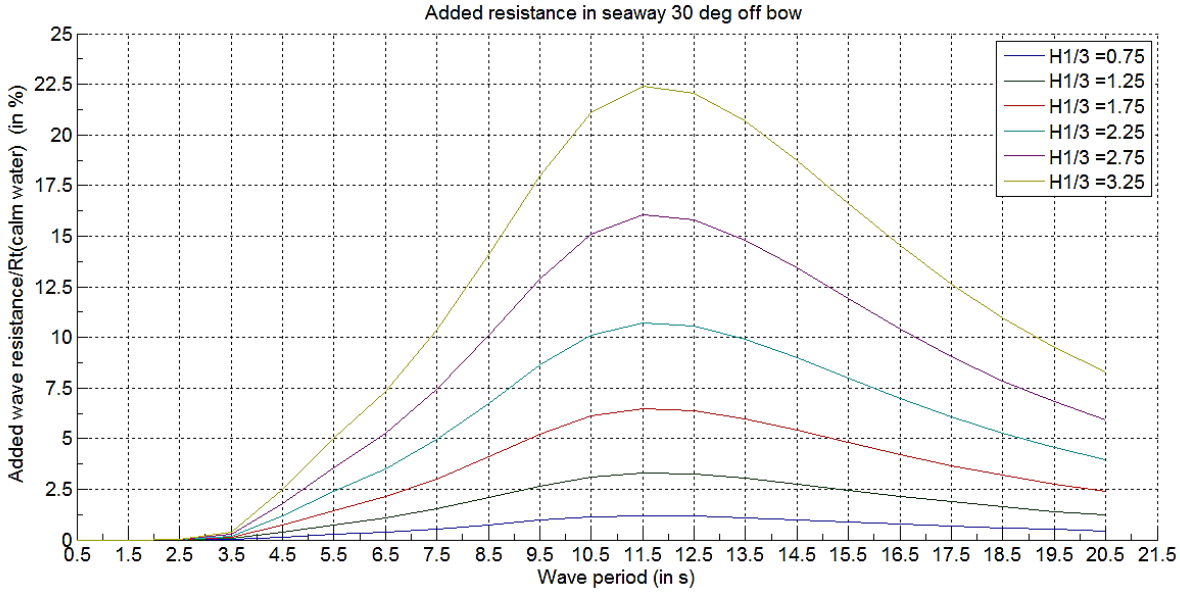

Figure- 57: Added wave resistance/ Rt (Calm water) (%) in seaway 30 deg off bow

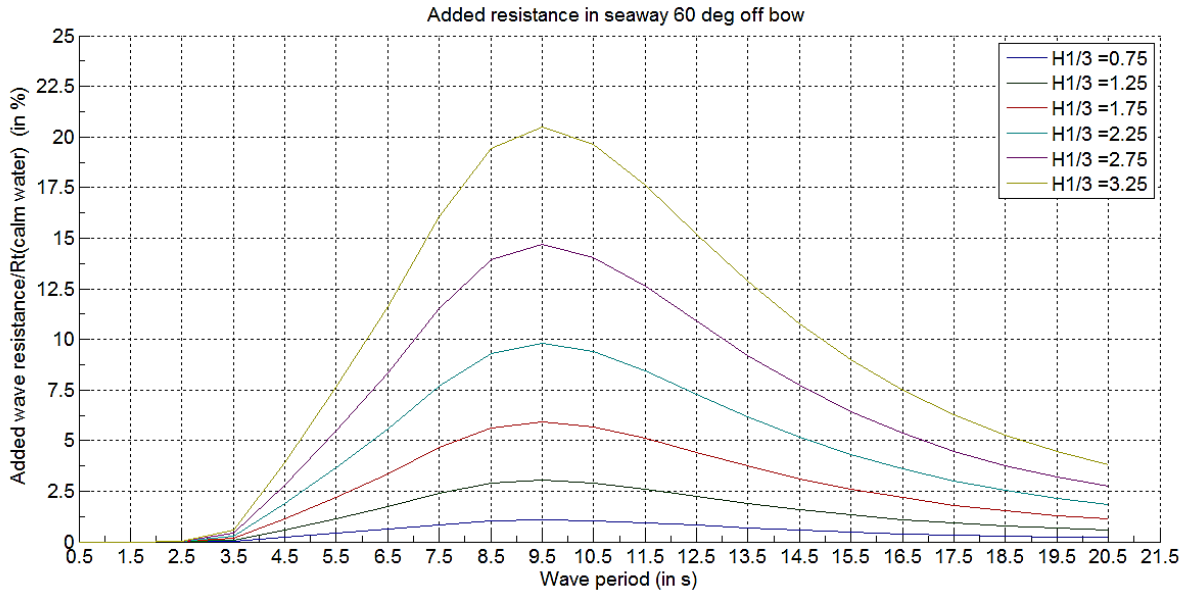

Figure- 58: Added wave resistance/ Rt (Calm water) (%) in seaway 60 deg off bow

As an example, Figures 56 to 58 show the added wave resistance related to total resistance in calm water due to different heading wave angles for operation condition 1 (V_1=15.5 knots and T_1=14.5m). It can be seen that while changing the wave heading angle from 180 deg to 150 deg and 120 deg, the peak period for different significant wave height becomes lesser and the maximum added wave resistance % related to total resistance in calm water becomes lesser and lesser. From the above results, it can be conclude that the direct optimization for total resistance in waves for moderate sea states can be done only for head waves for the safe side and for saving computation time. In order to choose the final optimal model for the direct optimization in sea states, the maximum added wave resistance comparison for two selected model with the base model was performed, as shown in Figure 59 and 60.

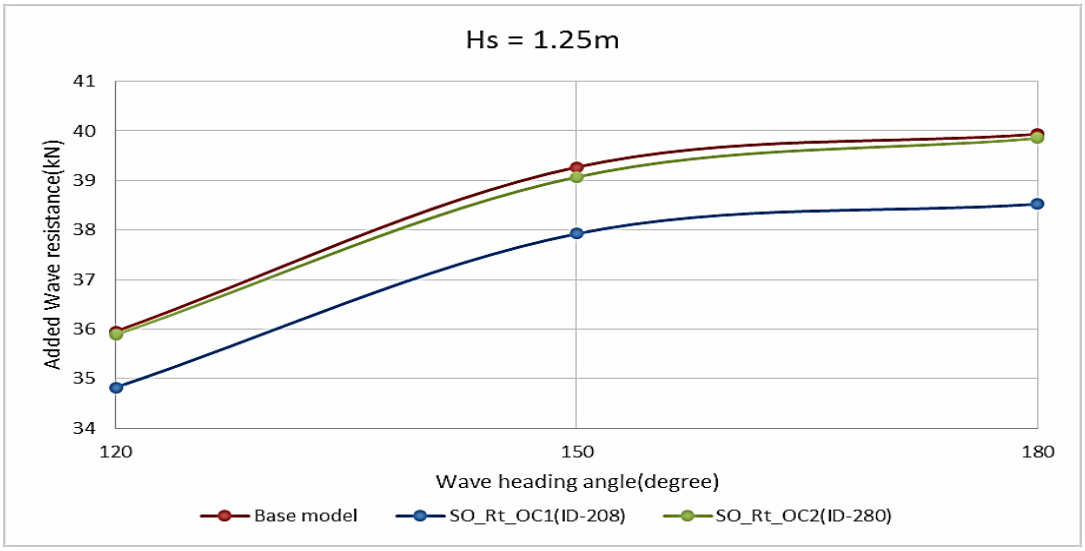

Figure- 59: Added wave resistance at V1=15.5knots, T1=14.5m and Hs=1.25m

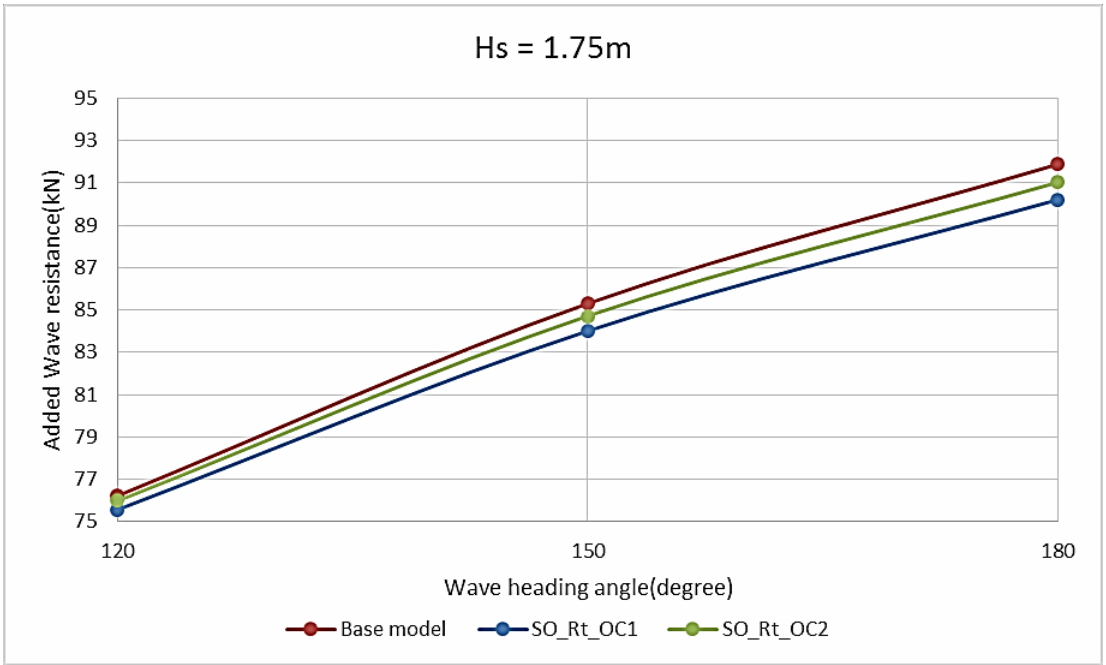

Figure- 60: Added wave resistance at V2=18knots, T2=15m and Hs=1.75m

From Figures 59 and 60, it shows that the optimal models selected from the direct optimization in sea states for head waves (180 deg) by means of SOBOL method have the improvement in other wave heading angles. But, the optimal model obtained from the objective function of minimizing the total resistance in waves for operation condition 1 has the greater improvement in both operation conditions when compared to the base model. Therefore, the optimal model named SO_Rt_OC1 (Design Index-208 in SOBOL) was selected as the final optimal model for the direct optimization in moderate sea states.

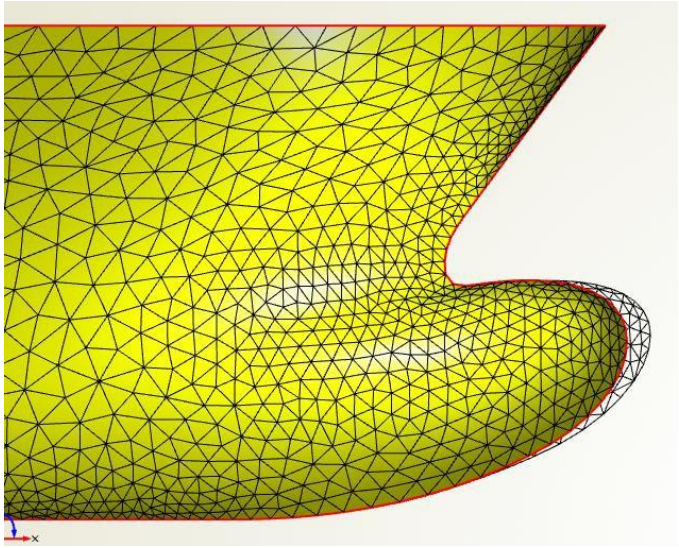

Figure- 61: Comparison of Geometry of Bulbous Bow in Longitudinal View

[Base model – Yellow, Optimal Model – Grey]

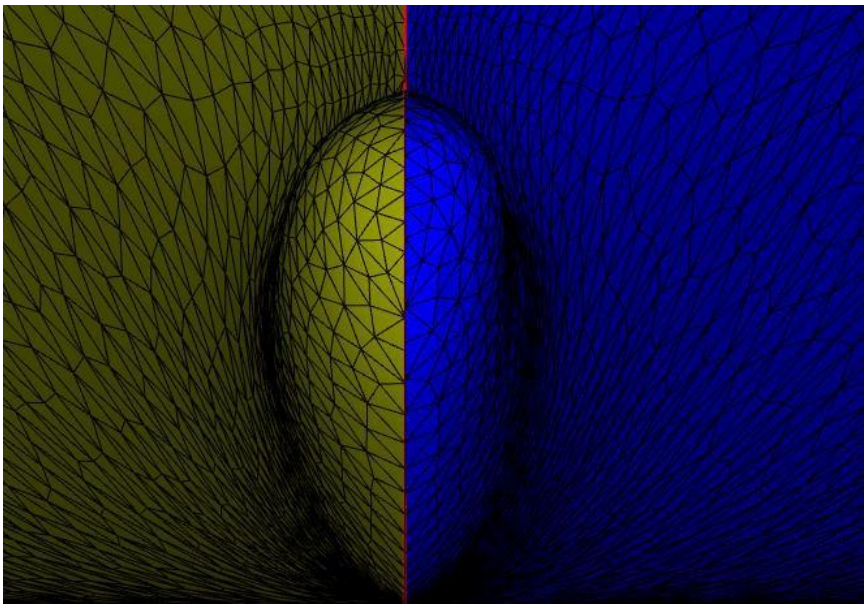

Figure- 62: Comparison of Geometry of Bulbous Bow in Transverse View

[Base model – Yellow, Optimal Model – Blue]

Figure 61 and 62 show the comparison of the geometry between base model and the final optimal model. The bulbous bow is a bit narrower and longer than the base model. The bulb tip elevation becomes a bit higher than the base model [Details can be seen in Table 16].

In conclusion, the selected design from the direct optimization presents a good behavior at variations of the wave heading angles and also has the improvement in the total resistance in sea states for the main operational velocities.

9. SUMMARY

Normally, the ship hull form is optimized in calm water condition without consideration of actual operating conditions in sea states in order to minimize the total resistance occurred by the hull while moving in the water. Instead of using sea margin to compensate the resistance created by waves, it cannot be said as a best approach to estimate the accurate power needed by the ship. In order to solve this problem, the optimization processes of the hull form in calm water condition, including in seaways as well are performed.

In this thesis, firstly, the closed review for modifying the parametric model of the initial model is performed and the most effective design parameters related to changing most for the hull form geometry are created. Besides, for calculating the most reliable and accurate results from the CFD solver, GL Rankine, the thorough understanding and testing of this CFD code is performed, followed by validation of its results with the experimental data from HSVA towing tank.

The coupling of the CFD solver to the optimization algorithms in the framework of CAESES is carried out for getting the automatic process of optimizing. In this thesis, the use of GL Rankine solver coupling with CAESES / Dakota interface for optimization is introduced. In order to receive the global optimum value of the calm water resistance, the study of DoEs in the design space is done first, followed by the single objective optimization for different speeds with Surrogate- based local optimization algorithm after selecting the best design from DoE. Not only single objective optimization for each speed, but also single objective optimization with different weighted function is performed while taking total resistance for both speeds into account of weighted function. Finally, the multi-objective optimization process is performed for both speed conditions at fixed draft by the use of Dakota/ Surrogate-based global optimization method.

In the stage of optimization in calm water condition, the different optimum designs for two speeds are then checked for their sensitivities by varying different drafts and compared for their performances with initial model. Since the optimization was done for two speeds with fixed draft, the different optimal models was analyzed for different operation scenario and compared with initial model's performance. And then, the different optimal designs for two speeds are then checked and compared for their performances in added wave resistance in seaways. Finally, the final optimal model for the first optimization stage is chosen by considering different analysis performed before and comparison of wave pattern, wave cut and geometry changes related to the initial model is performed.

In the second stage, the direct optimization in moderate sea states was performed for the selected wave scenario for two operation conditions. This process was performed only with the use of SOBOL in CAESES for finding 300 design variants and selected the optimal model for respective operation condition. Since the optimization was done only for head waves, the performance of the two selected models was analyzed for the different wave heading angles. The final optimal model for the direct optimization in moderate sea states was chosen by comparing the performance at different heading angles which gives the minimum total resistance in waves for the selected sea state.

As summary, table 17 shows the performance of the final optimal models chosen from the optimization in calm water condition and direct optimization in moderate sea states compared to the base model.

Table - 17: Performance Summary of the final optimal models for two operation conditions

		Design	CFD run (DoE+Opt)	Performance[1,2]	
				V =15.5kn T_1=14.5m	V = 18 kn T_2=15m
Optimization in calm water condition	DoE+ surrogate based local optimization	SO_V15.5	267	-6.92%	-3.14%
Optimization in sea states	DoE(SOBOL)	SO_Rt_OC1 (ID_208)	300	-7.5%	-1.36%

10.CONCLUSION AND RECOMMENDATIONS

10.1. Conclusion

Several conclusions can be done on regarding the optimization techniques used in this thesis and the analysis of CFD code in order to get the reliable results of the simulations. It saves a lot of times in simulating the necessary results by taking around 30 minutes for each simulation, steady flow computation or seakeeping analysis. In GL Rankine solver, it is necessary to adjust the panel grid sizes, the initial wave height positions in forward and aft of the ship, wave damping factor and relaxation factor to get the convergence. Those parameters are very sensitive and can lead to unstable and unreasonable output results for the simulation of the design variants generating from the optimizing algorithms. For achieving the good and feasible behavior in the optimization, the CFD solver set-up should modify for auto-selection of input parameters and stable penalization with more reliable result data.

In summary, the single objective method leads to a very good improvement for the condition set as objective. The optimization with different objective conditions included in the objective function by a weight presented a very low degree of improvement. In addition, it can also be concluded that, as expected, the weight is an efficient way to move the objective from one condition to another in a smooth way. The multi-objective optimization by means of genetic algorithm, MOGA, considering the high number of necessary designs leads to a very expensive method with high cost/benefits.

The result file for seakeeping computations of GL Rankine gives the average drift forces per amplitude squared. In order to find added resistance in waves from the result file, the specific wave scenario was fixed for each operation condition. While performing the direct optimization in moderate sea states, the seaway spectrum was used by Pierson-Moskowitz spectrum and analyzed only for the regular head waves.

In this thesis, the different optimization methods and procedures were used in order to minimize the total resistance of the ship in calm water and in moderate sea states. The final optimal models obtained from those optimization approaches gave the greater improvement when compared to the initial model. As conclusion, the proper selection of the optimization method for each case of study proves to be a key factor in order to achieve good results. The approaches in this work still require numerous improvements and also for the CFD solver set-up that should modify for auto-selection of input parameters and stable penalization with more reliable result data.

10.2. Recommendations

For penalization of the model in GL Rankine, it should be nice to follow the standard recommendation of the code developer such as 1% of LPP of ship for panel size in middle section and 0.7% for that in forward or aft section. It is wise to keep the default value for wave damping factor and relaxation parameter in the set-up (only needed to change if the solver cannot get the convergent solution) and adjust the initial wave height position in the forward and aft region carefully.

An adequate optimization method should be selected for each case of study; tests with simplified analyses should be performed for the selection. For the optimization processes it is important to have a good initial design that can be obtained via DoE (e.g. SOBOL method). It can be said that the optimization approaches in this work scope are not the complete task for the early design stage.

While performing the optimization process, the author took the results of wave, frictional and total resistances calculated from GL Rankine. It may lead to the difference from the actual result since GL Rankine is potential flow solver and it omits the viscous effects of the hull form. In order to check the error of the potential flow solver and to study the viscous effects, it is strongly recommended to simulate with another commercial RANS-codes not only for the initial model but also for the final optimal models obtained from this thesis work.

This work was performed only for the optimization of bulbous bow in calm water condition and the added resistance of the vessel due to head waves was calculated separately after optimization process. While calculating the added wave resistance, the author decided to calculate for most frequent sea state for both speed conditions. In order to get precise performance in waves, different wave scenario should be considered.

Finally, in the direct optimization approach in order to minimize the total resistance in waves, the author decided to use Design of Experiments (SOBOL) only since the computation time for each design is more than one hour. In order to get the good results, the optimization process should be done by using single objective or multi-objective algorithms.

Since the purpose of this thesis is to get the optimal design which has the better performance in calm water and in moderate sea states for the earlier design stage, the results obtained from overall analysis in this thesis are quite helpful and reliable for further detail analysis.

REFERENCES

[1] Harries S, February 2015, *Practical Shape Optimization Using CFD*, FRIENDSHIP SYSTEMS.

[2] H. Bagheri, H. Ghassemi & A. Dehghanian, March 2014, *Optimizing the Seakeeping Performance of Ship Hull Forms Using Genetic Algorithm*, the International Journal on Marine Navigation and Safety of Sea Transportation, DOI: 10.12716/1001.08.01.06.

[3] Zhang Ping, Zhu De-xiang and Leng Wen-hao, 2008, *Parametric Approach to Design of Hull Forms*. ScienceDirect Journal of Hydrodynamics, 20(6), 804-810.

[4] Abt, C.; Bade, S.D.; Birk, L.; Harries, S., September 2001, *Parametric Hull Form Design – A Step Towards One Week Ship Design*, 8th International Symposium on Practical Design of Ships and Other Floating Structures · PRADS 2001, Shanghai.

[5] Heinrich Söding, Alexander von Graefe, Ould el Moctar and Vladimir Shigunov, Sebastian Walter ,2012 ,*Computing Added Resistance in Waves –Rankine Panel Method Vs RANSE Method*.

[6] Justus Heimann, 2005. *CFD Based Optimization of the Wave-Making Characteristics of Ship Hulls*. Thesis (PhD). Technical University Berlin.

[7] Gregory J. Grigoropoulos and Dimitris S. Chalkias, 2009, *Hull-form optimization in calm and rough water*. Computer-Aided Design, 42 (2010), 977-984.

[8] H. Bagheri, H. Ghassemi, 2014. *Genetic Algorithm Applied To Optimization of the Ship Hull Form With Respect to Seakeeping Performance*, Transactions of Famena Xxxviii-3.

[9] Shahid Mahmood and Debo Huang, 2012, *Computational Fluid Dynamics Based Bulbous Bow Optimization Using a Genetic Algorithm*, Multihull Ship Technology, Key Laboratory of Fundamental Science for National Defense, Harbin Engineering University, Harbin 150001, China.

[10] Dakota Version 6.1, User Manual, *Chapter 14, Advanced Methods.*

[11] CAESES4.0.1, Tutorials, *Learn More: Dakota.*

[12] *https://www.caeses.com/about-us/r_a_d/persee/*

[13] *https://www.uni-due.de/persee/workpackage.shtml*

[14] Ould el Moctar, Vladimir Shigunov & Tobias Zorn, August 2012, *Duisburg Test Case: Post-Panamax Container Ship for Benchmarking*, Ship Technology Research Schiffstechnik VOL. 59/ NO. 3.

[15] Birk L and Harries S (Edt.), 2013, *Optimistic-Optimization in Marine Design, Chapter-5-geometric Modelling and Optimization by Stefan Harries,* 39th WEGEMT Summer School, Berlin, Germany.

[16] P. Ferrant, 2013, *Seakeeping Lectures 1&2, Page 19,* Ecole Centrale de Nantes, Ocean/ Master EMSHIP 2013 – 2014.

[17] Hochkirch K and Bertram V, *Slow Steaming Bulbous Bow Optimization for a Large Containership*.

[18] Alexander von Graefe, Bettar El Moctar and Vladimir Shigunov, 2014, *GL Rankine: User Manual, DNV GL*, Version 2014-04-03.

[19] ITTC Recommended Procedures and Guidelines, *Speed and Power Trials, Part 2 Analysis of Speed/Power Trial Data*, 7.5-04-01-01.2, Effective Date 2014, Revision 1.1.

[20] Vladimir Shigunov and Volker Bertram, 2014, *Prediction Of Added Power In Seaway By Numerical Simulation*, Conference Paper.

[21] Kai Graf, Marcus Pelz, Volker Bertram and H. Söding, March 2007, *Added Resistance in Seaways and its Impact on Yacht Performance*, the 18th CHESAPEAKE sailing yacht symposium.

[22] Martin Alexandersson, January 2009, *a Study of Methods to Predict Added Resistance in Waves Performed At Seaware AB,* Master Thesis, and KTH Centre for Naval Architecture STOCKHOLM.

[23] Harries S., *Optimization Course Nantes Friendship-Systems*, Ecole Centrale Nantes, 2013.

[24] Jan-Patrick Voß, *Accurate CFD prediction of added resistance in waves* , HSVA Newswave Newsletter, issue 2-15.

APPENDIX

A1. Study on Each Design Parameters

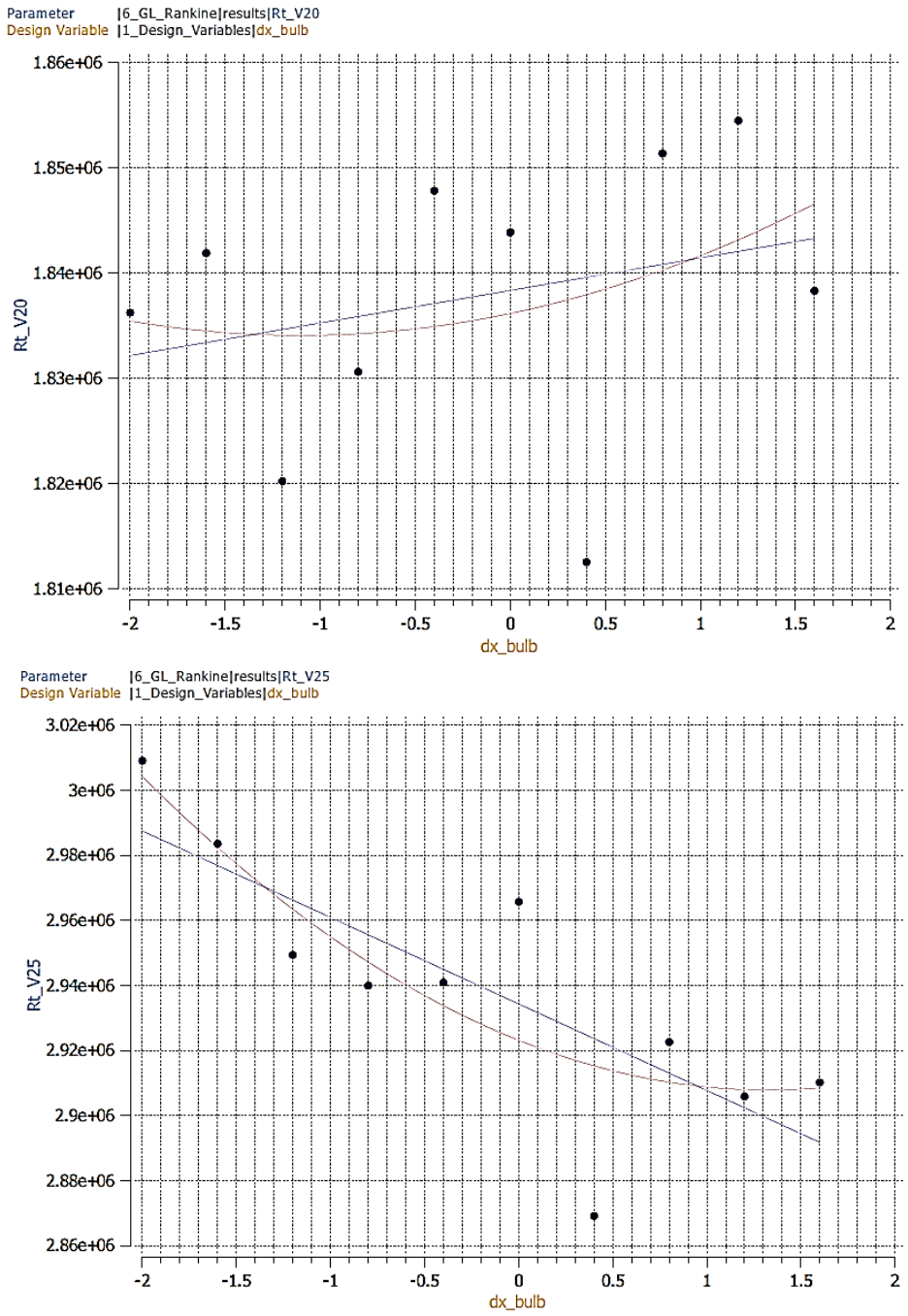

Figure- A1- 1: Influence of bulb length variable on ship total resistance

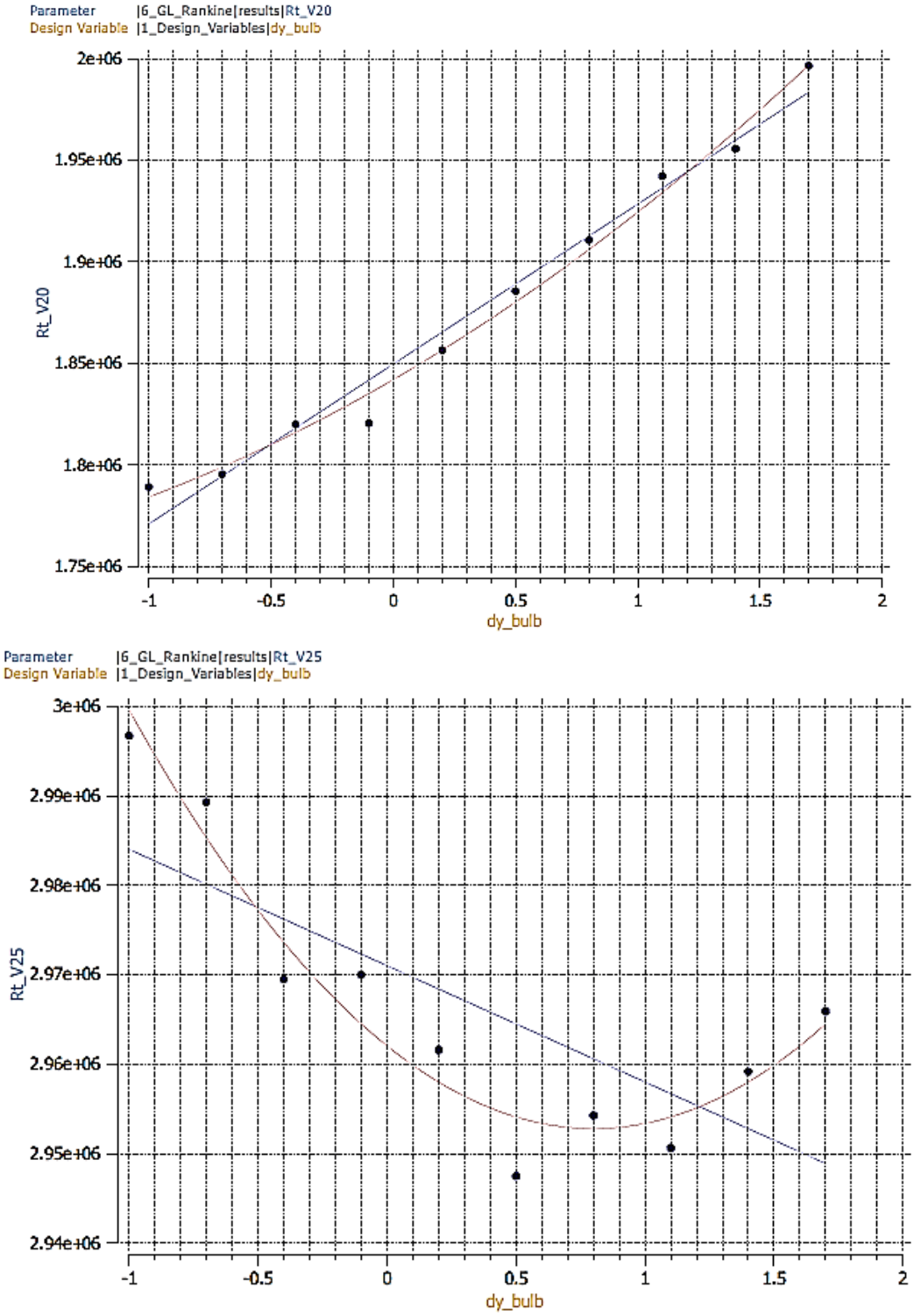

Figure- A1- 2: Influence of bulb width variable on ship total resistance

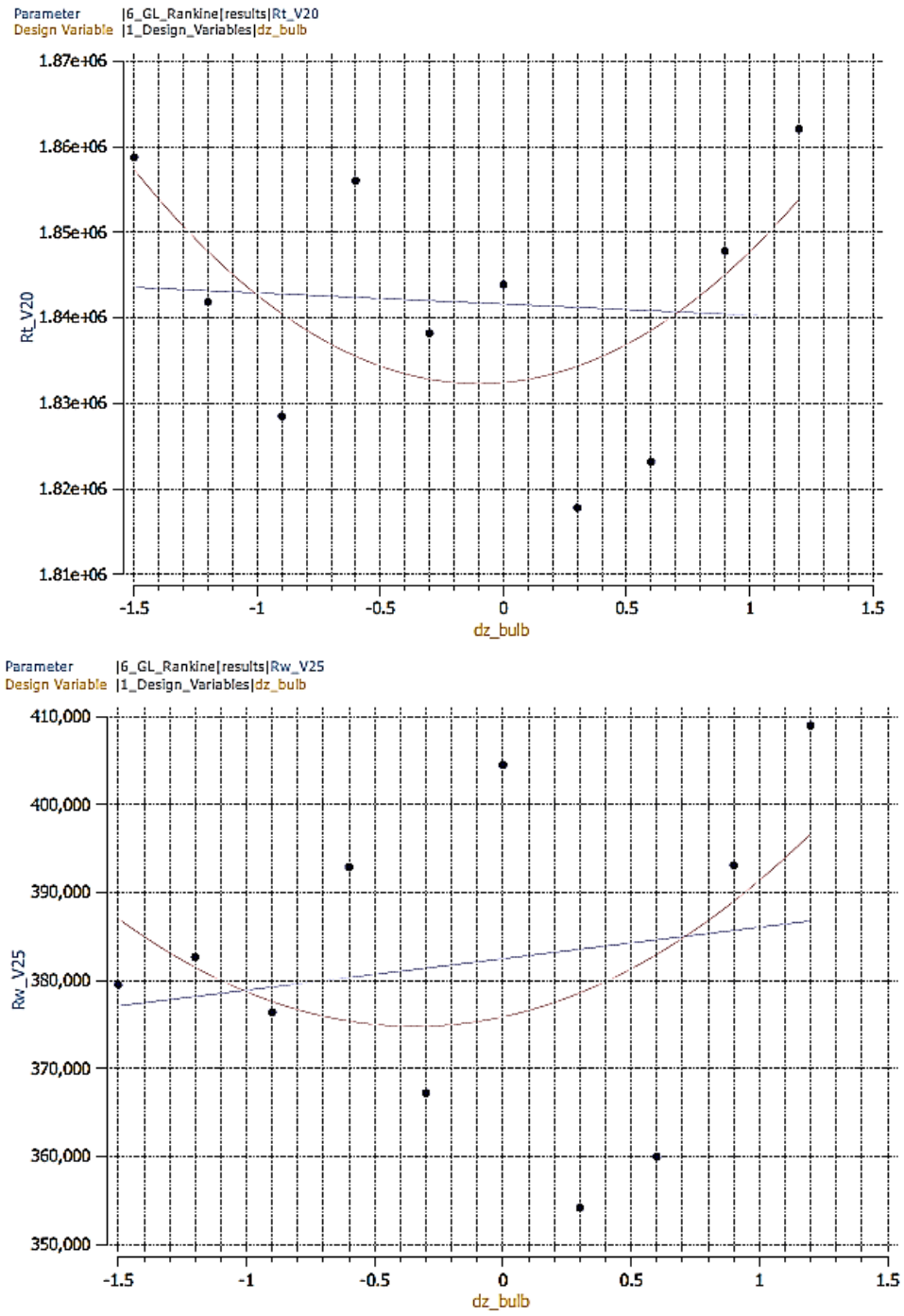

Figure- A1- 3: Influence of bulb tip elevation variable on ship total resistance

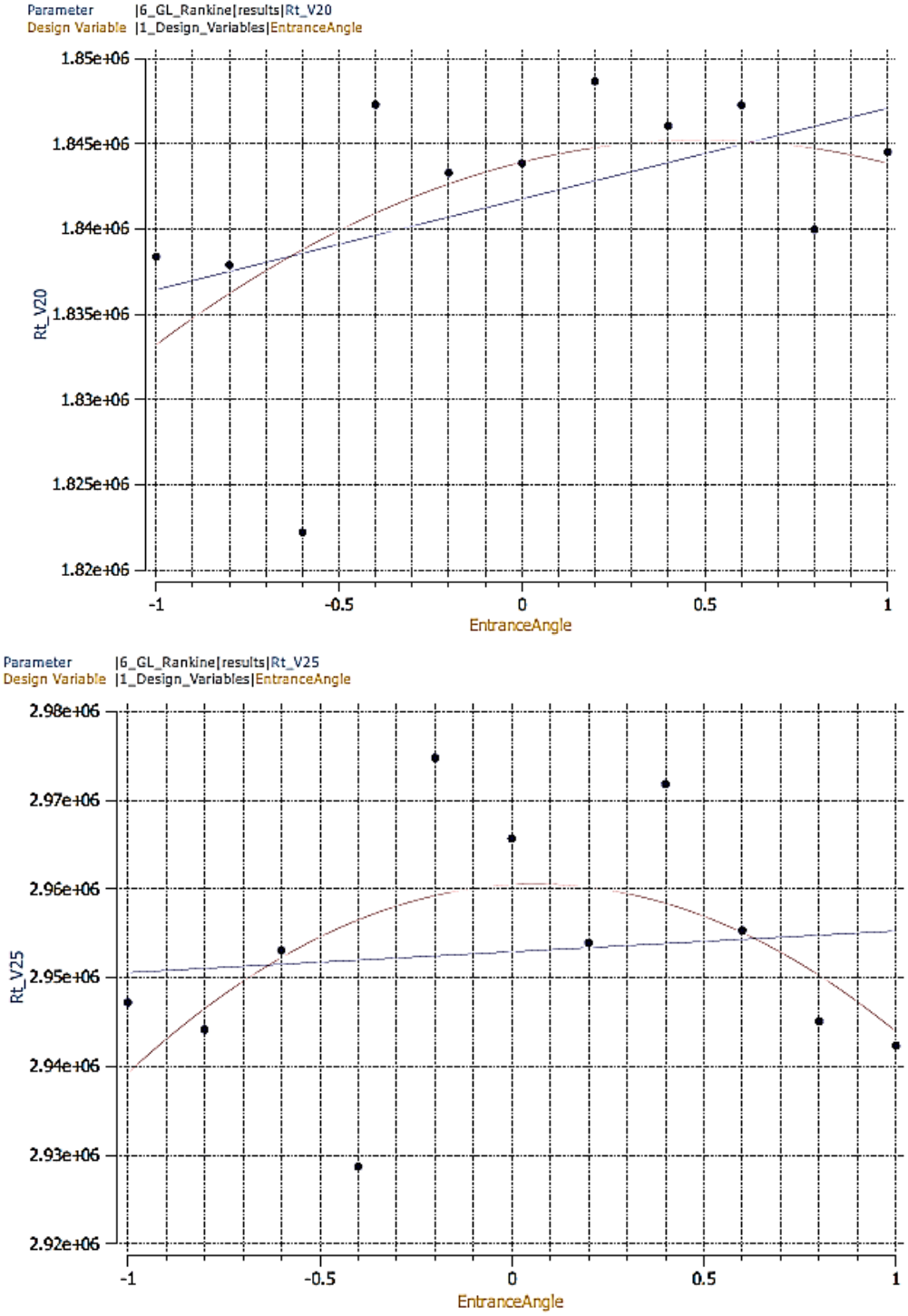

Figure- A1- 4: Influence of WL entrance angle variable on ship total resistance

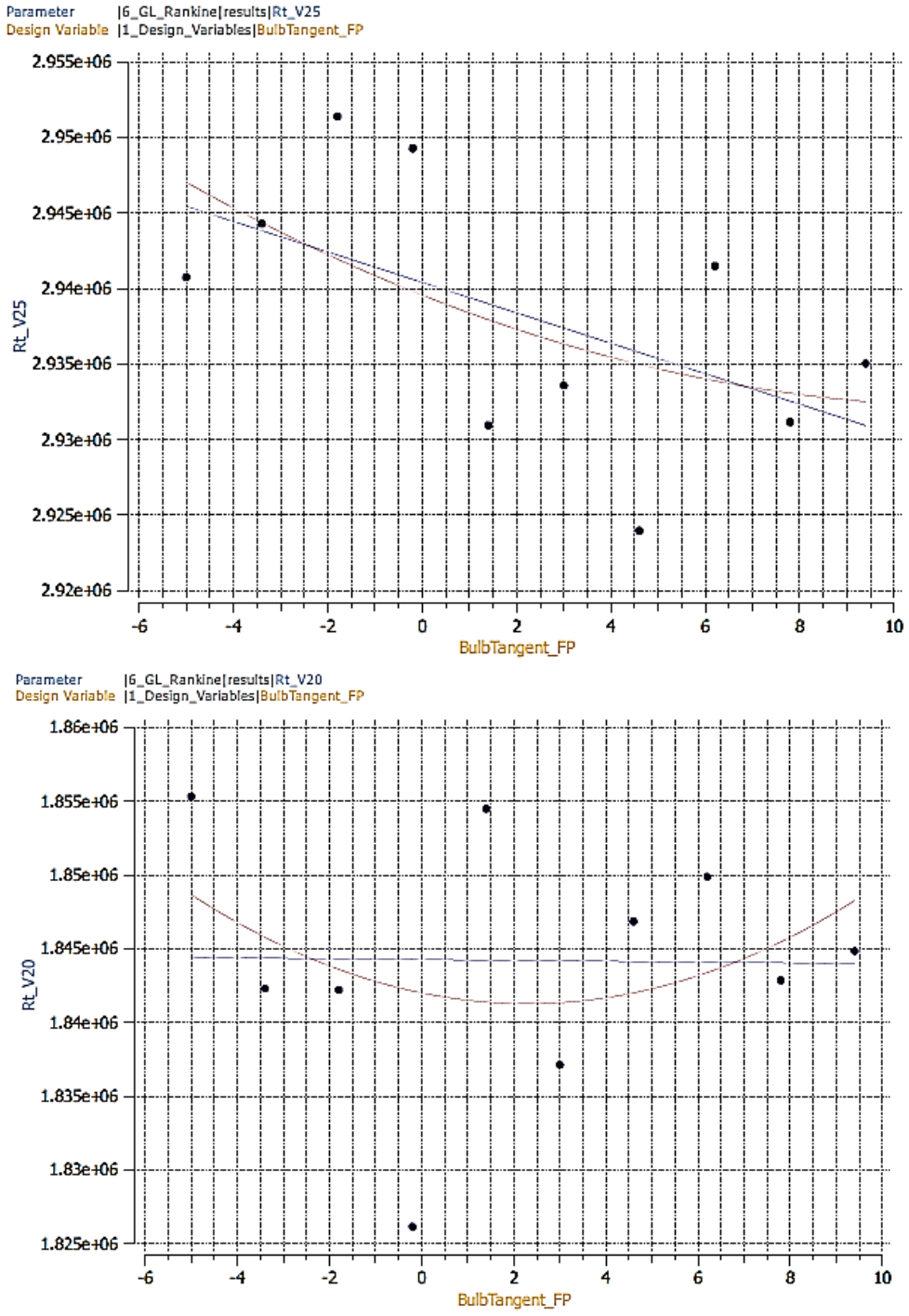

Figure- A1- 5: Influence of Bulb top tangent at FP variable on ship total resistance

A2. Set-up Input XML File for GL Rankine Solver

A2.1. Sample XML file for Steady Flow Computation

```
<GLRankine>
<Project version="1.0">
<Configuration>
<ProjectInfo>
<Generator>
<Name value="created by Tin"/>
<Version value="1.0"/>
</Generator>
<CreationTime timeStamp=""/>
<CreatedBy name="Tin"/>
<ProjectName value="DTC"/>
</ProjectInfo>
<Computations>
<Preprocessing>
<Bodies>
<Body>
<BodyDefinition name="dtc" sym="1">
<BodyParts>
<BodyPart name="part">
<Surface>
<ReadFromFile type="stl" fileName="DTC.stl"/>

<Transformations>

<Translation dx="0" dy="0" dz="-14.5" />

</Transformations>
<! -- <LimitPlane nx="0" ny="1" nz="0" d="0" /> -->

<WriteToFile type="vtk" fileName="surf.vtk" />
</Surface>

<BodyPanelGeneration>
<double name="lMid" value="3.5"/>
<double name="lBow" value="2.5"/>
<double name="lAft" value="2.5"/>
<double name="zBow" value="1.62008"/>
<double name="zAft" value="0.972048"/>
</BodyPanelGeneration>
</BodyPart>
</BodyParts>
<Transformations>
</Transformations>
<WriteToFile type="vtk" fileName="panels.vtk"/>
<WriteToFile type="shr2" fileName="body-def2.shr2"/>
</BodyDefinition>
```

```
</Body>
</Bodies>
<FreeSurface>
<SetDefaultParameterFor u0="7.9732" />
<FreeSurfaceDefinition>
<RectangularFreeSurface>
</RectangularFreeSurface>
<WriteToFile type="vtk" fileName="fs.vtk"/>
</FreeSurfaceDefinition>
</FreeSurface>
</Preprocessing>
<NonlinearSteadySimulation>
<Data>
<BodyData bodyName="dtc">
<double name="cogZ" value="8.46951" />
</BodyData>
</Data>
<Parameter>
<double name="u0"                value="7.9732" />
<double name="rho"               value="1025" />
<double name="g"                 value="9.81" />
<double name="relax" value="0.3"/>
<double name="relax0" value="1"/>
<double name="wdp"               value="0.001" />
<unsignedInt name="maxIter" value="100" />
</Parameter>
<Output>
<ResultFile>dump.shr2</ResultFile>
<LogFile>log.out</LogFile>
<VTKDirectory>data</VTKDirectory>
</Output></NonlinearSteadySimulation>
</Computations>
</Configuration>
</Project>
</GLRankine>
```

A2.2. Sample XML file for Seakeeping Computation

```
<? Xml version="1.0" encoding="UTF-8"?>

<GLRankine xmlns: xsi: xsi="http://www.w3.org/2001/XMLSchema-instance"
schemaVersion="1.0" xsi:
noNamespaceSchemaLocation="RankineConfig.xsd">
<Project version="1.0">
<Configuration>
<ProjectInfo>
<Generator>
<Name value="Manually created by Tin"/>
<Version value="1.0"/>
</Generator>
<CreationTime timeStamp="2009-09-29T13:00:59.99Z"/>
<CreatedBy name="Tin"/>
<ProjectName value="PerSee"/>
</ProjectInfo>
<Computations>
<SeakeepingLinear>
<Input>
<StationarySolution>dump.shr2</StationarySolution>
</Input>
<Data>
<BodyData bodyName="dtc">
<double name="GM" value="1.37" />
<double name="rollDamp" value="3" /> <! -- 3% -->
<double name="r_xx" value="20.25" />
<double name="r_yy" value="88.19" />
<double name="r_zz" value="88.49" />
<double name="r2_xy" value="0" />
<double name="r2_xz" value="0" />
<double name="r2_yz" value="0" />
</BodyData>
```

```
<WaveData>
<Waves omega="0.257" muList="180" />
<Waves omega="0.303" muList="180" />
<Waves omega="0.344" muList="180" />
<Waves omega="0.371" muList="180" />
<Waves omega="0.389" muList="180" />
<Waves omega="0.407" muList="180" />
<Waves omega="0.426" muList="180" />
<Waves omega="0.454" muList="180" />
<Waves omega="0.525" muList="180" />
<Waves omega="0.613" muList="180" />
<Waves omega="0.678" muList="180" />
<Waves omega="0.768" muList="180" />
<Waves omega="0.867" muList="180" />
        </WaveData>
</Data>
<FreeSurfaceGeneration>
<DefaultGeneration>
<double name="fsGridResolution" value="1.0" />
<double name="fsGridSize"                    value="1.0" />
</DefaultGeneration>
</FreeSurfaceGeneration>
<Parameter></Parameter>
<Output>
<ResultFile>tf_wo_v16kn.shr2</ResultFile>
<LogFile>log.out</LogFile>
</Output>
</SeakeepingLinear>
</Computations>
</Configuration>
</Project>
</GLRankine>
```

A3. Distribution of Design Variables by SOBOL in Design Space

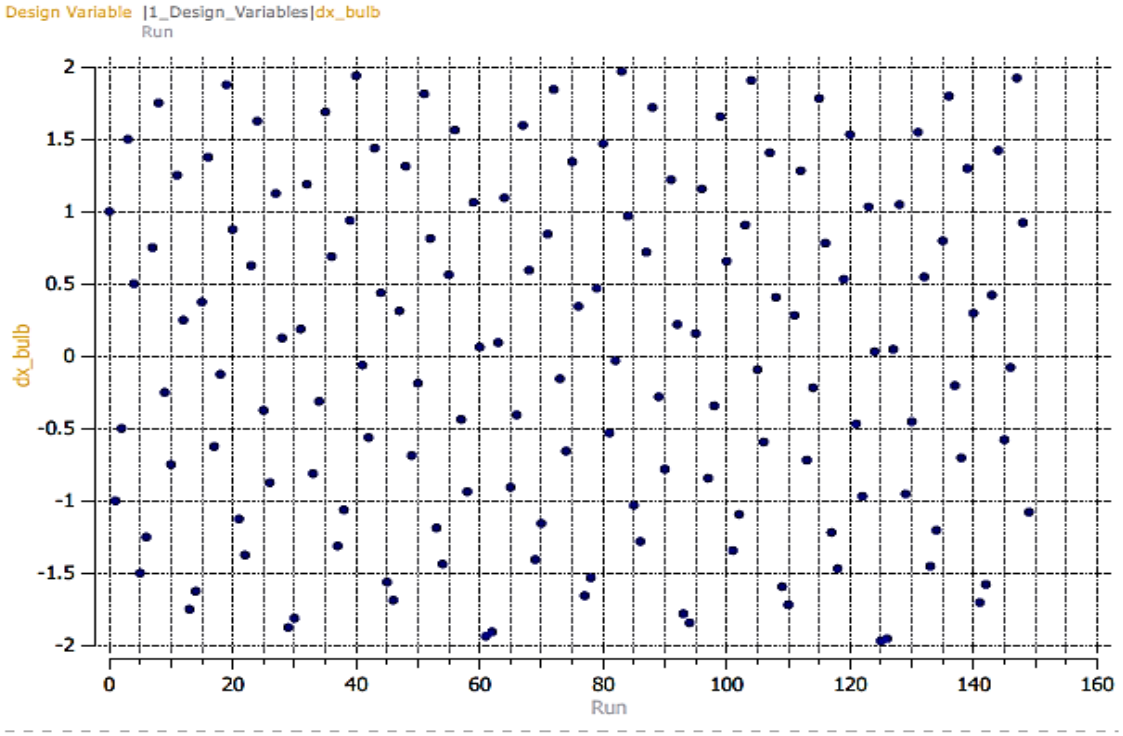

Figure-A3- 1: Distribution of the values of parameter “dx-bulb”

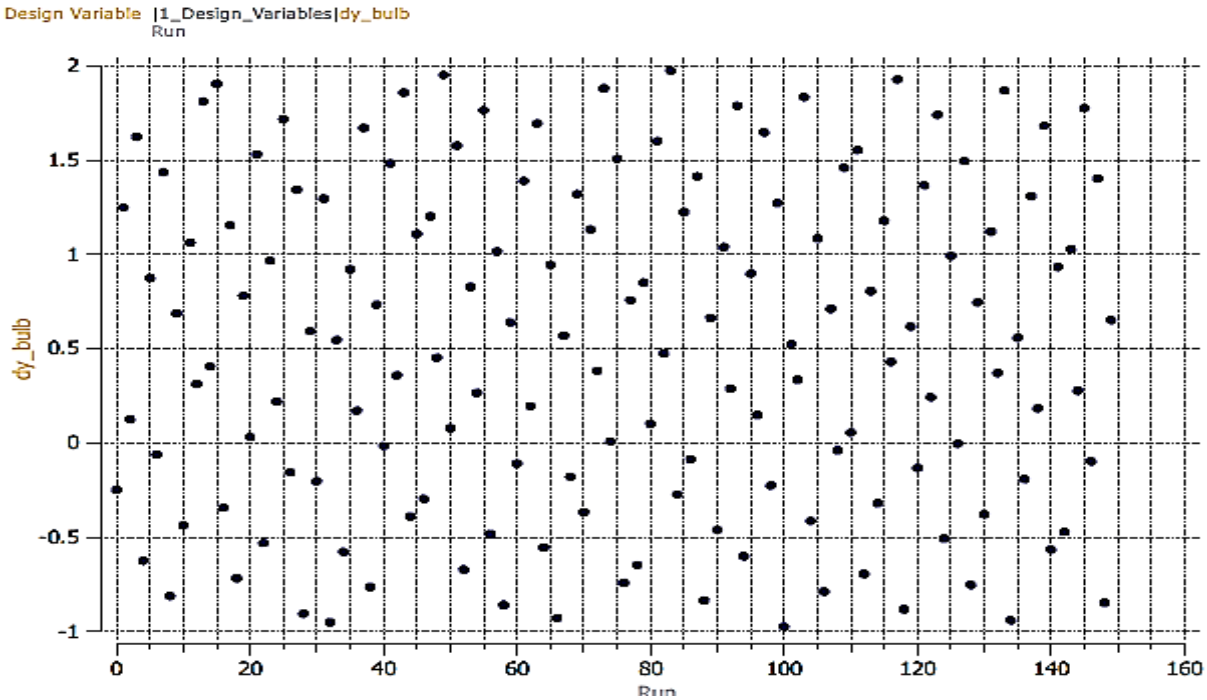

Figure-A3- 2: Distribution of the values of parameter “dy-bulb”

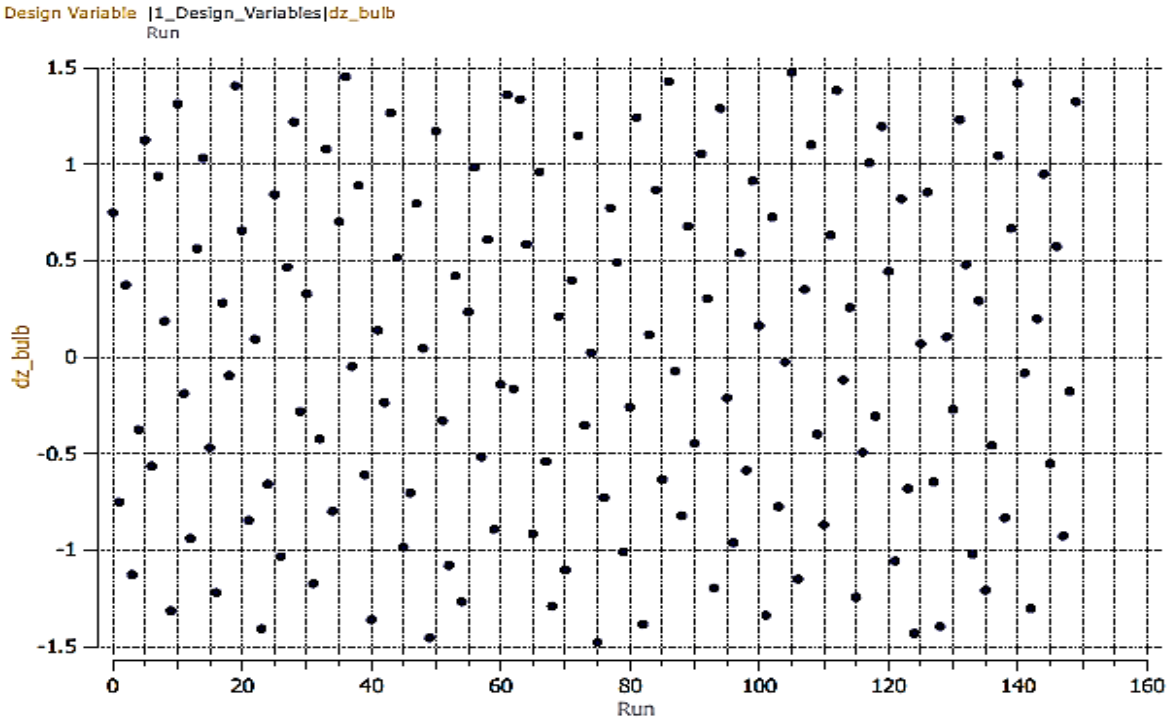

Figure-A3- 3: Distribution of the values of parameter “dz-bulb”

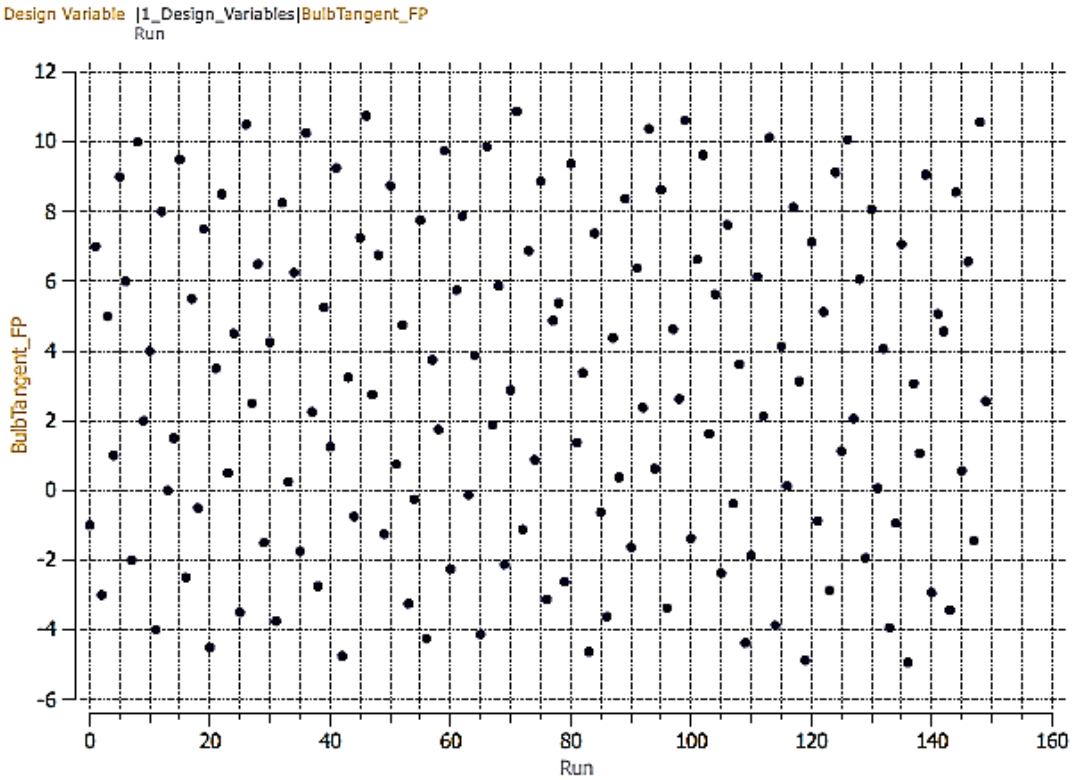

Figure-A3- 4: Distribution of the values of parameter “bulbTangent_FP”

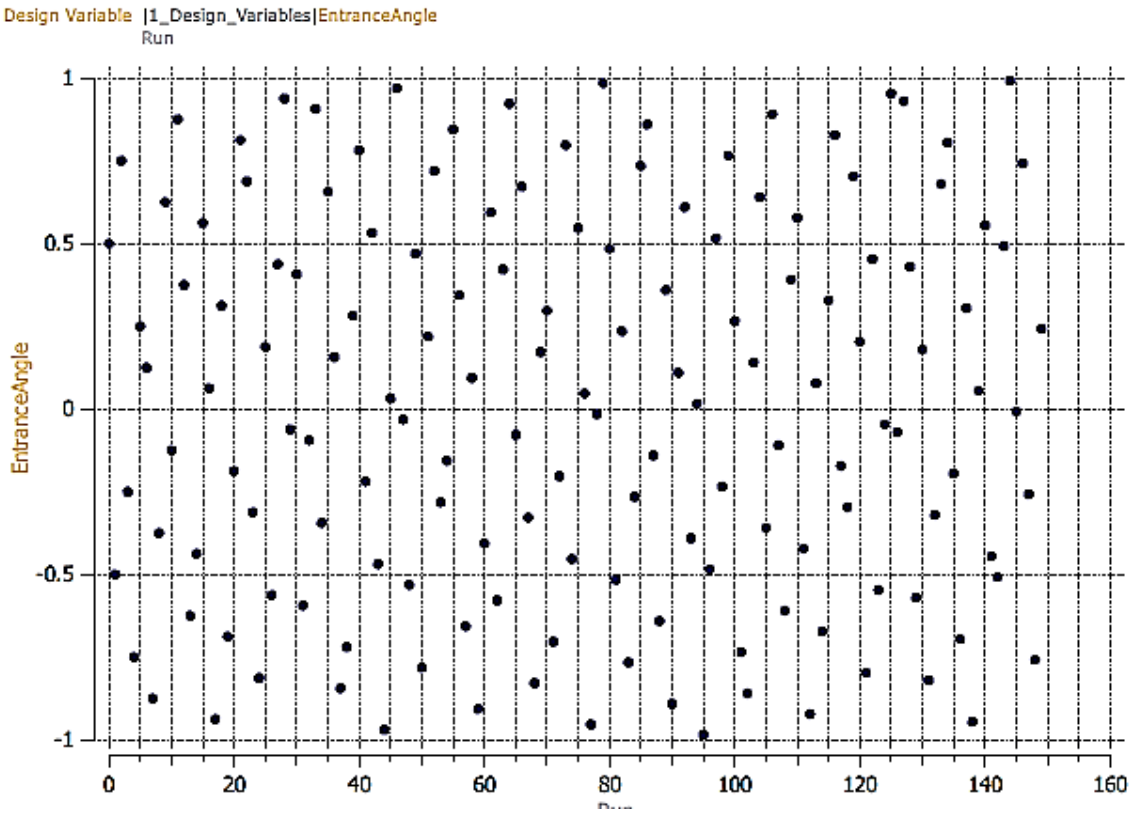

Figure-A3- 5: Distribution of the values of parameter "EntranceAngle"

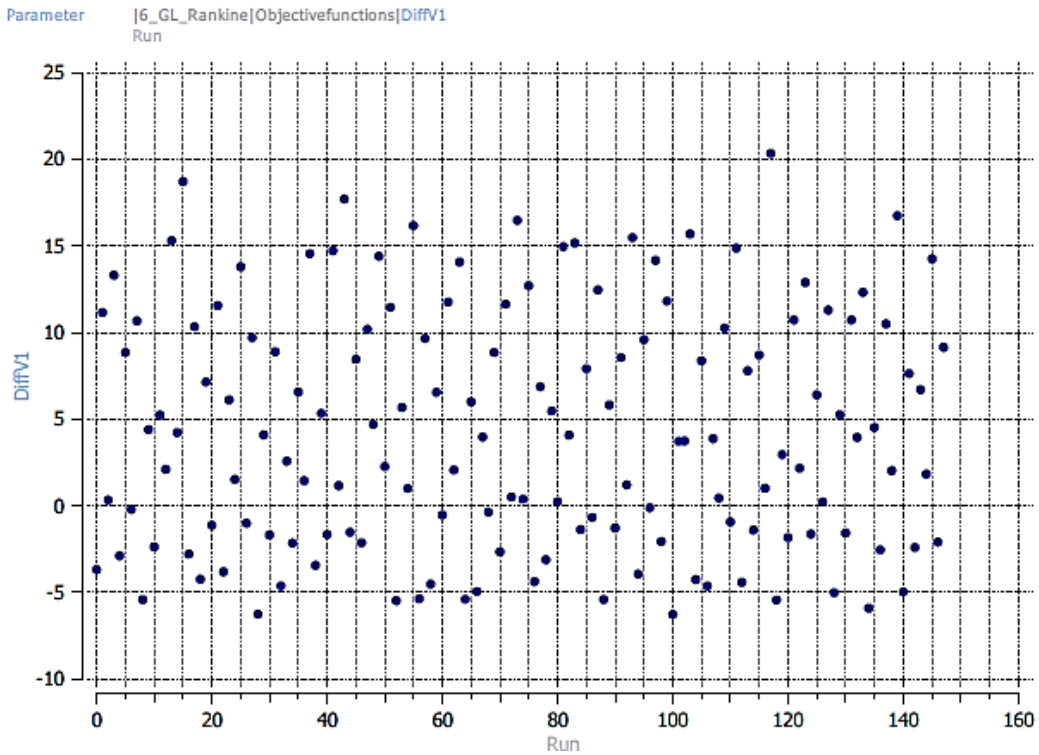

Figure-A3- 6: Distribution of the values of parameter "Difference in RTV1 from BM"

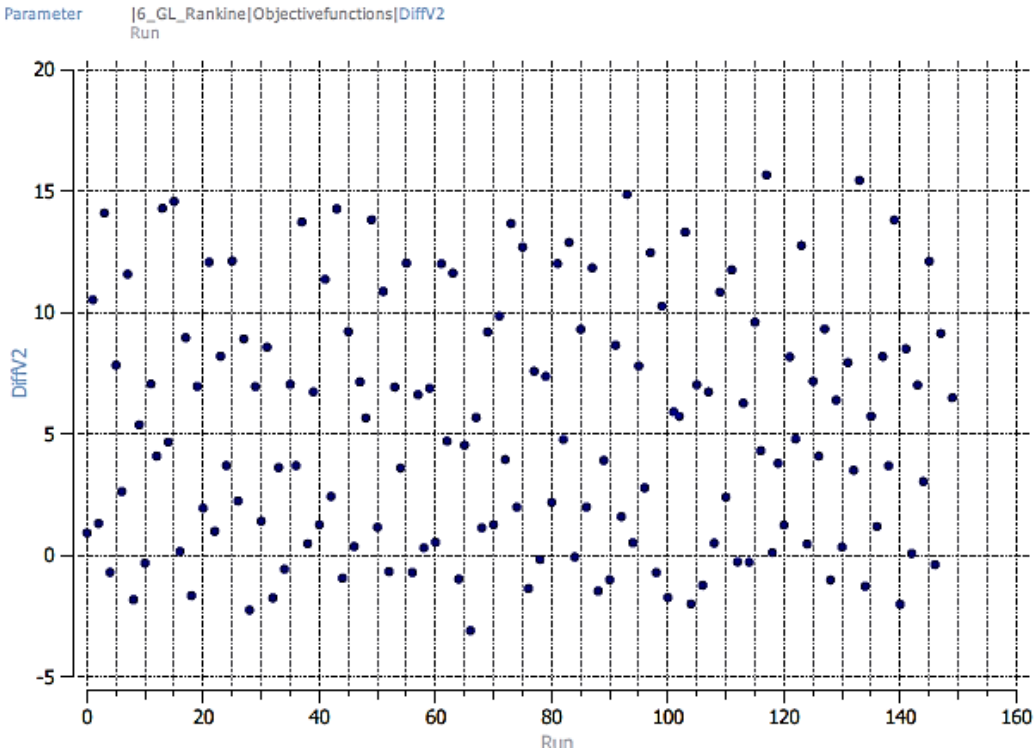

Figure-A3- 7: Distribution of the values of parameter "Difference in RTV2 from BM"

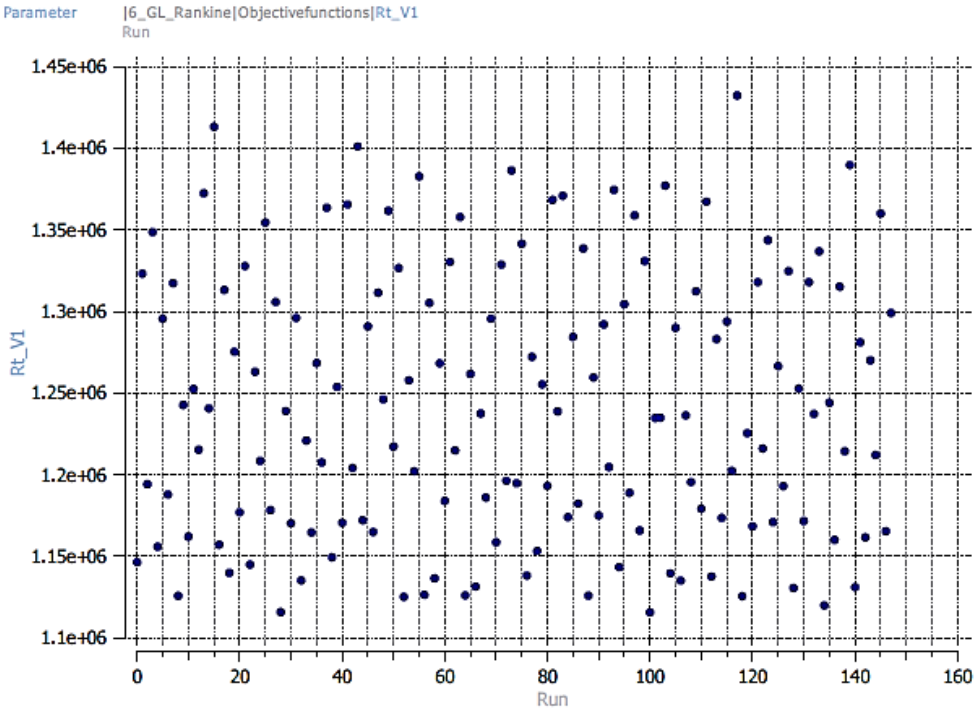

Figure-A3- 8: Distribution of the values of parameter "RTV1"

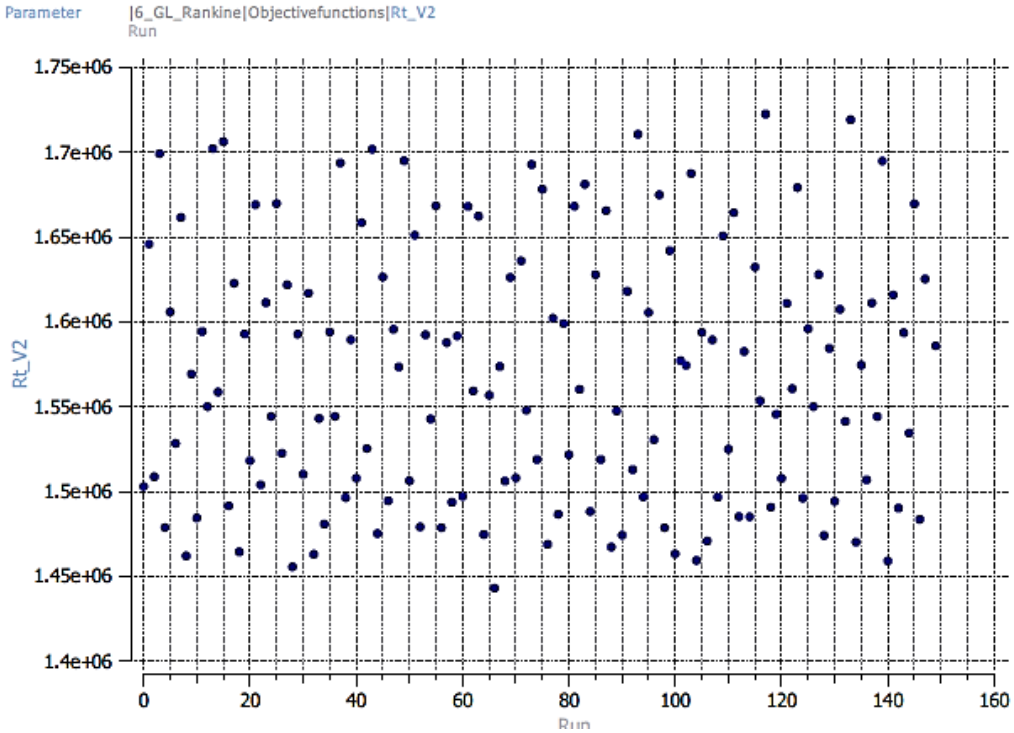

Figure-A3- 9: Distribution of the values of parameter "RTV2"

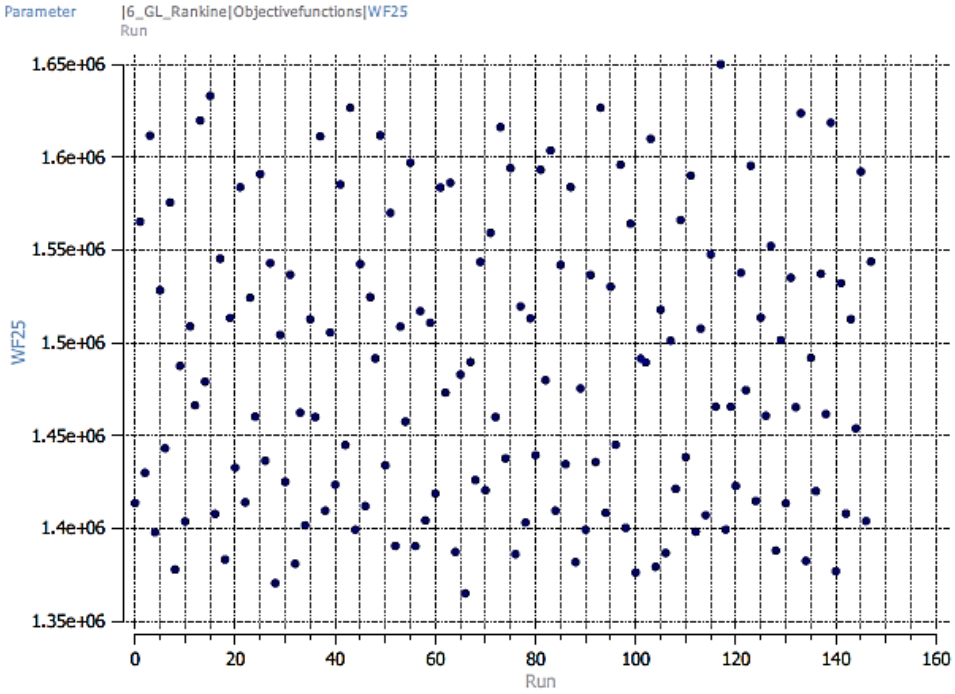

Figure-A3- 10: Distribution of total resistance with weight coefficient= 0.25

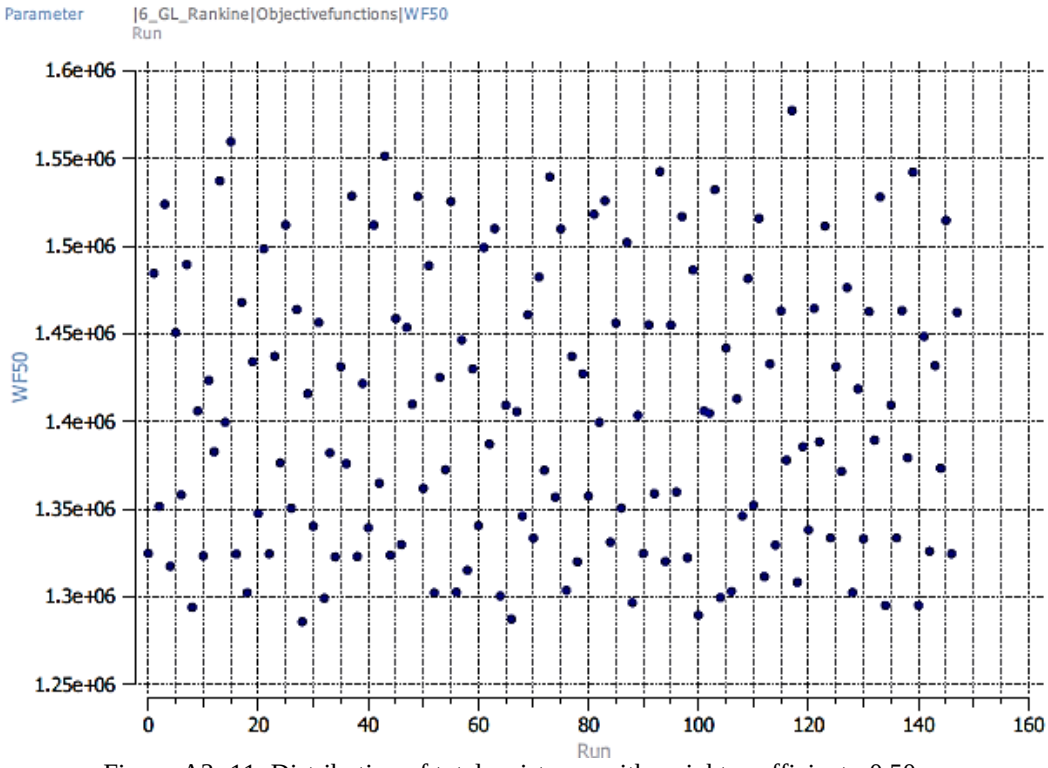

Figure-A3- 11: Distribution of total resistance with weight coefficient= 0.50

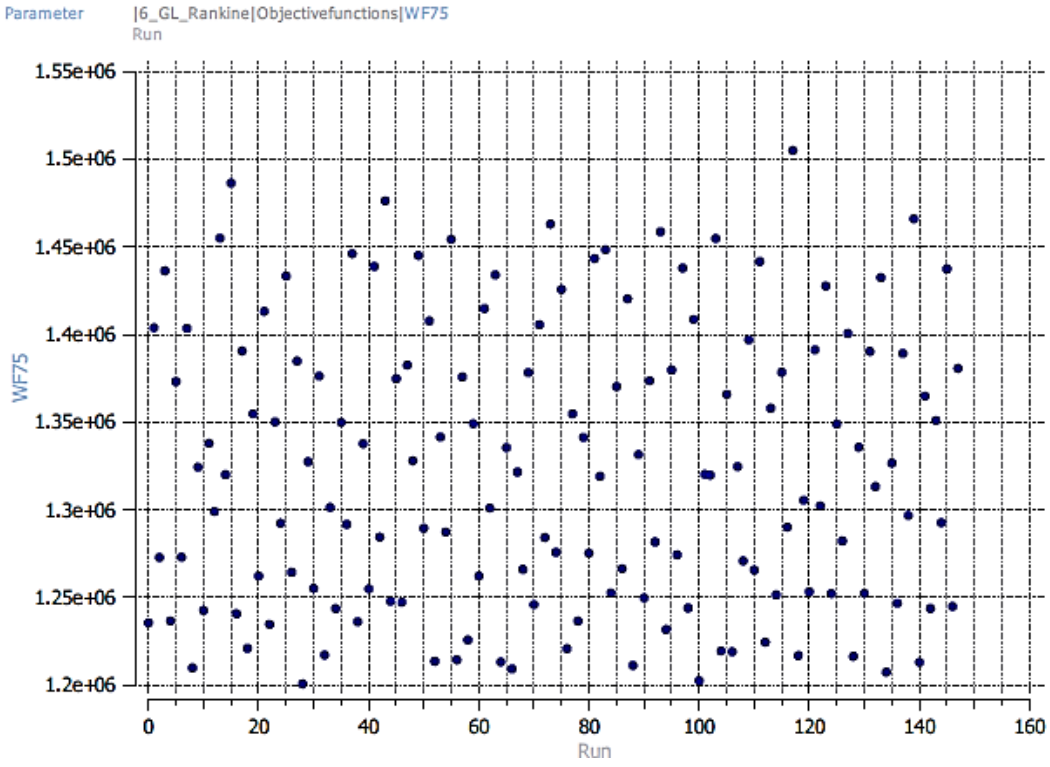

Figure-A3- 12: Distribution of total resistance with weight coefficient= 0.75

A4. Standard Template for Surrogate Based Global Optimization (CAESES)

environment tabular_graphics_data method_pointer = 'SBGO'

Method
id_method = 'SBGO' surrogate_based_global model_pointer = 'SURROGATE' approx_method_pointer = 'MOGA' replace_points
max_iterations = 300

Method
id_method = 'MOGA' moga
output silent
seed = 12345
population_size = 300
max_function_evaluations = 5000 initialization_type unique_random crossover_type shuffle_random num_offspring = 2 num_parents = 2
crossover_rate = 0.8 mutation_type replace_uniform mutation_rate = 0.08 fitness_type domination_count
replacement_type below_limit = 6 shrinkage_percentage = 0.9 convergence_type metric_tracker percent_change = 0.1
num_generations = 30
final_solutions = 10
model
id_model = 'SURROGATE' surrogate global gaussian_process surfpack trend constant
dace_method_pointer = 'SAMPLING' correction additive zeroth_order
reuse_points all import_points_file = 'model.dat'
method
id_method = 'SAMPLING' model_pointer = 'TRUTH' sampling
samples = 50
seed = 54321 sample_type lhs
model
id_model = 'TRUTH' single

variables continuous_design = 5
initial_point 0 0 0 0 0
lower_bounds -2 -1 -1.5 -5 -1
upper_bounds 2 2 1.5 11 1
descriptors '|1_Design_Variables|dx_bulb' '|1_Design_Variables|dy_bulb' '|1_Design_Variables|dz_bulb' '|1_Design_Variables|BulbTangent_FP' '|1_Design_Variables|EntranceAngle'

responses objective_functions = 2
nonlinear_inequality_constraints = 0
nonlinear_equality_constraints = 0 no_gradients
no_hessians

interface fork
analysis_driver = 'fdakota_client.exe' verbatim parameters_file = 'params.in' results_file = 'results.out' work_directory directory_tag
named 'design' file_save directory_save

asynchronous evaluation_concurrency = 24

A5. MATLAB Code for Calculating the Added Wave Resistance

```
% define Pierson-Moskowitz (ITTC) spectrum parameters
T = 0.5:1:20.5;
w1= [0.1;0.2;0.3;0.4;0.5;0.6;0.7;0.8;0.9;1.0;1.1];
Hs = 0.75:0.5:3.25;
load results.mat;   % results obtained from the GLRankine seakeeping computations
Fx_180= zeros (length (w1), 1);
Fx_150= zeros (length (w1), 1);
Fx_120= zeros (length (w1), 1);
count =1;
for i=1: length (w1)
Fx_180 (i) = -1*Results (count, 3);
Fx_150 (i) = -1*Results (count+1, 3);
Fx_120 (i) = -1*Results (count+2, 3);
count=count+3;
end
Raw1_180 (length (Hs), length (T)) =zeros ();
Radd_max_180 (length (Hs), 1) =zeros ();
Tp_180 (length (Hs), 1) =zeros ();
Raw1_150 (length (Hs), length (T)) =zeros (); Radd_max_150 (length (Hs), 1) =zeros ();
Tp_150 (length (Hs), 1) =zeros ();
Raw1_120 (length (Hs), length (T)) =zeros (); Radd_max_120 (length (Hs), 1) =zeros ();
Tp_120 (length (Hs), 1) =zeros ();

for k= 1: length (Hs)
        Raw_180= zeros (size (T));
        Raw_150= zeros (size (T));
        Raw_120= zeros (size (T));

for j= 1: length (T)
      S1= zeros (size (w1));
      for i= 1: length (w1)
         Af= 173*Hs (k) ^2/T (j) ^4;
         Bf= 691/T (j) ^4;
```

```
        S1 (i) = Af*w1 (i) ^-5*exp (-1*Bf*w1 (i) ^-4);
      end
      RAW_180 =S1.* Fx_180;
     Raw_180 (j) = 2*trapz (w1, RAW_180);
     If (j>1)
        if (Raw_180 (j)>Raw_180 (j-1))
           Radd_max_180 (k, 1) =Raw_180 (j); Tp_180
           (k, 1) = T (j);
        end
     end
     RAW_150 =S1.* Fx_150;
     Raw_150 (j) = 2*trapz (w1,RAW_150);
     if (j>1)
        if (Raw_150(j)>Raw_150(j-1))
           Radd_max_150(k,1)=Raw_150(j);
           Tp_150(k,1)= T(j);
        end
     end
     RAW_120 =S1.* Fx_120;
     Raw_120(j) = 2*trapz(w1,RAW_120);
     if (j>1)
        if (Raw_120(j)>Raw_120(j-1))
           Radd_max_120(k,1)=Raw_120(j);
           Tp_120(k,1)= T(j);
        end
  end
  end
  Raw1_180  (k,:)=  Raw_180/Rtcalmwater*100;
  Raw1_150  (k,:)=  Raw_150/Rtcalmwater*100;
  Raw1_120  (k,:)= Raw_120/Rtcalmwater*100;
end
```